Generation of a mouse model to study the temporal relationship between *BRAF*^{V600E} expression and *PTEN* silencing in melanoma development

Michelle Lamarche
Department of Biology, McGill University

October, 2011

A thesis submitted to McGill University in partial fulfillment of the requirements of the degree of Masters

Abstract

Metastatic melanoma is a devastating and poorly understood disease that is extremely resistant to current approved therapeutic regimens. The earliest and most common observed genetic alteration encodes constitutively active BRAF-V600E ($BRAF^{V600E}$) which promotes sustained activation of the BRAF-MEK-ERK MAP kinase signaling pathway. $BRAF^{V600E}$ is detected in 85% of human nevi and ~65% of metastatic melanomas. Progression from nevi to melanoma is thought to require the subsequent functional loss of at least one tumor suppressor gene, commonly *PTEN*. We have previously demonstrated that the concomitant activation of $BRAF^{V600E}$ and *PTEN* silencing led to the appearance of highly pigmented melanocytic skin lesions with histological features of melanoma. However, human tumors do not develop mutations simultaneously. Thus, to study melanoma progression *in vivo*, we will initiate $BRAF^{V600E}$ expression and *PTEN* silencing independently with Flp and Cre respectively. We have previously generated mice carrying a Flp-activated $BRAF^{V600E}$ allele ($BRAF^{FA}$), which expresses normal *BRAF* prior to Flp-mediated recombination, at which point $BRAF^{V600E}$ is expressed. Similarly, we have a conditional *PTEN* allele that becomes inactivated upon Cre-mediated recombination.

To separate $BRAF^{V600E}$ activation and *PTEN* silencing *in vivo*, I attempted to generate a transgenic mouse expressing inducible forms of Cre and Flp recombinases in a melanocyte-specific manner (pTyr:CreER and pTyr:FlpPR). The two constructs were co-integrated into the genome of C57BL/6 zygotes, generating five *Tyr:FC* founder strains. *In vitro* analysis of the constructs demonstrated melanocyte specificity and appropriate inducibility and specificity for recombination sequences. However, zero of five *Tyr:FC* strains demonstrated recombinase expression or function *in vivo*. The reason behind this lack of expression remains unknown but is most likely attributed to the co-injection technique, too few founder strains for analysis, or faults in the pTyr constructs.

Résumé

Le mélanome est une maladie dévastatrice et excessivement résistante aux thérapies actuelles sur laquelle nos connaissances sont très limitées. Un des événements génétiques initiateurs de la maladie, qui est également le plus fréquemment observé, est une mutation qui encode une forme constitutivement active de BRAF-V600E ($BRAF^{V600E}$), ce qui mène à une activation soutenue de la voie MAP kinase BRAF-MEK-ERK. $BRAF^{V600E}$ est détecté dans 85% des naevus et environ 65% des mélanomes métastatiques. On considère que la perte d'au moins un gène suppresseur de tumeur, par exemple *PTEN*, est nécessaire pour la progression d'un naevus à un mélanome. Nous avons précédemment démontré que l'activation de $BRAF^{V600E}$ couplée avec une perte d'expression de *PTEN* menait à l'apparition de lésions mélanocytiques hautement pigmentées avec certaines caractéristiques histologiques du mélanome. Par contre, les tumeurs humaines ne subissent pas de telles mutations de façon simultanée. Ainsi, pour étudier la progression du mélanome *in vivo*, nous allons initier l'expression de $BRAF^{V600E}$ et l'ablation de l'expression de *PTEN* de façon indépendante avec les recombinases Flp et Cre respectivement. Nous avons précédemment généré une souris portant un allèle de $BRAF^{V600E}$ activé par Flp ("Flp-activated", $BRAF^{FA}$) qui exprime une version normale de *BRAF* au préalable et $BRAF^{V600E}$ après la recombinaison par la Flp. Nous avons également un allèle de *PTEN* qui est inactivé suite à la recombinaison par la recombinase Cre.

Pour séparer l'activation de $BRAF^{V600E}$ et l'ablation de *PTEN in vivo*, j'ai tenté de générer une souris transgénique exprimant des formes inductibles des recombinases Cre et Flp spécifique aux mélanocytes (pTyr:CreER et pTyr:FlpPR). Les deux constructions ont été co-intégrées dans le génome de zygotes C57BL/6, ce qui a généré cinq lignées fondatrices. L'analyse *in vitro* a démontré que l'expression des constructions était spécifique aux mélanocytes et que l'induction des recombinases ainsi que leur spécificité pour les sites de recombinaison étaient appropriées. Par contre, l'expression ou l'activité de l'une ou l'autre des recombinases n'a été détectée dans aucune des cinq lignées *Tyr:FC*.

La cause derrière cette absence d'expression reste inconnue mais elle est probablement attribuable à la technique de co-injection, le nombre limité de lignées fondatrices ou des défauts dans les constructions pTyr.

Acknowledgements

I would first and foremost like to thank my supervisor Dr. Dankort for his continual guidance, optimism, and support. I have learned a great deal from his wealth of knowledge and research skills. Also, I would like to thank all the current and former Dankort lab members, specifically Rosalie McDonough, Guillaume Vandal, and Benjamin Geiling for their insightful conversations when troubleshooting problems that arose and for their assistance with experimental matters. Also, thank you to Guillaume for translating my abstract into French and Danielle Tenen for helping with tedious experimental analyses. Benjamin, Guillaume, and Kendall Dutchak also read portions of my thesis, providing insightful suggestions. All lab members have contributed to a cooperative and friendly working environment, providing a great place to work and study and making my time at McGill an amazing experience.

I would also like to thank the Moon lab for the use of their microscope and imaging equipment, without which documenting my results would not have been possible. Also, thank you to Alana Nguyen from the Bouchard lab for providing a working X-gal staining protocol that contributed significantly to my ability to analyze my experimental mouse strains.

And from McGill, I would like to thank the biology department for giving me the opportunity to study at this institution and my committee members Dr. Nilson and Dr. Muller. Also, thank you to the Animal Resource Center for ensuring the health and safety of the mice. Lastly, I would like to thank my family and friends for their support and encouragement throughout this process.

Table of Contents

List of Used Abbreviations

4-HT	4-hydroxytamoxifen
AP	alkaline phosphatase
ARF	p14, alternate reading frame
Avertin	2,2,2,-tribromoethanol
BAC	bacterial artificial chromosome
BRAF^{CA}	Cre-activated BRAF^{V600E} allele
BRAF^{FA}	Flp-activated BRAF^{V600E} allele
CAT	chloramphenicol acetyltransferase
CDK4	cyclin-dependent kinase 4
CDKN2A	cyclin-dependent kinase inhibitor 2A
CR	conserved region
CRD	cysteine-rich domain
DDR	DNA damage response
DOPA	dihydroxyphenylalanine
FAK	focal adhesion kinase
FAMM	familial atypical mole melanoma
HS site	DNAase I hypersensitive site
INK4A	p16, inhibitor of kinase 4A
IRES	internal ribosomal entry site
IVS	intervening sequence
LBD	ligand binding domain
MAPK	mitogen-activated protein kinase
MAR	matrix attachment region
MC1R	melanocortin-1-receptor
MDM2	murine double minute 2
MITF	microphthalmia-associated transcription factor
OIS	oncogene-induced senescence
PDK	phosphoinositide-dependent protein kinase
PI3K	phosphatidylinositol 3'kinase
PIP_3	phosphatidylinositol 3,4,5-triphosphate
PolyA	polyadenylation
RBD	RAS binding domain
RGP	radial growth phase
ROS	reactive oxygen species
RPE	retinal pigmented epithelium
RT	reverse transcriptase
SAHF	senescence-associated heterochromatin foci
SASP	senescence-associated secretory phenotype
SA-β-gal	senescence-associated beta-galactasidase
SMS	senescence-messaging secretome
SSM	superficial spreading melanoma
SV40	simian virus 40
TSG	tumor suppressor gene
VGP	vertical growth phase
X-gal	5-bromo-4-chloro-3-indolyl-β-galactopyranoside
YAC	yeast artificial chromosome
α-MSH	alpha-melanocyte stimulating hormone
β-gal	beta-galactasidase

1. Introduction to Melanoma

Melanoma is the most deadly form of skin cancer, accounting for 80% of all skin cancer related deaths[1]. In 2010 it was reported that the lifetime risk for developing melanoma for Caucasians is 1 in 37 for males and 1 in 56 for females[2]. The most common form of skin cancer is superficial spreading melanoma (SSM) accounting for 70% of all melanoma cases[3]. SSM occurs on intermittently UV-exposed skin and is commonly found in individuals with fair skin. The greatest risks for SSM development are a genetic pre-disposition, intermittent sun exposure, severe childhood burns, and an abundance of melanocytic nevi (commonly known as moles)[4,5].

The exact mechanism leading to melanoma development still remains unknown; however, the theory that tumor formation is the result of multiple genetic disruptions over time is widely accepted[6,7]. It is thought that in most cases melanoma begins with the formation of a nevus, a benign precursor. A melanocyte gains heightened proliferative capacity, likely due to an activating mutation in an oncogene, and undergoes a number of replications before entering a growth arrested state[8]. These lesions can remain benign for decades whereby most of them will not progress to melanoma. However, at some time point after nevus formation a cell may reacquire proliferative capacity, most likely due to additional genetic alterations or disruptions. Once the cell begins to proliferate again, an *in situ* lesion forms where the cells grow outwards within the plane of the epidermis. At this point, the disease is in the radial growth phase (RGP) and may remain at this stage for 1-5 years[3]. If caught during the RGP, the disease can most often be cured through surgery. If left to progress, the cells may enter the vertical growth phase (VGF) where they gain the capacity to break through the basement membrane. Once the basement membrane has been breached, the cells can invade other areas of the body and take up residence in secondary organs, most often the skin, lungs, liver, and brain[9]. Although this description outlines the typical progression of melanoma development, there are many variations to how a single cell may lead to melanoma development. For example, melanoma may

develop without an initial visible benign lesion. In another mechanism, a lesion progresses directly from a benign nevus to the VGP, bypassing the RGP. In any case, once the disease has reached the metastatic phase, there are few treatment options available as seen by the median survival of 6 months and a 5 year survival rate for less than 10% of patients[1].

Melanomas are known for their chemo- and radiotherapy resistance making these cancers notoriously difficult to treat. Dacarbazine, a methylating agent, is the most widely used therapy for the treatment of metastatic melanoma. Previous clinical trials have determined that dacarbazine confers a 5.6-7.8 month median survival rate and 7-12% average response rate, as determined by tumor shrinkage, demonstrating the difficulty of treating advanced stage melanoma[10-13]. Despite research being focused heavily on discovering new therapies, there has been little improvement over the last few decades until recently, with most treatments outright failing or with patients relapsing quickly after treatment[3]. Despite these clinical failures, there have been two new radically different therapies approved by the FDA within the last year. These two drugs function through two very different approaches: ipilimumab, is an immune system modulator, which functions in a cell autonomous fashion, while vemurafenib, (PLX4032, marketed as Zelboraf by Hoffman-La Roche Inc), is a small molecule inhibitor targeting a specific activating mutation in the BRAF kinase ($BRAF^{V600E}$) frequently found in melanoma[14]. Phase 2 clinical trials testing vemurafenib yielded a median response duration of 6.7 months. The phase 3 clinical trial compared the efficacy of vemurafenib to dacarbazine in a randomized trial of 675 patients harbouring *BRAF* mutations at codon 600. Interim results analyzed at 6 months post-treatment initiation demonstrated response rates of 48% and 5%, and overall survival rates of 84% and 64% for vemurafenib and dacarbazine respectively[15]. Due to the unprecedented response rates of the phase 2 and 3 trials, the drug was approved before phase 3 was completed. Vemurafenib now represents the most effective treatment option available, as well as the first melanoma tumor specific therapy.

Despite the apparent success of vemurafenib and other $BRAF^{V600E}$ tumor expressing inhibitors, almost all patients relapse. Unlike relapses seen in Gleevec-treated CML patients, acquired resistance to vemurafenib is not due to subsequent mutations in the BRAF kinase, but rather due to a variety of mechanisms, not all of which have been identified[16-20]. Analysis of human tumor biopsies before and after treatment has led to the identification of potential candidates conferring this acquired resistance. Three genetic alterations discovered in this manner function to restore heightened mitogen-activated protein kinase (MAPK) activity: oncogenic mutation in NRAS found upstream of RAF[18]; oncogenic mutation in MEK found downstream of RAF[20]; and an upregulation in COT, a MAPK agonist that activates ERK in a MEK-dependent manner[16]. Other alterations, such as the upregulation of the receptor tyrosine kinase beta-type platelet-derived growth factor receptor (PDGFRβ), conferred resistance in a MAPK-independent manner[18]. *In vitro* analysis has also been useful at identifying potential resistance conferring candidates. Two alterations identified in this manner are the upregulation of CRAF[16,17], a different RAF protein capable of restoring heightened MAPK activity, and the upregulation of the insulin-like growth factor 1 receptor (IGF-1R) which can signal through both the MAPK and phosphatidylinositol 3'kinase (PI3K) pathways[19]. Additional cooperating genetic events are continuing to be identified. Identification of these events may provide insight into alternative targets that are viable points of therapeutic intervention.

Development of effective treatment options could be assisted by a more thorough understanding of the physiological processes and aberrations underlying malignant conversion. To this end, we have previously generated a mouse model that allows for the concomitant expression of $BRAF^{V600E}$, an activating mutation of the BRAF kinase commonly found in nevi and metastatic melanoma, and silencing of the *PTEN* tumor suppressor (where *PTEN* silencing refers to the elimination of the PTEN phosphatase domains through the deletion of exons 4 and 5), commonly found lost in late stage melanomas[21]. Induction of both mutations results in the rapid formation of highly metastatic melanoma. A better understanding of the cooperation of these two genetic alterations in

melanomagenesis could be achieved through the use of a model allowing for independent control of these two mutations. Such a model would allow for the assessment of different stages within tumor development that may have varying degrees of susceptibility to therapeutic intervention.

1.1 Melanoma genetics

1.1.1 Familial melanoma

Melanoma can arise due to a genetic predisposition (familial melanoma), somatic mutations (sporadic melanoma), or a combination of both. Two highly penetrant cancer susceptibility loci, cyclin-dependent kinase inhibitor 2A (*CDKN2A)* and cyclin-dependent kinase 4 (*CDK4)*, are commonly associated with familial atypical mole melanoma (FAMM) syndrome[5,22,23]. FAMM is characterized by a genetic predisposition to cutaneous melanoma, commonly with at least one affected family member and an abundance (> 50) of atypical nevi displaying architectural disorder and nuclear atypia[5,23]. Up to 40% of familial melanomas have mutations affecting the *CDKN2A* locus[3]. This locus is unique in the mammalian genome because it encodes two different proteins ($p16^{INK4A}$ and $p14^{ARF}$ or $p19^{ARF}$ in mice, referred to as INK4A and ARF respectively)[24]. INK4A is named for its role as the inhibitor of kinase 4A and ARF after its discovery as the product of translating an alternate reading frame of the *CDKN2A* locus. INK4A and ARF each have unique first exons (1α and 1β respectively), but share exon 2[25].The generation of two proteins by translating alternate reading frames of the shared exon generates two completely different proteins with unique protein sequences[25]. INK4A and ARF are tumor suppressors that indirectly block cell cycle progression upon aberrant or oncogenic stimuli, with ARF acting through the p53 pathway and INK4A acting through the pRB pathway[26]. In a normal cell, p53's activity is maintained at a basal level through the action of its negative regulator, the E3 ubiquitin ligase murine double minute 2 (MDM2)[27]. Following DNA damage, p53 accumulates and induces a cell cycle arrest to allow the damage to be repaired or to activate an apoptotic program[28,29]. This accumulation of p53 is mediated by ARF's association with MDM2, which prevents it from

targeting p53 for degradation[26,30,31]. INK4A inhibits CDK4 activation by binding CDK4 and preventing its association with cyclin D, thereby preventing the phosphorylation and inactivation of pRB[32]. Hypophosphorylated pRB binds E2F transcription factors, preventing them from directing the expression of genes necessary for progression through the cell cycle G1/S checkpoint[33]. Loss of INK4A therefore results in progression through this checkpoint. Further evidence supporting the importance of the CDK4/INK4A interaction comes from the analysis of a rare CDK4 mutation, a missense mutation at codon 24 (R24C), that fails to bind INK4A also resulting in progression through the cell cycle[34].

In familial melanoma, germline disruption of the *CDKN2A* locus most often occurs by point mutation, followed by loss of heterozygosity in tumors[35]. These mutations are commonly found in exon 2 or 1α, thus disrupting the function of either both proteins, or just INK4A[36]. Mutations affecting only exon 1β have been identified[37,38], but are not as common as the first two suggesting a greater importance of INK4A in suppressing melanoma development. Furthermore, the high frequency of *CDKN2A* mutations may explain why p53 and pRB mutations are relatively rare in melanoma[30,39]. One theory is that melanoma formation requires disruption in both the p53 and pRB pathways, thus mutations in the single *CDKN2A* locus, affecting two tumor suppressors simultaneously achieves this more easily than disruptions of two independent gene loci[24].

A third weakly penetrant gene is the melancortin-1-receptor (*MC1R)* gene encoding the receptor that binds alpha-melanocyte stimulating hormone (α-MSH) released by keratinocytes following UVB irradiation[3,40,41]. Upon stimulation, melanocytes produce melanin in specialized organelles called melanosomes that are transported within melanocytic dendrites and deposited directly into keratinocytes. Within keratinocytes, melanin becomes localized to the apical surface of the nucleus thereby shielding the DNA from incoming UV, and thus preventing UV-induced DNA damage[40]. MC1R stimulation leads to INK4A upregulation, MAPK pathway activation and microphthalmia-associated transcription factor (MITF) expression, among other responses[42-44]. There are up to 30 allelic variations of *MC1R*[45], all of which convey varying degrees of

melanoma susceptibility due to their varying abilities to respond to α-MSH and induce a protective response against the damaging UV radiation. Three variants in particular give rise to a red hair, fair skin, freckled phenotype and are commonly associated with increased melanoma susceptibility due to an impaired ability to bind α-MSH[46].

1.1.2 Sporadic melanoma

Despite a clear familial component, over 90% of melanomas are sporadic, appearing to result from mutations within a few key pathways[3,5,47]. The *CDKN2A* locus is mutated in up to 50% of sporadic melanomas[24]. In contrast to familial melanoma where point mutation is the predominant cause of INK4A and ARF functional impairment, large genomic deletions of the *CDKN2A* locus are observed in sporadic melanoma[48]. Another gene commonly mutated in melanoma is *c-KIT*[49]. This receptor tyrosine kinase, encoded by the mouse *White spotting (W)* locus, plays an important role in melanocyte development, migration and survival[50,51]. *c-KIT* activating mutations or gene duplications have been found in different types of melanomas, such as cutaneous melanomas on chronically UV-exposed skin (28%) and acral and mucous membrane melanomas (up to 39%)[49]. The exact role c-KIT plays in tumor formation is still largely unknown; however, it is found upstream of RAS activation, and therefore likely contributes to the upregulation of RAS activated signalling cascades such as the MAPK and PI3K/AKT pathways[51]. In fact, members of these two pathways are frequently mutated in melanomas on intermittently sun exposed skin, commonly resulting in SSM. Both of these pathways are discussed in detail below.

1.1.3 The MAPK signalling pathway

MAPK pathway activation results in physiological responses such as cell growth, proliferation, and differentiation. The membrane bound monomeric GTPase RAS is activated following stimulation by extracellular growth factors such as fibroblast growth factor and hepatocyte growth factor[52,53]. There are three *RAS* genes: *NRAS*, *KRAS*, and *HRAS*. Protein products from all three loci are capable of activating downstream effectors[54]. Activated RAS recruits and

activates effector proteins, including the RAF serine/threonine kinase, the initiating kinase of the RAF-MEK1/2-ERK1/2 MAPK cascade[55]. Activated ERK regulates the activity of cytoplasmic and nuclear proteins including those regulating cell migration and metabolism, as well as transcription factors regulating the expression of genes regulating cell growth and differentiation[56].

1.1.4 Activation of BRAF by RAS

There are three *RAF* genes: *A-, B-,* and *C- RAF*[57]. *CRAF* was the first *RAF* gene cloned and is therefore sometimes referred to as *RAF-1*[58]. However, *BRAF* appears to have the highest level of sequence conservation with invertebrates, such as *Drosophila melanogaster* and *Caenorhabditis elegans* and is therefore most likely the ancestral form[59]. RAF proteins have three conserved regions: conserved region 1 (CR1) and CR2 are regulatory domains and CR3 contains the kinase domain (Fig. 1-1). The kinase domain contains a negatively charged regulatory region (N-region), a glycine-rich loop, and the activation segment (containing the catalytic domain)[59]. Within CR1 are the RAS binding domain (RBD) and the cysteine-rich domain (CRD), both of which are responsible for RAF's association with RAS. Irrespective of its GTP-bound state, RAS associates loosely with the CRD of RAF proteins; however, RAS only binds the RBD upon activation. Through these domains RAS recruits RAF to the membrane and induces conformational changes within the RAF proteins facilitating its subsequent activation by kinases[57]. RAF activation requires phosphorylation at key sites within its activation domain (Fig. 1-1). RAF proteins are phosphorylated on residues within their activation segment: T^{452} and T^{455} for ARAF, T^{599} and S^{602} for BRAF, and T^{491} and S^{494} for CRAF[57]. Also, within the N-region of CR3, RAF proteins have SSYY motifs that are phosphorylated by a second kinase, most likely Src, prior to activation: S^{298}SYY for ARAF and S^{338}SYY for CRAF[60]. For full activity, ARAF and CRAF must be phosphorylated on the first serine and last tyrosine of the motif. In contrast, the corresponding BRAF motif (S^{446}SDD) is constitutively phosphorylated at S^{446}. Furthermore, aspartic acid residues replace tyrosine residues and are phosphomimetic (Fig. 1-1)[57,61]. The difference in activation requirements (phosphorylation of 4 sites in ARAF and CRAF, but only

2 in BRAF) could explain why BRAF has a higher basal level activity[8] and why it is more commonly found de-regulated in cancers[57].

1.1.5 Mutations of the MAPK pathway in melanoma

Increased MAPK signalling is found in many cancers, including melanoma. Of the three *RAS* genes, *NRAS* is the most commonly mutated gene in melanoma; both in primary tumors (33%) and metastases (26%)[62]. As part of the Cancer Genome Project in 2002, The Wellcome Trust Sanger Institute identified 14 different mutations of the *BRAF* locus commonly found in cancer cell lines and tumor samples[63]. One mutation, a *T1799A* missense mutation encoding an amino acid substitution of valine for glutamic acid at codon 600, $BRAF^{V600E}$, accounts for 80% of all *BRAF* mutations in cancer, 92% of *BRAF* mutations in melanoma, and is found in ~65% of metastatic melanomas[63]. Codon 600, located on exon 15 is between the two key BRAF phosphorylation sites (T^{599} and S^{602})[63]. The V600E amino acid substitution de-stabilizes the inactive form of the protein, rendering the kinase constitutively active resulting in continuous MAPK signalling[64]. $BRAF^{V600E}$ has a 500-fold increased basal level BRAF activity relative to the wild type protein[64]. This mutation occurs somatically, consistent with the observation of early embryonic lethality in mice ubiquitously expressing $BRAF^{V600E}$ *in utero*[65]. Given congenital nevi are known to harbour the $BRAF^{V600E}$ mutation[66], mutation must occur at some point late in development or after birth. The exact mechanism of how this mutation is induced is unclear. Given $BRAF^{V600E}$ is commonly found in lesions on intermittently sun-exposed skin, the T→A transversion is uncharacteristic of UV-induced mutations, commonly found as C→T or CC→TT mutations[67]. Furthermore, the mutation is detected at high frequency in thyroid[68], colorectal[69], and ovarian cancers[70], all of which are not exposed to UV radiation. Thus, the source of *BRAF-T1799A* mutation must not be UV radiation, at least not directly. While *NRAS* and *BRAF* are both frequently in melanoma, these mutations are thus far mutually exclusive[63,71,72]. Given that RAS and BRAF are within the same linear pathway, *BRAF* mutations are unnecessary in the presence of an already heightened MAPK signalling due to activated RAS. In fact, activating mutations in both *RAS* and *BRAF* within the same cell could lead to

superactivation of the MAPK pathway and would likely lead to a protective response, such as senescence or cell death, rather than cell proliferation or growth[6].

1.1.6 $BRAF^{V600E}$-induced senescence

$BRAF^{V600E}$ is found in ~85% of nevi, lesions that are thought to be benign precursors to melanoma[71]. The drastic increase in basal level activity of $BRAF^{V600E}$ leads to an initial increase in cell proliferation causing the formation of a melanocytic lesion that at some point later is followed by the induction of a senescent-like state[8], forming a nevus. Senescence was first observed in primary human fibroblasts where the cells were able to replicate a certain number of times before entering a growth arrest[73,74], later attributed to telomere attrition[75]. Each time a cell replicates, its telomeres shorten slightly due to the inability of DNA polymerase to completely replicate the lagging strand. Once the telomeres have reached a certain minimal length, the telomere ends are sensed as double stranded DNA breaks and trigger a DNA damage response (DDR), resulting in accumulation and activation of p53[76]. These cells remain metabolically active but become unresponsive to mitogenic stimuli[77]; these cells have entered a state of replicative senescence. More recently, it has been demonstrated that oncogene over-expression can rapidly induce a growth arrest resembling replicative senescence, in the absence of telomere attrition. This tumor suppressive growth arrest was termed oncogene-induced senescence (OIS)[78]. It had long been known that "oncogenic" RAS (most often $HRAS^{V12}$) was insufficient to transform primary human or rodent fibroblasts unless the cells were initially immortalized by carcinogens[79] or coupled with the co-expression of what were then called "nuclear oncogenes" (v-Myc[80] or Adenoviral E1a[81], to target pRB-family members). Indeed when Lowe's group expressed $HRAS^{V12}$ in primary fibroblasts the cells entered a stable cell cycle arrest with characteristics similar to those for replicative senescence[78]. When $HRAS^{V12}$ expression is coupled with loss of p53 or INK4A in rodent cells or expression of Adenoviral E1A in human cells, senescence is by-passed[78]. Serrano and Lowe hypothesized that this OIS is a tumor suppressive mechanism protecting the host from aberrant proliferative

signals[78]. Subsequent to this, two groups determined that RAS-induced OIS was due to aberrant RAS-MAPK signalling[82,83]. The first *in vivo* evidence of OIS resulting from upregulated MAPK signaling comes from the study of melanocytic nevi: benign lesions that often harbor *BRAF-T1799A* mutations. Human $BRAF^{V600E}$ containing nevi stain positive for senescent markers[8]. Indeed human nevi contain many hallmarks of senescent cells (as described below), importantly the absence of cells undergoing proliferation, INK4A upregulation, and senescence associated beta-galactasidase (SA-β-gal) activity[8].

1.1.7 Oncogene-induced senescence

Within the last decade, the knowledge surrounding OIS has grown immensely. It has become apparent that no set criteria can be used to identify a senescent cell because the exact mechanism of senescence induction can vary widely between cells depending on factors such as the oncogene being over-expressed, the tumor suppressors expressed, and the cell type among others. There are no unique senescence markers and therefore it is necessary to analyze the cells for multiple senescence-associated markers in order to differentiate senescent cells from quiescent or terminally differentiated cells. The strictest criteria is the inability of cells to divide, specifically that cells are senescent if they have entered an irreversible growth arrest. Also, the morphology of cultured senescent cells will differ from actively dividing and quiescent cells: in general, senescent cells are flatter, larger and contain larger nuclei than their non-senescent counter parts[84]. Another characteristic is the production of reactive oxygen species (ROS), which are produced in response to MAPK signaling[85]. Heightened MAPK signaling (which commonly results in senescence induction) therefore results in increased levels of ROS[86], causing DNA damage resulting in a DDR. DDR are visible through the production of DNA damage foci, commonly present in senescent cells[77]. The most commonly used senescence marker is the expression of SA-β-gal activity. β-gal activity is detectable in senescent fibroblasts and keratinocytes *in vitro*, but not in actively growing, pre-senescent, quiescent, or terminally differentiated cells[87]. The increased lysosomal content of senescent cells allows for detection of residual lysosomal β-gal expression at a sub-optimal

pH[88]. Interestingly, while the presence of SA-β-gal activity is commonly used to identify senescent cells, the role of this enzyme, if any, in senescence induction and/or maintenance has yet to be identified. Furthermore, in most cases senescence induction appears to require activation of either the p53 or INK4A-pRB tumor suppressor pathways, or a combination of both[89]. As such, the upregulation of components of these pathways (such as INK4A, ARF, p53, and p21) are commonly used as senescence markers[90]. An upregulated INK4A maintains pRB in the hypophosphorylated state, indirectly suppressing the expression of cell cycle progression E2F target genes[32]. These genes may also be silenced through the pRB-dependent global rearrangement of chromatin generating senescence associated heterochromatin foci (SAHFs)[91]. SAHFs are small highly condensed chromatin regions that commonly contain modified histones such as lysine 9 methylation of histone 3. SAHFs can be found in regions of the genome where they induce a stable repression of genes necessary for progression through the cell cycle, contributing to an irreversible growth arrest[91]. The p53 tumor suppressive pathway is activated in response to cellular stresses such as DNA damage and oncogenic signaling (oncogenic stress)[29]. Abberant mitogenic signals induce ARF expression resulting in p53 accumulation due to ARF's binding with MDM2, inhibiting MDM2's association with p53[30,31]. Once active, p53 transcriptionally activates p21, a key regulator of p53 senescence that prevents cell cycle progression by inhibiting cyclin-dependent kinases[92]. Although these two pathways appear to play an important role in senescence induction, they are not uniquely responsible for this cellular response. This highlights gaps in our understanding of OIS and the need to identify the other mechanisms controlling the induction of senescence in response to oncogenic stress.

There are some cellular processes underlying OIS that are just beginning to be revealed. The senescence associated secretory phenotype (SASP) and the senescence-messaging secretome (SMS) refer to the mixture of chemokines and cytokines released by cells undergoing oncogenic stress. These signals alter gene expression within the cell, as well as modify the microenvironment of the extracellular matrix and provide stimulation to the surrounding cells[89,93]. SASPs

can play a pivotal role in OIS induction and maintenance. For example interleukin 6 (IL-6) and IL-8 are required for the induction and maintenance of $BRAF^{V600E}$-induced senescence *in vitro*[94]. IL-6 and IL-8 have a cell autonomous role in OIS induction and maintenance, while at the same time act as a paracrine signal for cell proliferation. Furthermore, components of the inflammatory network are upregulated in response to IL-6 and IL-8 activity[94]. Inflammatory factors induce pro-oncogenic responses such as proliferation and migration. Further studies are required to determine exactly how these interleukins or how specific SASPs and SMSs are able to control senescence induction, maintenance, and eventual escape allowing for progression to metastatic disease, while at the same time providing proliferation signals to the neighboring cells. In any case, all studies that have observed $BRAF^{V600E}$-induced senescence have seen a concomitant loss of a tumor suppressive component prior to disease progression indicating the need for additional genetic disruptions on the path to melanoma development.

The mechanism of OIS escape due to loss of a tumor suppressor gene (TSG) that plays a role in OIS induction and maintenance, such as INK4A and ARF, may be more easily hypothesized than those with an unknown involvement in OIS. The *CDKN2A* locus is not found functionally ablated in all tumors, leading to the need to identify roles of other tumor suppressors in this process. More specifically, what other tumor suppressors may be involved in malignant conversion and by which cellular processes following TSG loss.

1.1.8 The PI3K/AKT signaling pathway in melanoma

Another pathway commonly mutated in melanoma is the PI3K/AKT pathway. PI3K is a heterodimeric membrane bound lipid kinase that, like BRAF, can be activated by RAS[95]. PI3K phosphorylates membrane lipids such as phosphatidylinositol 4,5-bisphosphate (PIP_2) at the number 3 position, forming phosphatidylinositol 3,4,5-trisphosphate (PIP_3)[96]. PIP_3 recruits proteins such as the serine/threonine kinase AKT (also known as Protein Kinase B, PKB) and phosphoinositide-dependent protein kinase (PDK)1 to the membrane[96,97]. Once in close proximity, AKT is activated by phosphorylation at Thr308 and Ser473 by

PDK1 and an uncharacterized PDK2 respectively[98,99]. Activated AKT regulates downstream players involved in cellular functions such as cell growth and proliferation (GSK3β, p27, p21) and cell survival and apoptosis (NF-κB, PRAS40, BAD)[100-103]. There are 3 AKT proteins: AKT1, AKT2, and AKT3. Heightened AKT3 activity is detected in 43-60% of melanomas[104]. Due to AKT3's location within the PI3K/AKT pathway, this upregulated activity can be the result of multiple upstream genetic changes. Firstly, upregulated RAS or PI3K result in increased AKT activation. As previously mentioned, *NRAS* is commonly mutated in melanoma resulting in increased PI3K signaling. Conversely, while PI3K is upregulated in a variety of cancers, such as colon and prostate cancers[105], it is only over-expressed in about 3% of melanoma[106], and therefore does not contribute significantly to the increased AKT activity in melanoma. Lastly, heightened AKT activity commonly occurs due to a functional loss of the PI3K antagonist phosphatase and tensin homologue found on chromosome ten (*PTEN*, also called *MMAC1* and *TEP1* due to the simultaneous identification of the locus by three different groups[107-109]), which is functionally ablated in up to 60% of melanomas[110].

1.1.9 PTEN's role as a tumor suppressor

PTEN is a tumor suppressor protein that is most well known for its role as a PI3K antagonist. PTEN is composed of an N-terminal catalytic region that contains both protein and lipid phosphatase domains, and a C-terminal region responsible for binding lipids as well as being important for the protein's stability[111]. Thus far, the majority of PTEN's tumor suppressive role has been attributed to its lipid phosphatase domain. PTEN is a negative regulator of the PI3K/AKT pathway where it removes the number 3 phosphate on PIP_3 added by PI3K[112], inhibiting the activation of AKT. Naturally occurring PTEN mutants harboring a G129E point mutation within the lipid phosphatase domain lose the ability to inhibit cell cycle progression in a *PTEN* null renal carcinoma cell line, demonstrating the important role of this domain[113]. Germline *PTEN* mutations, such as C124R in exon 5, underlie the development of three autosomal dominant diseases that are characterized by increased susceptibility to malignant tumors:

Cowden disease, Bannayan-Zonana syndrome, and Lhermitte-Duclos disease[114-116]. With this in mind, 20-30% of the genetic alterations of the *PTEN* locus affect exon 5, the location of the lipid phosphatase domain[117]. Loss of PTEN activity is also commonly achieved through genetic alterations affecting the entire gene, such as promoter methylation, chromosomal deletions, or frameshift mutations[118,119]. Similar to $BRAF^{V600E}$, homozygous *PTEN* deletion *in utero* results in embryonic lethality, demonstrating that *PTEN* loss in tumors is the result of somatic genetic alterations[120].

Although PTEN's tumor suppressive role has mostly been attributed to its lipid phosphatase domain, the importance of other domains within the protein are being acknowledged for their participation in tumor suppression. For example, the focal adhesion kinase (FAK) is a PTEN protein target. PTEN dephosphorylation of FAK is important for inhibiting cell migration and invasion[121]. Also, protein-protein interactions of PTEN with other tumor suppressors, such as p53, are modulated through PTEN's C-terminus[122]. PTEN directly associates with p53 in the nucleus, increasing p53's stability and its transcriptional activity by modulating p53's DNA binding capacity[122]. With this in mind, PTEN loss can result in instability of p53 function, potentially disrupting p53's tumor suppressive and senescence induction roles within the cell.

1.1.10 The cooperation of $BRAF^{V600E}$ activation and *PTEN* loss in melanoma

PTEN loss is more often associated with melanoma progression rather than initiation as reflected by the loss of PTEN activity in 63% of melanomas and only 8% of benign nevi[110]. It is thought that part of the pro-tumorigenic effect of PTEN loss is upregulated AKT3 activity. AKT3 activity is relatively absent in nevi, whereas increasing levels of activated AKT3 are correlated with malignant progression with elevated levels of active AKT3 in up to 77% of metastatic melanomas[123]. Increasing levels of AKT3 activity correspond closely with the trend of PTEN loss. Similar to the relationship between *NRAS* and *BRAF*, mutations in *NRAS* and *PTEN* are mutually exclusive[124]. Both PI3K/AKT and MAPK pathways are activated downstream of RAS and therefore *RAS* activating

mutations result in heightened activity of both pathways, rendering *BRAF* and *PTEN* mutations unnecessary and potentially detrimental to the cell. Subsequent mutations in either of these genes could promote superactivation of their respective pathways, potentially resulting in senescence induction or cell death. Interestingly, *PTEN* is functionally silent in about 20% of $BRAF^{V600E}$ expressing late stage melanomas[72]. These data suggest that *BRAF* activating mutations and PTEN loss may cooperate to cause metastatic melanoma. The mechanism underlying this cooperation has yet to be uncovered.

1.2 Transgenic mouse models using tyrosinase regulatory regions

Mouse models can be used for dissecting genetic interactions between different proteins in disease development. Regulatory regions of genes uniquely expressed in melanocytes can be used to express cDNAs of interest in a melanocyte-specific manner. In melanoma studies, the regulatory regions of the tyrosinase gene are often found directing the expression of genes to be analyzed.

1.2.1 Dissecting the tyrosinase locus

Tyrosinase (EC 1.14.18.1) is located at the *c*-locus on mouse chromosome 7 spanning 80kb and encodes 5 exons[125,126]. Tyrosinase is a key enzyme in melanin synthesis responsible for catalyzing the first two biochemical steps: the hydroxylation of tyrosine to dihydroxyphenylalanine (DOPA) and the subsequent oxidation of DOPA to dopaquinone, which is finally converted into eumelanin or phoemelanin[127]. These reactions mainly occur in cell types of two distinct cell lineages: the neural crest-derived melanocytes found in the skin, hair follicles, choroid, and iris and in the optic cup-derived retinal pigmented epithelium (RPE). Tyrosinase expression is first detected in the RPE at embryonic day 10.5 (E10.5) and in melanocytes of the hair follicle at E16.5[128]. Expression in the migrating melanoblasts, melanocyte precursor cells, has been detected as early as E10.5 but is more pronounced by E12.5[129]. Despite the different lineages, the tyrosinase expressed in both cases is from the same gene locus. This differential expression in two different cell types leads to questions of how tyrosinase expression is

regulated and what drives expression in the two cell lineages. A summary of the below described regulatory regions is found in Figure 1-2.

1.2.1a The minimal tyrosinase promoter

As an initial step in understanding the regulatory regions directing melanocyte-specific expression, the minimal region of the tyrosinase promoter was identified. A 5' deletion series generating promoter fragments (6.1kb, 3.7kb, 0.27kb, and 0.08kb) were tested for their ability to direct melanocyte-specific expression of a chloramphenicol acetyltransferase (CAT) reporter *in vitro*[130]. The expression level was relatively uniform for the three largest fragments, but decreased significantly when driven by the 80bp promoter fragment identifying 270bp of the 5' flanking sequence as sufficient to direct, albeit weak, tyrosinase expression. Promoter fragments (270bp, 2.6kb, and 5.5kb) driving tyrosinase expression were successful at rescuing the albino phenotype *in vivo* and directed expression in both neural crest and optic cell-derived cell lineages[128,130-133]. The albino phenotype is a result of a point mutation within the tyrosinase gene that renders the enzyme inactive, and therefore impedes melanogenesis[134,135]. All promoter sizes directed relatively equal expression levels, but much lower than wild type levels and appear to be affected by integration position. An 11bp consensus sequence known as the M-box is located within the first 105bp of the promoter region and is conserved between the promoter regions of the mouse tyrosinase related protein-1 gene, another melanocyte-specific protein, and the human tyrosinase gene[136,137]. The M-box contains a CANNTG consensus sequence known as an E-box that is characteristic of a recognition sequence for basic helix-loop-helix transcription factors, such as MITF, a transcription factor regulating tyrosinase expression[136-138]. Furthermore, while the M-box is necessary for melanocyte-specific expression, it is not sufficient on its own, indicating the need for additional regulatory elements[139].

1.2.1b The tyrosinase enhancer

When portions of the tyrosinase locus upstream (-17.6kb to -74.4kb) and downstream (+0.4kb to +95.8kb) regions were mutated, high levels of

melanocyte-specific expression was observed[125] leading to the conclusion that all the major regulatory regions are contained within the first 17.6kb sequence directly upstream of the transcription start site. In accordance with this, a DNAase I hypersensitive site (HS site) is located 15kb upstream of the transcription initiation site within a 200bp "core enhancer"[140,141]. DNAase I sites are strong indicators of regulatory regions as they signal areas of the chromatin that are less tightly packed, thus making themselves accessible to trans acting factors[142,143]. Two other groups identify this HS site and surrounding regions at -12kb[144,145]. I have compared the enhancer sequences to currently available genomic sequence and confirm that the site is found 15kb upstream of the transcription start site. The 200bp core enhancer also contains palindrome sequences and transcription factor binding sequences, such as Sox10 and activator protein-1 binding sequences, highlighting the importance of this region in regulating expression *in vivo*[144,146]. When fused to a tyrosinase promoter region (270bp), this core enhancer is sufficient to increase melanocyte-specific expression levels[144,146,147]; however, it additionally confers positional sensitivities to the construct[147]. Within 3.6kb spanning the core enhancer are matrix association regions (MARs)[140,141]. MARs function to insulate genes from the effects of the surrounding chromatin thus protecting transgenes from position effects and are most commonly found surrounding regulatory elements[148,149]. When this 3.6kb enhancer region was fused with portions of the tyrosinase promoter (2.5kb and 5.5kb), position-independent and copy number dependent expression levels were seen in most cases[141,144]. To better understand the difference in position effect between the 3.6kb enhancer region and the 200bp core enhancer, different regions of the 3.6kb enhancer were fused to the 2.5kb tyrosinase promoter[150]. When the 2.3kb 5' region of the enhancer was fused to 2.5kb of the promoter immediately upstream of the transcription start site, three results of interest were observed: the loss of enhanced expression in neural crest-derived cells, maintenance of position-independence, and increased expression in the RPE[150]. This leads to the conclusions that sequences in the 5' region of the 3.6kb enhancer contain the MARs and protect the transgene from position effects, and the remaining

sequences contain positive regulatory regions directing tyrosinase expression in neural crest-derived cells and potentially negative regulatory regions for the RPE. Furthermore, while a single study has observed increased expression levels in both neural crest and optic cup-derived cells using transgenes directing tyrosinase cDNA through the use of the 3.6kb enhancer and 5.5kb promoter[144], the majority of studies have seen increased expression levels in only the neural crest derivatives[140,141]. Camacho-Hubner and Beerman have observed not only an increase in neural crest-specific expression, but also repressed expression in the RPE[147]. Discrepancies of this sort, as in variation of tissue specificity for the same regulatory regions, is commonly observed throughout the above described mouse models, as well as those described below and summarized in Figure 1-2.

1.2.2 Transgenic mouse models containing tyrosinase regulatory regions

1.2.2a Mouse models directing Cre expression

The Cre/loxP system has become a useful tool that can be used in any cell type and any cellular environment. Cre is a P1 bacteriophage site specific recombinase that mediates recombination between two 34bp loxP sites[151]. Mice expressing Cre under the control of tyrosinase regulatory elements are capable of activating/inactivating genetically manipulated genes containing loxP sites in a melanocyte-specific manner. These transgenic mice can be used to circumvent the embryonic lethality of knocking out certain genes by allowing for the inactivation at a later time point in development. Tonks *et al.* developed a melanocyte-specific Cre expressing transgenic mouse line using a fusion of the 3.6kb enhancer region with the 270bp minimal promoter (*TEC* strain)[129]. To monitor functional Cre expression in developing tissues, the *TEC* mice were mated with *Z/AP* reporter mice. *Z/AP* mice express β-galactasidase (β-gal) prior to Cre-mediated recombination and alkaline phosphatase post-recombination[152]. Analysis of a *TEC* strain harbouring the *Z/AP* allele revealed Cre activity beginning at E10.5, becoming more pronounced by E12.5. At this time, Cre expression was observed in the melanoblasts of the skin, the precursor to melanocytes, and in some of the developing nerves. In adult mice, expression was not only seen in the melanocytes, but also in regions of the brain, neural tissue, and the RPE. In a

separate study using a similar transgene containing a larger portion of the tyrosinase promoter (2.5kb in place of the 270bp) to direct Cre expression, *Cre* RNA was detected in the cutaneous melanocytes and the brain and Cre activity in the skin as well as in other neural crest derivatives: the central nervous system and some peripheral nerves[153].

1.2.2b Mouse models directing inducible Cre expression

In order to obtain spatial and temporal control of Cre activity *in vivo*, transgenic mice expressing an inducible form of Cre were developed. A modified hormone binding domain of the estrogen receptor (ER^{T2}) was fused to the 3' end of the Cre recombinase to generate $CreER^{T2}$. $CreER^{T2}$ has 3 mutations (G400V/M543A/L544A) within the hormone binding domain that render this domain unresponsive to endogenous estrogen, yet susceptible to activation by estrogen analogues, such as 4-hydroxytamoxifen (4-HT)[154]**.** Prior to 4-HT administration, the estrogen binding domain is sequestered in the cytoplasm bound to heat shock protein 90 (HSP90)[155]. Upon 4-HT treatment, the estrogen binding domain is released from HSP90 allowing the recombinase to enter the nucleus where it mediates recombination between loxP sites[154,155]. Expression of *CreER^{T2}* cDNA was directed to cutaneous melanocytes using a fusion of the 3.6kb and 2.5kb tyrosinase enhancer and promoter sequences[156]. The ability to control Cre activity temporally and spatially was assessed through the use of *Rosa26^{tm1Sor}* Cre reporter mice ($R26^{Cre}$), which harbour the lacZ gene downstream of transcription stop sites flanked by loxP sites at the ubiquitously expressed *Rosa26* locus[157]. These mice express β-gal in cells that have undergone prior Cre-mediated recombination, and can therefore be identified through X-gal staining. Upon recombinase activation, β-gal activity was observed in regions of the hair bulge and melanocytes in adult mice or in the melanoblasts of developing embryos. Of interest was the absence of any activity in the brain, peripheral nerves or RPE. In a separate study, a similar transgenic line was generated: *Tyr:CreER^{T2}* [158]. Here, *CreER^{T2}* expression was directed by 9.1kb of tyrosinase regulatory elements (3.6kb enhancer and 5.5kb promoter). The *CreER^{T2}* cDNA was flanked by a rabbit β-globin intervening sequence (IVS, sequence containing

an intron) to the 5' end and a truncated SV40 polyadenylation sequence at the 3' end (Fig. 1-3A). When *Tyr:CreER*^{T2} mice harbouring the *R26*^{Cre} allele were treated topically with 4-HT within a week of birth, β-gal activity was detected in the cutaneous melanocytes of 2 week old mice (Fig. 1-3B). Similar results were obtained when mice 3-6 months old were treated systemically. In all described cases studied for this transgenic mouse, Cre activity was observed exclusively in the cutaneous melanocytes, identifying the suitability of this mouse model for use in studying melanocyte biology.

1.3 Mouse models of melanoma

Animal models are a useful tool for dissecting physiological processes *in vivo*. Genetic interactions commonly observed in human tumor samples can be tested *in vivo* using mouse models.

1.3.1 Transgenic melanoma mouse models

Transgenic mouse strains expressing the simian virus 40 (SV40) early region containing the small and large tumor antigens (T-antigens, disrupting both the pRB and p53 pathways[159] and promoting transformation through negative regulation of the protein phosphatase 2A family of phosphatases[160]), under the control of 2.5kb of the tyrosinase promoter (*Tyr:SV40E*) developed spontaneous melanomas, primarily the ocular type[161]. Melanoma susceptibility varied between transgenic strains. Cutaneous melanoma was rare, particularly in the strains demonstrating high melanoma susceptibility, likely due to early fatality attributed to the ocular melanoma and its associated metastases. When skin from the high susceptibility strains was grafted onto low susceptibility strains, cutaneous melanoma developed in 25-100% of the recipient strains, with variation depending on the donor strain's susceptibility[162]. Also, when the low susceptibility strains were treated with UV radiation, about 20% of the mice developed cutaneous melanoma with metastatic potential[163]. The *Tyr:SV40E* model demonstrates the ability to induce melanoma using an *in vivo* model. The utility of this model in discerning collaborating genetic disruptions is limited due to the wide range of cellular targets affected by the SV40 T-antigens. A model

that demonstrates the role of pathways frequently mutated in melanoma would give insight into cooperating events in melanomagenesis.

1.3.2 Modelling genetic interactions with the *CDKN2A* locus

The *CDKN2A* locus, encoding INK4A and ARF, is frequently mutated in melanoma (as described above). To understand INK4A's role in tumor development, a genetically engineered mouse model (GEMM) containing a germ-line knock out of the *CDKN2A* locus (*INK4A*$^{\Delta 2/3}$) was generated[164]. This GEMM contains deleted exons 2 and 3 in order to closely mimic the frequently observed exon 2 deletion in human malignancies, and therefore also eliminates ARF function. Mice homozygous for the *INK4A*$^{\Delta 2/3}$ allele displayed highly penetrant tumor formation (69% developed tumors), whereas 0% of wild-type or mice hemizygous for *INK4A*$^{\Delta 2/3}$ developed tumors. The homozygous knock-out mice do not develop melanoma, but rather B-cell lymphomas and fibrosarcomas[164]. When coupled with *PTEN* heterozygosity, ~10% of mice developed melanoma[165]. These results highlight the requirement for additional cooperating genetic alterations in melanomagenesis. PTEN loss partially mimics activating *RAS* mutations and as previously described, *RAS* and *PTEN* are both frequently mutated in melanomas. A transgenic mouse line expressing oncogenic HRAS (*HRAS*^{G12V}) under the control of tyrosinase enhancer and promoter regions was also generated: *Tyr-ras*[166]. The activating *HRAS*^{G12V} mutation was chosen because *NRAS* and *HRAS* activating mutations naturally occur in human nodular melanoma[167] and the functional loss of the *CDKN2A* locus prevents HRAS^{G12V}-induced senescence[78]. *Tyr-ras* mice rarely developed cutaneous melanoma, and in all such cases, analysis of the tumors identified a dysfunctional *CDKN2A* locus[166]. Furthermore, *Tyr-ras INK4A*$^{\Delta 2/3}$-- mice rapidly developed melanoma, with the tumors resembling human nodular melanomas. A second model that doxycycline-inducibly expressed *HRAS*^{G12V} in the *INK4A*$^{\Delta 2/3}$-- background demonstrated the need for RAS over-expression in tumor maintenance[168]. In this model, the tumors that developed resembled those seen in the above described *Tyr-ras INK4A*$^{\Delta 2/3}$-- model; however, when the doxycycline was removed, tumor regression occurred. Furthermore, as previously stated, *NRAS* is the most commonly mutated *RAS* gene

in melanoma. In fact, 95% of familial melanomas with germline mutations in the *CDKN2A* locus contain activating mutations at codon 61, such as $NRAS^{Q61K}$ [169]. Ninety-four percent of *CDKN2A* null transgenic mice expressing $NRAS^{Q61K}$ in a melanocyte-specific manner (*Tyr:N-Ras*^{Q61K}), developed melanotic, multifocal cutaneous melanoma within 6 months[170]. The tumors resembled human cutaneous melanoma and frequently metastasized to the lungs, liver and lymph nodes.

1.3.3 Mouse models expressing $BRAF^{V600E}$

It was not until The Wellcome Trust Sanger Institute identified the high frequency of *BRAF* mutations in melanoma that the kinase received attention for its role as an oncogene. There have now been three mouse models, all published within two months of each other[21,171,172], generated in an attempt to discern the mechanism through which $BRAF^{V600E}$ functions and identify cooperating genetic events that are required for malignant transformation. Transgenic mice expressing human $BRAF^{V600E}$ under the control of tyrosinase regulatory elements develop melanocytic hyperplasias uniformly within their dermal layer[172]. The presence of SA-β-gal activity and increased INK4A levels suggests the melanocytic lesions are senescent. A transgenic line displaying high transgene expression levels developed melanomas occasionally (10%). Analysis of the tumors revealed absent or reduced levels of INK4A, as well as increased phospho-Erk and phospho-Akt suggesting cooperating genetic events contributed to the malignant transformation of these lesions[172]. When the $BRAF^{V600E}$ allele was coupled with null alleles of *CDKN2A* or *p53*, melanoma quickly ensued, by-passing senescence induction and demonstrating the cooperation of these loci with $BRAF^{V600E}$ expression in melanoma development[172].

The use of transgenic mice is limited when studying the effects of naturally occurring mutations because transgenic technology does not control for transgene expression levels. This becomes particularly problematic for proteins such as BRAF that can cause dramatically different cellular effects within a given cell type ranging from increased proliferation to growth arrest depending on expression levels[173]. With this in mind, to ensure that physiological changes are in

fact due to the *BRAF*^{V600E} expression and not due to abnormal expression levels based on integration position or other transgenic technology side-effects, two groups generated GEMMs expressing a Cre-inducible *BRAF*^{V600E} allele at the endogenous *BRAF* locus[174,175]. In both models, *BRAF*^{V600E} expression led to the development of nevi-like lesions[21,171]; however, the two models differed in the requirements for malignant transformation. In Dhomen *et al*.'s model, BRAF^{V600E} was sufficient to induce melanoma formation (54% within 12 months), none of which metastasized. The incidence of melanoma increased when the *BRAF*^{V600E} expression was coupled with INK4A loss (ARF remained intact). No metastases were observed[171]. In the other model (described more thoroughly below), BRAF^{V600E}-induced melanoma formation required the cooperation of *PTEN* silencing[21].

In order to mimic the progression of BRAF^{V600E}-induced human melanoma, a mouse model needs to express two wild type copies of the *BRAF* gene prior to inducing the *T1799A* mutation in one of the alleles at some point after birth. Also, any genetic manipulations of the *BRAF* locus needs to retain endogenous expression levels and ratios of the BRAF isoforms that result from differential splicing and different transcriptional and translational start sites. Keeping these features in mind, Dankort *et al.* generated a GEMM carrying a Cre-Activated *BRAF*^{V600E} allele (*BRAF*^{CA}) at the endogenous *BRAF* locus (Fig. 1-4A). This model has two copies of wild type *BRAF* prior to *BRAF*^{V600E} induction of one of the alleles, mimicking somatic mutations found in normal human cancers. This allele was used in conjunction with a conditionally silent *PTEN* allele: exons 4 and 5 are flanked by loxP sites allowing for Cre-mediated ablation of *PTEN* phosphatase function (Fig. 1-4B)[120]. To study the interactions of *BRAF*^{V600E} expression and *PTEN* silencing in melanoma, an inducible form of Cre (CreER^{T2}) under the control of tyrosinase regulatory sequences was used to direct inducible Cre function to melanocytes (*Tyr:CreER*^{T2}, as described above). When *BRAF*^{V600E} expression was induced, increased proliferation of melanocytes resulted in the formation of lesions resembling human nevi that failed to progress to melanoma. These results are consistent with the above described studies where BRAF^{V600E}

was shown to induce OIS in melanocytes. When *PTEN* was ablated in the absence of $BRAF^{V600E}$ expression, no phenotype was observed. When $BRAF^{V600E}$ expression and *PTEN* silencing were induced simultaneously, disease quickly ensued. Hyperpigmented lesions were observed within 7-10 days and melanoma developed within 2-3 weeks, and all mice required euthanasia within 50 days of treatment. Upon histopathological analysis, local invasion of the cells into the dermis was observed as well as metastases seen in the lymph nodes and lungs[21]. These results represent evidence supporting the cooperation of the activating $BRAF^{V600E}$ mutation and *PTEN* silencing in melanoma development.

The mechanism of PTEN cooperation remains unknown. PTEN stabilizes p53 in the nucleus[122] and therefore PTEN loss may contribute to the breakdown of the p53 pathway involved in senescence induction and maintenance. However, *PTEN* silencing induces senescence in the prostate through upregulation of p53, contradicting the above hypothesis[176]. Therefore to better understand the role *PTEN* silencing plays in $BRAF^{V600E}$-induced melanomagenesis, it would be useful to build a model that would temporally separate $BRAF^{V600E}$ expression and *PTEN* silencing. Such a model would allow for the functional analysis of different signalling pathways, such as the MAPK, PI3K/AKT, INK4A/pRB, and ARF/p53 pathways, before and after *PTEN* silencing following $BRAF^{V600E}$ activation, and at time points surrounding malignant transformation.

1.4 Summary of Intent

We have previously demonstrated that concomitant $BRAF^{V600E}$ expression and *PTEN* silencing leads to rapid melanoma formation. In order to better understand this cooperation and gain a better temporal understanding of disease progression, we need to control oncogene activation and TSG loss independently. To do this experimentally, a Flp-Activated $BRAF^{V600E}$ allele was generated ($BRAF^{FA}$, Dankort unpublished. Fig. 1-4A). This allele is analogous to the $BRAF^{CA}$ allele, save for the replacement of loxP sites with Flp-Recognition Target (Frt) sequences. Through the use of an inducible Flp recombinase, the $BRAF^{V600E}$ mutation can be induced independent of *PTEN* silencing. This model relies upon

the expression of melanocyte-specific and independently inducible forms of Cre and Flp recombinases. With this in mind, I set out to generate a transgenic mouse that would express inducible Cre and Flp recombinases specifically in melanocytes and whose activity is under the control of unique hormone analogues. Using this system, a more natural model of disease progression can be used whereby $BRAF^{V600E}$ is induced at some early time point, resulting in the formation of a nevus. At any given time point during or after nevus formation, *PTEN* loss can be induced and disease outcome can be assessed.

2. Materials and Methods

2.1 Basic techniques and standard solutions

All basic techniques, solution preparations, and cloning were as described Sambrook *et al.*[177]

2.2 DNA manipulation/ Plasmid generation/ Expression plasmid constructs

2.2.1 Bacterial growth

All entry vectors or expression plasmids were grown in Turbo (NEB), Mach1 (Invitrogen), or DH10B bacteria (Invitrogen). Gateway destination vectors were grown in ccdB Survival™ 2 T1 Phage-Resistant bacteria (Invitrogen). Bacteria were grown in LB medium or on bacterial agar plates containing 40μg/mL carbenicillin, 25μg/mL kanamycin, or a mixture of 40μg/mL carbencillin and 50μg/mL chloramphenicol depending on the selective marker contained within the plasmid. DNA was isolated from bacterial cultures using standard mini-, midi-, or maxiprep protocols.

2.2.2 Creation of gTyr gateway destination vector

The intervening (IVS) and polyadenylation sequences (PolyA) from pTyr:CreER^{T2} (referred to as pTCE-B) were PCR-amplified with GoTaq (Promega, Cat. M3001) using the forward and reverse primers ML021 and ML022 for the IVS and ML023 and ML024 for the PolyA (Table 2-1). Ten picograms of pTCE-B template DNA was added to a 20μL final reaction volume containing 1x GoTaq buffer, 1.5mM $MgCl_2$, 0.2mM dNTP, 1unit (0.2μL) of GoTaq and 0.5μM of each primer. Following an initial denaturation step at 94°C for 3 minutes, the DNA underwent 30 rounds of amplification (94°C for 45 seconds to denature the DNA, 55°C for 30 seconds to allow the primers to anneal, 72°C for 90 seconds for DNA extension), followed by a final extension step of 10 minutes at 72°C to ensure all DNA had been fully extended and to add an 'A' to the 3' end of each strand of DNA (Bio-Rad MyCycler Thermal Cycler) to allow for easy entry into the TOPO pCR2.1 vector. Both PCR products were cloned into

TOPO pCR2.1 (Invitrogen, Cat. K204040) and various plasmid clones were sequence verified. The IVS and PolyA were inserted into pBluescript as *SacII-KpnI* fragments to form pBS-IVS and pBS-PA respectively. The IVS was excised from pBS-IVS as a *BglII-BamHI* fragment and inserted into the *BglII* site of pBS-PA to produce pBS-PA/IVS. The tyrosinase enhancer and promoter were excised from pTCE-B as an *XmaI* fragment and inserted into the *XmaI* site of pBS-PA/IVS and screened for orientation to produce pPIEP. This vector was made into a Gateway destination vector by inserting reading frame B of the Gateway Conversion System (Invitrogen, Cat. 11828-029) into the *StuI* site of pPIEP, thus producing gTyr.

2.2.3 Generation of melanocyte-specific expression vectors

pENTR-βGal, pENTR-mCherry, pENTR-FlpPR, and pENTR-CreER were obtained from Rosalie McDonough. These cDNAs were inserted into gTyr using Gateway recombination technology, specifically the LR reaction. Two hundred nanograms of gTyr was mixed with 100-150ng of the entry vector in question in a final volume of 10μL containing 2μL LR Clonase II reaction mix (Invitrogen, Cat. 11791020). Reaction was incubated at room temperature for 16 hours, transformed into MachI or DH10B bacteria, and plated on carbenicillin bacterial plates.

2.2.4 Sequencing

All sequencing was completed by the McGill University and Génome Québec Innovation Centre using the Sanger Sequencing method. Table 2-2 outlines the primers used to sequence pTCE-B, pTyr:CreER and pTyr:FlpPR.

2.3 Cell culture

2.3.1 Cell lines and growth conditions

B16 F10 melanoma and NIH 3T3 fibroblast cell lines were graciously donated by Dr. Teodoro and Dr. Park (McGill University Goodman Cancer Center) respectively. Cells were cultured in complete media consisting of Dulbecco's Modified Eagle Medium (DMEM) supplemented with L-glutamine,

pyruvate, and 4.5 g/L glucose (Wisent, Cat. 319-005-CL) containing 0.9 IU/mL penicillin, 90 µg/mL streptomycin (Wisent, Cat. 450-201-EL), 9% fetal bovine serum (Gibco, Cat. 12483-020), and 9mM Hepes (Wisent, Cat. 330-050-EL). Cells were grown at 37°C in 5% CO_2. For normal cell maintenance, cells were passaged once they reached 90% confluency and were split 1:10. To do this, cells were washed once in warm 1xPBS and trypsinized with 0.25% trypsin- 1xEDTA (Invitrogen, Cat. 25200-056) for 2 minutes at 37°C. Trypsin was inactivated with 5mL complete media and cells were centrifuged at 1200RPM for 3 minutes. Cell pellets were resuspended in 10mL media, and split as desired.

2.3.2 Fluorescence microscopy

Cells were imaged using equipment from Quorum technologies Inc. Cells were observed using the Leica DM IL LED Fluorescence microscope (11521258). Cells were excited using an X-Cite 120Q System (P010-00153) and fluorescence was filtered with FITC/Cy2 (ET-49002) and TRiTC/Cy3 (ET-49005) filter sets for GFP and DSRed respectively. Imaging was recorded using a QICAM FAST 1394 camera and Qcapture imaging software (QIC-F-M-12-C).

2.3.3 Transfections

Cells were plated at a cell density of $4x10^5$ cells per well of a 6 well dish 24 hours prior to transfection. Each well was transfected using 2.5µL Lipofectamine 2000 (Invitrogen, Cat. 11668-019) per 1µg DNA in Opti-MEM (OMEM) with a final volume of 200µL. The Lipofectamine, DNA (2-4µg per well), and OMEM transfection mixture was incubated at room temperature in Falcon 2058 tubes for 25 minutes to allow DNA micelles to form before being added to cells that were washed twice in 500µL warmed OMEM, and left in 800µL OMEM. Cells were transfected at 37°C for 2 hours before transfection mix was removed and replaced with warmed complete media.

2.3.4 Testing melanocyte specificity of gTyr

B16 F10 and NIH 3T3 cells were co-transfected with 1µg of each Mxi-eGFP + pTyr:mCherry, Mxi-eGFP + pTyr:βGal, or pTyr:mCherry + pTyr:βGal.

Forty-eight hours post-transfection, the cells were observed under fluorescence and subsequently stained for β-gal activity.

2.3.5 Detection of β-galactosidase activity in cultured cells

Cells were washed once in 1xPBS, fixed for 10 minutes at room temperature in 3mL cold fixative solution (2% formaldehyde, 0.2% glutaraldehyde in 1xPBS), and washed twice in cold 1xPBS. One millilter pre-warmed X-gal stain (2mM $MgCl_2$, 4mM potassium ferricyanide, 4mM potassium ferrocyanide, and 1mg/ml 5-bromo-4-chloro-3-indolyl-β-galactopyranoside (X-gal) in 1xPBS) was added to each well and incubated in the dark at room temperature for 72 hours.

2.3.6 Detection of recombinase activity in culture cells

B16 F10 cells were triple-transfected with either pTyr:CreER or pTyr:FlpPR with both Cre (Addgene: 13769, pCALNL-DsRed) and Flp (Addgene: 13772, pCAFNF-GFP) reporter plasmids. Twenty-four hours post-transfection the cells were treated with 1nM 4-hydroxytamoxifen (4-HT; Sigma, Cat. H6278) or mifepristone (Sigma, Cat. M8046) dissolved in EtOH at a stock concentration of 1mM, or EtOH solvent control. Twenty-four hours later the cells were observed under fluorescence**.**

2.4 RNA analysis

2.4.1 Non-quantitative RT-PCR expression analysis

2.4.1a RNA extraction from cell cultures

B16 F10 and NIH 3T3 cells were washed once in 1xPBS and trypsinized using 0.25% Trypsin-1xEDTA for 2 minutes at 37°C. Trypsin was inactivated by the addition of 3mL complete media and $5x10^6$ cells were pelleted. Cell pellets were homogenized using QIAGEN QIAshredders (Cat. 79654) prior to RNA extraction using the QIAGEN RNeasy kit (Cat. 74104).

2.4.1b RNA extraction from tissue samples

Mice were anesthetised using 0.016mL Avertin (2,2,2,-tribromoethanol, Sigma Cat. T48402) per gram mouse weight and the right flank of the mouse was shaved using an electric razor. Samples of $1cm^3$ or smaller of the following tissues were isolated, quick frozen in liquid nitrogen, and stored at -80°C: breast, small intestine, large intestine, spleen, liver, kidney, lung, thymus, heart, eye, fore-brain, hind-brain, ear, and shaved flank. Tissue samples were isolated and frozen at least 24 hours prior to RNA extractions.

One whole ear or $1cm^2$ piece of shaved flank was ground up under liquid nitrogen using a mortar and pestle previously chilled with liquid nitrogen. RNA was extracted from these skin grounds or from $0.5cm^3$ sized other tissue using 1mL TRizol reagent (Invitrogen, Cat.15596-026) following manufacturer's instruction and resuspended in 35-45µL DEPC-treated water.

2.4.1c cDNA Generation

One microgram of RNA was treated with DNase in a 10µL volume using DNase I amplification grade (Invitrogen, Cat. 18068-015). cDNA was generated using 4µL of random primed (using 0.5µg of primers) DNase treated RNA in a final volume of 20uL containing 1x GoScript buffer, 1.5mM MgCl2, 0.5mM dNTP, 20 units rRNasin RNase inhibitor, and 1µL of GoScript Reverse Transcriptase (Fischer Cat. PRA5000). Samples were initially incubated at 25°C for 5 minutes to allow complete primer annealing, followed by 60 minutes at 42°C for DNA extension, and finally the reverse transcriptase was inactivated at 70°C for 15 minutes. One microliter of cDNA was used per PCR reaction.

2.4.1d RT-PCR of melanocyte-specific and non-specific genes

cDNA was tested for melanocyte specific and non-specific RNA following the conditions outlined in Table 2-3. Following an initial 3 minute denaturation step at 95°C, cDNA went through 35 rounds of amplification (25 seconds at 95°C for DNA denaturation, 30 seconds at the appropriate annealing temperature to allow the primers to anneal, 45 seconds at 72°C for DNA extension) all followed by a final incubation at 72°C for 3 minutes to ensure all DNA strands were

synthesized (Bio-Rad MyCycler Thermal Cycler). For nested PCR reactions, 2µL of PCR product from reaction one was added to a final volume of 25µL for reaction two. PCR products were visualized by DNA gel electrophoresis in 1.8% agarose.

2.4.2 Quantitative RT-PCR (qRT-PCR)

2.4.2a qRT-PCR Set-up

Different amounts of pTyr:CreER and pTCE-B (0µg, 0.5µg, 0.75µg, 1µg, 2µg, 3µg, and 4µg) were transfected into B16 F10 cells. The amount of DNA in each transfection was equalized to 4µg using salmon sperm DNA. Each condition was transfected in duplicate, and each duplicate was analyzed in triplicate. Two independent midipreps of each pTyr:CreER and pTCE-B were tested. Forty-eight hours post-transfection, the cells were harvested, homogenized using QIAGEN QIAshredders (Cat. 79654), and the RNA extracted using the QIAGEN RNeasy kit (Cat. 74104). cDNA was generated as described above using random primers. RNA expression levels between conditions were measured using qRT-PCR with SYBR green (Finnzymes DyNAmo Flash SYBR Green qPCR kit, ThermoScientific, Cat. F-415L). One microliter of random primed cDNA was added to a total 10µL (0.5µM of each forward and reverse primers, and 1x master mix consisting of the hot-start version of a modified *Tbr* DNA polymerase, SYBR Green I, optimized PCR buffer, 2.5mM $MgCl_2$, and dNTP mix including dUTP) and analyzed using a BIO-RAD C1000 Thermal Cycler and CFX96 Real Time detection System. The forward and reverse primers ML132 and ML134 amplified a 150bp fragment within Cre (Table 2-1). Following a 7 minute incubation at 95°C to initially denature the cDNA and to heat activate the DNA polymerase, the cDNA underwent 39 rounds of amplification (10 seconds at 95°C to denature the DNA, 15 seconds at 62°C to allow the primers to anneal, and 15 seconds at 72°C for the DNA extension) followed by a final extension of 60 seconds at 72°C and a melt curve from 65°C to 95°C to ensure purity of the amplified product. Fluorescence data was captured prior to each DNA extension step and after each temperature increase for the melt curve. Five standards (1fg/µL, 10fg/µL,

100fg/μL, 1pg/μL, 10pg/μL) of three different pTyr:CreER or pTCE-B plasmids were analyzed with each experiment.

2.4.2b Analysis of qRT-PCR Results

A standard curve was generated by plotting average Ct value vs. Log number of molecules using the average Ct values from the five standards for each experiment. The number of molecules for the standards was calculated using an average nucleotide weight of 660g/mol and an average plasmid size of 14,912kb (average of pTyr:CreER and pTCE-B). The number of RNA molecules for each experimental sample was calculated using the equation for the line of best fit from the standard curve. The number of RNA molecules was corrected for the number of molecules detected for the salmon sperm negative control transfection. An average number of RNA molecules and 95% confidence interval were calculated for each condition using all 6 samples of that condition (ie. transfected in duplicate, and each duplicate analyzed in triplicate).

2.5 Animal studies

2.5.1 Mice previously generated

The *Rosa26tm1*^{Sor}, β-Gal Cre reporter mouse[157] (*R26*^{cre}) is in a BL6 background and was purchased from The Jackson Laboratories. All other mice used, aside from the generated *Tyr:FC* strains, were of a mixed background. Mice carrying Cre- or Flp- Activated *BRAF* alleles (*BRAF*^{CA} and *BRAF*^{FA} respectively) were generated by Dr. Dankort[174] (*BRAF*^{FA}, unpublished). The conditional *PTEN* mice were obtained from Dr. Pandolfi of the Sloan-Kettering Institute in New York and contain loxP sites flanking exons 4 and 5[120]. *Tyr:CreER*^{T2} mice were obtained from Marcus Bosenberg at the University of Vermont[158]. Nomenclature for the alleles used are outlined in Table 2-4.

2.5.2 Generation of *Tyr:FC* mice

One hundred micrograms of both Tyr:FlpPR and Tyr:CreER transgenes were excised with BspEI, separated on a 0.8% agarose gel, and purified using QIAGEN QIAquick Gel Extraction Kit (Cat. 28704). To increase DNA yield from

the extraction columns, the DNA/dissolved agarose mixture was spread out over 10 columns and the DNA was eluted in sets of 5 columns at a time. The eluate from column one was added to column two and used to elute the DNA from column two, and so on. The final eluates from the two sets of five columns were combined. Purified Tyr:FlpPR and Tyr:CreER were mixed 1:1 before injection.

Pro-nuclear micro-co-injection of Tyr:CreER and Tyr:FlpPR was completed by the McGill Transgenic Mouse facility. The purified transgene solution was injected into the pronuclei of fertilized BL6 oocytes. Offspring carrying the transgene(s) were identified by PCR (refer to Table 2-1).

2.5.3 Genotyping

To extract DNA, 5mm long tail samples were incubated in 50µL lysis solution (25mM NaOH, 0.2mM disodium EDTA, pH 12) at 100°C for 20 mins, centrifuged at 15,000RPM in a microcentrifuge for 5 minutes, mixed with 50µL neutralization solution (40 mM Tris-HCl, pH 5), vortexed briefly and centrifuged for 5 minutes at top speed. Differences in alleles were detected by PCR using the primers outlined in Table 2-1. One microliter of extracted DNA was added to a final 25µL reaction mix containing 0.75µL Taq (produced in-house), 0.15mM dNTP, 0.15mM forward and reverse primers, 0.2mM spermadine, and 1xGoTaq buffer. Following an initial 3 minute denaturation step at 95°C, DNA went through 35 rounds of amplification, or 33 in the case of FlpPR, (25 seconds at 95°C for DNA denaturation, 30 seconds at 60°C, or 66°C for FlpPR and CreER, for 30 seconds to allow the primers to anneal, and 45 seconds at 72°C for DNA extension), all followed by a final incubation at 72°C for 3 minutes to ensure all DNA strands were synthesized (Bio-Rad MyCycler Thermal Cycler). PCR products were visualized by DNA gel electrophoresis in 2% agarose.

2.5.4 Activation of Cre and Flp recombinases in mice

2.5.4a Treatment of mice for nevi and melanoma development

Tyr:FC and *Tyr:FC PTEN*$^{lox/lox}$ or *Tyr:CreER*^{bos} and *Tyr:CreER*^{bos} *PTEN*$^{lox/lox}$ mice were crossed with *BRAF*^{CACA} and *BRAF*^{CACA}*; PTEN*$^{lox/lox}$ or *BRAF*^{FAFA} and *BRAF*^{FAFA}*; PTEN*$^{lox/lox}$ mice respectively. Pups were treated

topically on three separate days within the first week of birth with 25mg/mL 4-HT (Sigma, Cat. H6278) in DMSO for Cre activation or 27.7mg/mL mifepristone (Sigma, Cat. M8046) in DMSO for Flp activation. Both drug solutions were prepared before use and were stored at -20°C protected from light. The drug was applied to the right ear and flank, and entire tail using dedicated thin paintbrushes.

2.5.4b In utero activation of Cre and Flp recombinases

Tyr:FC experimental or *Tyr:CreER*^{bos} control mice were mated with *R26*$^{cre/cre}$ reporter mice. Males to be used in the mating were kept in the cage alone for at least 48 hours prior to introducing the female(s). Female(s) were added to the cage no earlier than 6pm on the day of mating. Females were checked for plugs by 8:30am over the following 6 days. Mornings where plugs were observed were identified as embryonic day 0.5 (E0.5).

Pregnant females were injected intraperitoneally with 2mg tamoxifen per 40g body weight on the mornings of E10.5, E11.5, and E12.5. Alternatively for Flp activation, pregnant females were injected intraperitoneally with mifepristone (0.3mg to 2mg per 40 g body weight) with or without progesterone on embryonic days ranging from E10.5 to E13.5. In an attempt to decrease the toxicity of the mifepristone, progesterone (0.5 mg per treatment) was administered concurrently.

Tamoxifen (Sigma, Cat. T5648) was dissolved in sterilized corn oil to 10mg/ml. One hundred milligrams of mifepristone (Sigma, Cat. M8046) was first dissolved in 700µL DMSO before being suspended in 20mL sterile corn oil to produce a 4.84 mg/mL solution. Two hundred milligrams of progesterone (Sigma, Cat. P0130) was dissolved in 40mL sterile corn oil to produce a 5mg/mL solution. Each solution was pre-made, aliquoted and stored at -80°C .

2.5.4c X-gal embryo staining

On E13.5, pregnant females were anesthetised with 0.016ml Avertin per gram mouse weight, the uterus excised and the embryos transferred into cold 1xPBS. The embryos were washed twice in a 10cm dish with cold PBS without rocking for 5 minutes, transferred to 2ml round bottomed microtubes and fixed in

1.2mL β-gal fix solution (0.02% glutaraldehyde, 0.1M PO4, 5mM EGTA, 2mM $MgCl_2$) on ice without rocking for 25 minutes. Embryos were then transferred to a 12 well dish, washed twice in 2mL wash solution (0.1M PO4, 2mM MgCl2, 0.01% Na-deoxycholate, 0.02% Nonidet P-40) for 5 minutes with rocking at room temperature and stained for 48 hours at 37°C in 2mL pre-warmed β-gal stain per embryo (0.1M PO_4, 2mM $MgCl_2$, 20mM tris-HCl pH 7.3, 0.01% Na-deoxycholate, 0.02% Nonident P-40, 5mM potassium ferricyanide, 5mM potassium ferrocyanide, and 1mg/ml X-gal). Embryos were washed twice in 2mL 1xPBS with rocking at room temperature for 5 minutes before being stored in 4% formaldehyde in 1xPBS.

Prior to genotyping, embryos were cleared in glycerol/PBS: each embryo was incubated in 50% glycerol at 4°C with rocking for 48 hours before being transferred to 2mL 80% glycerol for another 48 hours at 4°C with rocking. The tail and hindlimbs were resected from the embryo and subjected to digestion with proteinase K (100mM Tris-HCl, pH 8.8; 5mM EDTA, pH 8.0; 0.2% SDS; 200mM NaCl; 100μg/mL proteinase K) at 55°C for 16 hours. Digest was diluted 5-fold with double distilled water, vortexed, and centrifuged for 5 min at 15,000RPM in a microcentrifuge. One microliter of extracted DNA was used per genotyping reaction. Embryos were genotyped for FlpPR, CreER and $R26^{cre}$.

3. Results

We have previously demonstrated that the concomitant *BRAF*^{V600E} activation and *PTEN* silencing results in rapid melanoma formation[21]. The model used to demonstrate this interaction is reliant on technologies where oncogene activation is co-incident with tumor suppressor gene (TSG) silencing. We have generated a novel inducible *BRAF* allele that expresses *BRAF*^{V600E} in response to Flp-mediated recombination (*BRAF*^{FA}). This new allele permits one to independently regulate oncogene expression and TSG loss when both Cre and Flp recombinases are expressed in melanocytes.

3.1 Creating and characterizing Tyr:CreER and Tyr:FlpPR for the generation of transgenic mice

In order to independently initiate oncogene expression (*BRAF*^{V600E}) and TSG silencing (*PTEN*) in a temporally controlled and melanocyte-specific manner, melanocyte-specific vectors directing the expression of inducible forms of Flp and Cre (FlpPR and CreER, described below) were needed.

3.1.1 Sequencing pTyr:CreER^{T2}

We obtained the same plasmid (pTyr:CreER^{T2}, which we refer to as "pTCE-B"), from Marcus Bosenberg that was used to generate the *Tyr:CreER*^{T2} mice (referred to as *Tyr:CreER*^{bos})[158]. At the time of receiving pTCE-B, little sequence information was known aside from a minimal restriction map (Fig. 1-3A). Sequence information was initially obtained using primers specific to CreER^{T2}, the only region where sequence information was available. Also, a more detailed restriction map was generated to identify the location of *EcoRI* and *XbaI* restriction sites (Fig. 3-1A). *EcoRI* and *XbaI* fragments were shotgun cloned into the corresponding sites of pCR2.1 and sequenced using T7 and M13R primers. Sequence comparisons to the mouse genomic tyrosinase locus helped identify the tyrosinase enhancer and promoter regions contained within pTCE-B. The corresponding mouse genomic sequences were used to generate new primers that ultimately led to the complete sequencing of pTCE-B (Fig. 3-1B). Once the

sequence information was compiled, the precise origins and endpoints of the intervening sequence (IVS), and the polyadenylation signal (PolyA) were delineated through the use of internet blast searches (Fig. 3-1A). The IVS contains an intron and any other sequence, such as splice sites, that are not included in the post-processed mRNA. It was originally named as such due to its location between exons[178] and is now more commonly simply referred to as an intron. The IVS for the pTCE-B construct was taken from the rabbit β-globin gene and the PolyA from the simian virus 40 (SV40).

3.1.2 Generation of a universal melanocyte-specific vector

To aid in generating multiple tyrosinase-driven transgenes, I sought to create a vector to express any cDNA of interest using Gateway recombinase™ technology. With the pTCE-B sequence and annotation in hand, I set out to create a melanocyte-specific destination vector (gTyr). This vector was generated in a stepwise fashion: pTCE-B was used as a PCR template to obtain the IVS and PolyA sequences, whereas the tyrosinase enhancer and promoter were excised as a single *XmaI* fragment (Fig. 3-2). The IVS and PolyA were included in the final vector because the introduction of an intron helps to increase the nuclear export and expression of a transgene up to 300 fold[179,180] and PolyA sequences ensure the addition of a polyadenylated tail for correct mRNA processing. Furthermore, this plasmid was made Gateway compatible by inserting a Gateway negative selection cassette (reading frame B of the Gateway Conversion system) between the IVS and PolyA making the resulting vector (gTyr) universal by allowing entry of any cDNA contained within a TOPO entry vector.

3.1.3 Characterization of melanocyte-specific plasmids

3.1.3a gTyr is melanocyte-specific in vitro

To assess melanocyte-specific expression of gTyr, I transfected melanoma and fibroblastic cell lines (B16 and NIH 3T3 cells, respectively) (Fig. 3-3) with either pTyr:βgal or pTyr:mCherry to direct the expression of β-gal and a red fluorescent protein respectively. Previous studies expressing similar transgenes have concluded melanocyte specificity based on the differential

expression observed in a B16 melanoma-derived cell line versus expression in NIH 3T3 mouse fibroblasts, and therefore these cell lines were used for comparison[130,136,153]. To monitor transfection efficiency each plasmid was cotransfected with pMxi-eGFP, which directs ubiquitous expression of enhanced green fluorescent protein (eGFP) by virtue of the CMV promoter enhancer. Despite comparable transfection efficiencies, β-gal activity was only detected in the B16 cells (Figure 3-3B). There was very little mCherry expression and this was later attributed to the cDNA in use and not due to the lack of pTyr activation. These data demonstrate that gTyr directs cell specific expression.

3.1.3b pTyr:CreER and pTyr:FlpPR are functional in vitro

To independently regulate Cre- and Flp- dependent recombination in a melanocyte-specific manner, I have additionally created pTyr:CreER and pTyr:FlpPR plasmids expressing a 4-HT-inducible Cre recombinase ($CreER^{T2}$) and a mifepristone-inducible Flp recombinase ($Flp^{OE}PR*$). pTyr:CreER contains the P1 bacteriophage Cre recombinase fused to a triple mutated (G400V/M543A/L544A) ligand binding domain (LBD) of the estrogen receptor that renders the domain unresponsive to endogenous estrogen, yet susceptible to activation by estrogen analogues such as 4-HT[154]**.** pTyr:FlpPR contains a codon optimized and 37°C stable *S. cerevisiae*-derived Flp recombinase (Flp^{OE})[181,182] fused to a modified version of the LBD of the progesterone receptor (PR*)[182,183], rendering the domain unresponsive to endogenous progesterone, yet activated by analogues such as mifepristone. We refer to these optimized recombinase fusions as CreER and FlpPR.

To determine if pTyr:CreER and pTyr:FlpPR were functional, these plasmids were co-transfected with both Cre and Flp reporter plasmids into B16 melanoma cells. Both pTyr:CreER and pTyr:FlpPR display high specificity for their target sequence and are only activated in response to their respective hormone agonists, 4-HT and mifepristone respectively (Fig. 3-3C,D). These data confirm that pTyr:CreER and pTyr:FlpPR are functional *in vitro*.

3.1.3c pTyr:CreER and pTCE-B are induced transcriptionally to the same level in vitro

To determine if the pTyr constructs produced similar levels of Cre-fusion transcripts compared to the plasmid used to make the *Tyr:CreER*^{bos} mice, levels of transcription from pTyr:CreER and pTCE-B were directly compared. Specifically, increasing amounts of each plasmid were transfected into B16 F10 melanoma cells and the *Cre* RNA quantified by qRT-PCR. Each concentration was transfected in duplicate and the RNA from each transfection was analyzed in triplicate. The entire experiment was completed twice using independent plasmid preparations. The overall expression profile is comparable between the pTyr:CreER and pTCE-B plasmids (Fig. 3-4). Unfortunately, transfection efficiency was not controlled for eliminating the possibility of pooling the data, leaving overall trends to be used for analysis. In the case of either pTyr:CreER or pTCE-B, increasing amounts of transfected plasmid correlates with increasing *Cre* expression levels (Fig. 3-4). In each separate experiment, there are conditions that demonstrate a statistical difference in the RNA expression; however, the majority of DNA concentrations yield RNA expression levels that are the same within 95% confidence intervals. These data lead to the conclusion that the two plasmids are induced transcriptionally to similar levels.

3.2 Pro-nuclear microinjection of pTyr:CreER and pTyr:FlpPR generated five *Tyr:FC* strains

Having demonstrated that pTyr:CreER and pTyr:FlpPR direct melanocyte-specific expression and that the recombinases are functional *in vitro*, transgenic mice were derived by pro-nuclear injection. Using this technique, linear DNAs co-integrate randomly in tandem repeats in one location of the genome (>90% of the time) and are subjected to coincident transcriptional regulation[184-188]. If individual transgenic lines were made for each transgene, there could be differences in expression levels based on the location in the genome where the DNA integrates. Also, when *Tyr:FlpPR* and *Tyr:CreER* mice are mated together to obtain progeny with both transgenes, the two loci would segregate

independently of each other according to Mendelian genetics (Fig. 3-5A). To avoid these problems, equal molar ratios of linear pTyr:CreER and pTyr:FlpPR were co-injected into fertilized C57BL/6 eggs for the purposes of generating transgenic mice with *Tyr:CreER* and *Tyr:FlpPR* as cointegrants or, for simplicity's sake, *Tyr:FC* mice (Fig. 3-5A). Five hundred and four C57B6 zygotes were co-injected with the transgenes and only 287 of these zygotes developed into the two cell stage. Two hundred and sixty seven of these were transferred to surrogate mothers to eventually give rise to 40 founder strains. Of these founder strains, seven genotyped positive for at least one of the transgenes, and five of these passed the transgenes on to their progeny (Fig. 3-5B,C). All progeny from these five strains are consistently genotyped for both *CreER* and *FlpPR* and thus far none of the strains have demonstrated independent movement of the two transgenes, leading to the conclusion that the transgenes are co-integrated in all five strains.

3.3 Characterization of the *Tyr:FC* mice

After identifying strains carrying the transgenes, the mice were characterized based on two parameters: expression and function of the recombinases.

3.3.1 CreER and FlpPR are not expressed in melanocytes of *Tyr:FC* mice

In order to characterize *in vivo* transgene expression, RNA extracted from *Tyr:FC* and *Tyr:CreER*^{bos} mouse tissue was analyzed by reverse transcription PCR (RT-PCR). To triage the strains for further analysis, total RNA was obtained from the skin (both ear and flank skin) and the liver (as a negative sample). To increase sensitivity and specificity, nested PCR primers spanning the transgene intron were designed. This assay would distinguish fully processed RNA from unspliced nuclear RNA or genomic DNA. PCR products of 354bp and 926bp, 316bp and 926bp, and 428bp and 1009bp are produced from spliced and unspliced *Tyr:CreER*^{bos}, *Tyr:CreER* and *Tyr:FlpPR* respectively. The *Tyr:CreER*^{bos} samples were consistently positive for spliced RNA, whereas inconsistent results were observed for the *Tyr:FC* strains. In a few cases,

unspliced *Tyr:CreER* was detected in skin samples; however this detection was not reproducible. The RNA samples in question were again treated with DNase I and +/- reverse transcriptase samples were analyzed yielding negative results in all cases. Therefore, the identified *Tyr:CreER* PCR product was most likely due to incomplete DNA removal by DNase treatment prior to analysis for those given samples. Neither spliced nor unspliced *Tyr:CreER* or *Tyr:FlpPR* was consistently detected for any of the five *Tyr:FC* strains (Fig. 3-6). The ability to detect tyrosinase RNA confirms the presence of melanocytic RNA within the sample extracted from the skin, and therefore both the *CreER* and the *FlpPR* were not detectably expressed.

3.3.2 Characterizing function of FlpPR and CreER in *Tyr:FC* strains

I also sought to determine if *Tyr:CreER* and *Tyr:FlpPR* were expressed using two independent functional assays: expression of a surrogate marker in Cre-reporter mice and biological readouts for $BRAF^{V600E}$ expression and *PTEN* loss.

3.3.2a Tyr:FC strains do not induce nevi or melanoma formation

Given that our ultimate goal is to use *Tyr:FC* mice to build melanoma models, transgene function was assessed *in vivo*. Specifically, I assessed the ability of CreER and FlpPR to respectively activate $BRAF^{CA}$ and $BRAF^{FA}$ alleles (Fig. 1-4A) to induce nevi formation. Additionally, these experiments were conducted in conjunction with a conditionally silenced *PTEN* allele ($PTEN^{lox/lox}$, Fig. 1-4B) and the mice were monitored for melanoma formation. Within the first week of birth, the pups were treated topically three times with either 64.5mM 4-HT or mifepristone (for Cre and Flp respectively) or a 1:1 molar mixture of the two drugs, in the case of $BRAF^{FA};PTEN^{lox/lox}$, to activate the recombinase(s). The concentration used for the two drugs were as published before for 4-HT administration[21]. Activation of FlpPR by topical mifepristone administration has yet to be published and therefore the same concentration as for 4-HT was applied. All $Tyr:CreER^{bos}$ $BRAF^{CA/+}$ mice treated with 4-HT developed nevi 100% of the time within 4 weeks of treatment (Fig. 3-7, Table 3-1). None of the *Tyr:FC* strains harbouring the $BRAF^{CA}$ or $BRAF^{FA}$ alleles developed nevi with analyses extending

to 11 weeks post-treatment (Fig. 3-7, Table 3-1). Similar results were seen when the strains were assessed for melanoma formation. One hundred percent of *Tyr:CreER*^{bos} *BRAF*$^{CA/+}$*; PTEN*$^{lox/lox}$ mice rapidly developed melanoma and required euthanasia within 4 weeks (Fig. 3-8A, Table 3-1). However, of the *Tyr:FC* strains tested, none of the *Tyr:FC BRAF*$^{CA/+}$*; PTEN*$^{lox/lox}$ mice ever developed nevi or tumors, with analyses extending to 11 weeks (Fig. 3-8A, Table 3-1). Additionally I failed to detect nevi or melanoma in mifepristone/4-HT treated *Tyr:FC7 BRAF*$^{FA/+}$*; PTEN*$^{lox/lox}$ mice with analyses up to 7 weeks post-treatment (Fig. 3-8B, Table 3-1). These data suggest that the *Tyr:FC* strains do not express functional Cre and Flp recombinases.

3.3.2b Tyr:FC strains do not have functional Cre activity in utero

Recombinase function was also tested through the use of reporter mice. The strains were first analyzed for Cre activity due to the availability of the *Tyr:CreER*^{bos} control strain, using the *Rosa26*^{tm1Sor}, βGal Cre reporter (*R26*^{Cre})[157]. Other studies have demonstrated tyrosinase-driven Cre activity in melanocytes within the developing embryo through the use of Cre reporter mice[129,153,156]. Indeed, melanocytes migrating to the skin are detected in *Tyr:Cre* mice by embryonic day E10.5 (and more pronounced by E12.5) in embryogenesis[129]. I additionally sought to characterize *Tyr:FC* expression in the developing embryo. To this end, *Tyr:FC* and *Tyr:CreER*^{bos} mice harbouring the *R26*^{Cre} allele were treated *in utero* with 2mg tamoxifen (which will be metabolized into 4-HT, the compound required for CreER activation, with just over 10% efficiency[189]) per 40g mouse weight on E10.5-E12.5 and analyzed by whole mount X-gal staining on E13.5, as determined by Yajima *et al.*[156]. One hundred percent of the *Tyr:CreER*^{bos} *R26*$^{Cre/+}$ embryos were positive for β-gal activity in the melanocytes, whereas no *Tyr:FC2 R26*$^{Cre/+}$*, Tyr:FC3 R26*$^{Cre/+}$*,* or *Tyr:FC5 R26*$^{Cre/+}$ embryos displayed positive activity (Fig. 3-9A, Table 3-1). Interestingly 1 (of 10) *Tyr:FC7 R26*$^{Cre/+}$ embryo stained positive for β-gal activity. Following the staining procedure, each embryo was genotyped for both *CreER* and *FlpPR*. The presence of *FlpPR* confirmed that this *Tyr:FC7* embryo was in fact a *Tyr:FC* embryo and the Cre activity observed was not due to a mixed up *Tyr:CreER*^{bos}

embryo. The ability to detect positive Cre activity in the melanocytes of *Tyr:FC7* embryos was not reproducible and therefore it was concluded that strain 7 also had non-functioning Cre *in utero*.

3.3.3 Identifying a suitable dose and timing of mifepristone injection for Flp activation

Given that pTyr:CreER and pTyr:FlpPR function similarly *in vitro* (Fig. 3-3), and that they are co-integrated in the genome, it is likely that they would have similar expression levels *in vivo*. In the same manner that CreER function was tested *in utero*, I sought to test FlpPR activity using a *Rosa26* Flp reporter strain (*Rosa26*^{tm2Dym})[190]. Contrary to CreER activity, FlpPR has yet to be tested *in utero* in this manner and therefore a suitable dose for activating FlpPR *in utero* has yet to be identified. Mifepristone was developed as an abortion drug[191] and therefore, I initially attempted to identify a regimen of mifepristone administration that would allow for FlpPR activation while at the same time avoid abortion. The LBDs -PR and -ER are activated by similar levels of mifepristone and 4-HT *in vitro*[154,183]. With this in mind, I injected 15% (to represent the limited efficiency of 4-HT production) and 100% of the tamoxifen dose (dose referring to the moles of tamoxifen per 40g animal weight) on E10.5-E12.5 and analyzed the mice for mifepristone's abortive capacity. Both dosages resulted in abortion. Due to mifepristone's solubility properties, it first needed to be dissolved in a minimal amount of DMSO prior to being re-suspended in sterile corn oil (35µl/mL corn oil). To ensure that the solvent was not the cause of the abortions, the solvent alone was injected. The volumes tested were those that corresponded to the volume of mifepristone in solvent that would have been injected to achieve both 15% and 100% the tamoxifen dose. Both levels were non-abortive. In an attempt to negate the abortive effect of mifepristone, pregnant females were injected with progesterone (at the suggested does of 0.5mg per day[192]) at the same time as mifepristone administration on embryonic days ranging from E10.5 to E13.5 (Table 3.2). In one case, the progesterone was administered 5 hours prior to the mifepristone injection in an attempt to "pre-load" the female with enough progesterone that it would not suffer the effects of the progesterone analogue.

Despite trying various induction times and concentrations, all mifepristone administrations resulted in embryo abortion, thus I was unable to assess FlpPR activity *in utero*.

4. Discussion

4.1 The *Tyr:FC* strains are non-functional

In order to temporally separate oncogene activation from tumor suppressor gene (TSG) silencing, I constructed a melanocyte-specific expression system inducible for Cre and Flp activity. I generated pTyr:CreER and pTyr:FlpPR using transcription control elements from the *Tyr:CreER*^{bos} transgene. pTyr:CreER and pTCE-B directed equivalent *Cre* mRNA expression levels as analyzed by qRT-PCR after transfection into B16 melanoma-derived cells (Fig. 3-3). Although pTyr:FlpPR was unable to be analyzed in this manner due to the absence of a comparable control, the regulatory regions directing pTyr:FlpPR expression are identical to those in pTyr:CreER. Thus, I would expect relatively equal expression levels as well. When tested *in vitro*, the plasmids demonstrated melanocyte specificity and inducibility by their respective hormone analogues (Fig. 3-3). Given that pTyr:CreER and pTyr:FlpPR function the same as pTCE-B *in vitro*, they should function similarly *in vivo*. There was one instance where it appeared as though *Tyr:FC7* may have functional Cre activity: the *Tyr:FC7 R26*$^{cre/+}$ embryo positive for β-gal activity (Fig. 3-9). Given that this result was observed once, and that strain 7 was negative for melanoma development when harbouring the *BRAF*$^{CA/+}$*; PTEN*$^{lox/lox}$ genotype, the most dramatic observable phenotype, I am unable to conclude that *Tyr:FC7* is functional. There are two possible reasons for the positive *Tyr:FC7 R26*$^{cre/+}$ embryo: sporadic recombination between the loxP sites at the *Rosa26* locus, or a random genetic alteration within the genome of the positive embryo that either caused the lacZ gene to be expressed or that "unsilenced" *Tyr:CreER*. The *R26*^{cre} reporter strain is commonly used and sporadic recombination has not been reported thus far. In any case, the lack of positive phenotype for any of the other functional assays confirms that the *Tyr:FC7* strain, along with the other four *Tyr:FC* strains are non-functional. Potential reasons for this lack of expression are outlined below.

4.2 Transgene silencing is most likely at the transcriptional level

The absence of detectable RNA in the skin tissue leads to the hypothesis that the lack of functional *Tyr:FC* strain is due to transgene silencing at the transcriptional level and not due to faulty recombinase function. When making transgenic strains, there is almost always at least one strain that does not show transgene expression[144,147]. Therefore, in this case, the simplest explanation for the lack of functional *Tyr:FC* strain is the limited number of founder strains screened. Although five strains should be sufficient given the approximate 85% success rate with similar transgenes[129,144,153,158,193,194], it is entirely possible that a transgene expressing strain would have been identified had we more strains to screen. Unfortunately, the only mechanism to test this hypothesis would be to re-inject the 1:1 mixture of *Tyr:CreER* and *Tyr:FlpPR* and analyze more founder strains. At this point, to re-generate the *Tyr:FC* mice it would be advantageous to make some alterations in the event that this is not the explanation.

4.2.1 Transgene silencing could be due to integration site

The lack of expression in transgenic mice is often thought to be due to the transgene insertion site within the genome. If transgenes insert into a heterochromatic region, it is unlikely that the transgenes will be expressed due to the inability of trans-acting factors to bind with the regulatory elements. One mechanism to help minimize position effects is to add insulator sequences to the ends of the transgene[195]. Insulator sequences function by preventing the interaction of regulatory elements of adjacent genes, as well as to provide a barrier to heterochromatin-spreading from adjacent regions, thus leaving the chromatin open for transacting factors to regulate gene expression[195]. As for the *Tyr:CreER* and *Tyr:FlpPR* transgenes, they already contain insulator-like sequences: the 3.6kb tyrosinase enhancer contains MARs which function to isolate transgenes from position effects[140,141,196]. It has been hypothesized that transgenes may be better protected from position effects if flanked by these MAR sequences[150], similar to insulator sequences, and the two transgenes in question only contain MARs on their 5' end. However, by virtue of co-integration, we

know that there are at least two transgenes inserted in each strain; therefore, it is likely that at least one of these transgenes is flanked by its own MARs located at its 5' end and by the MARs of a second inserted copy, located at its 3' end. There remains the possibility that in each case there is a single copy of each transgene inserted and that they are each directed away from each other. If this was the case, it may be useful to include insulator sequences. Another mechanism to eliminate position-effects would be to build a targeting construct that can be inserted into a known ubiquitously expressed locus. A locus previously used for gene targeting in this manner is the *Rosa26* locus[197,198]. In order to take advantage of this mechanism, we would need to include both transgenes in a single construct. A mechanism to include both CreER and FlpPR expression in a single targeting vector would be to generate a bicistronic vector expressing both FlpPR and CreER from the same promoter. Possible methods of generating bicistronic vectors are discussed below.

4.2.2 Transgene silencing could be due to the co-injection technique

Another possible, although less easily explained reason for the absence of expression is the co-injection technique. Transgenic mice are commonly used in cancer research and it has been widely shown that multiple copies of the transgene will frequently insert in tandem at a single site[184]. The first study to demonstrate co-integration of two separate transgenes was in 1989. In this study, human α and β globin genes were co-injected into the mouse genome[199]. Both genes were expressed leading to the production of functional human haemoglobin. In another study, one group took advantage of the fact that transgene expression can be affected by the expression levels of surrounding DNA and co-injected a highly expressed transgene with a weakly expressed transgene in order to "rescue" the expression of the weakly expressed gene[186]. In this study, expression of the weakly expressed transgene increased 200-fold over the expression levels of the independently integrated transgene. Furthermore, two different groups demonstrate the use of a minigene as a "marker transgene"[200,201]. In these studies, the researchers co-injected a tyrosinase expressing minigene with the transgene of interest. When injected into albino mice, positive transgene expression is easily

identified by rescue of the albino phenotype. This system appears to simplify the initial screening process significantly, particularly in the early 1990's when molecular techniques were not as advanced as they are today. However useful these minigenes appear to be, there have not been any published studies where these marker minigenes have been used. In fact, there has been a limited number of studies demonstrating the use of co-injection despite the technique first being used over two decades ago. This raises the question, is the lack of publications using co-injection due to the fact that negative results are rarely published? It is possible that this technique has been attempted previously and other groups have also achieved non-expressing transgenic mice.

It is difficult to imagine a mechanism whereby co-injection would be detrimental, when injection of a single transgene is commonly successful with integration of the transgene in tandem repeats. This is particularly puzzling in the case of the *Tyr:FC* mice where the 2 transgenes injected are extremely similar and differ only in the cDNA being expressed; all the regulatory regions are identical. One hypothesis is that co-injection of an equimolar ratio of 2 transgenes decreases the expression level of each transgene by approximately half. Transgenes under the control of similar tyrosinase regulatory regions have observed copy number dependent expression levels. While the disadvantage to this is clear when considering the expression of a protein product such as tyrosinase, where levels of product can directly relate to the amount of pigment produced, this is not the case with Cre and Flp recombinases that are only required to be present for a short time, or in a limited amount because the result of their action is permanent. Also, if this were the case for the *Tyr:FC* strains, the mRNA should still be detectable. In one study expressing *Cre* under the control of the same tyrosinase 3.6kb enhancer and a smaller promoter (2.5kb) (*Tyr:Cre*), one transgenic line had a single transgene integrated[153]. Analysis of this strain demonstrated that it functioned equally well as the strain with 4 copies integrated. Also, *Cre* mRNA was detected in the skin tissue of 3-week old mice using a single round of PCR[153]. With this in mind, even if the *Tyr:FC* strains only had a single copy of each transgene integrated, it should still be possible to detect the mRNA (particularly

when using a nested PCR) and recombinase activity. Again, this leads to the conclusion that the strains are silenced at the transcriptional level.

To determine if co-injection is the problem, we could co-inject pTCE-B and pTyr:FlpPR and assess Cre function. Given that pTCE-B is the exact plasmid used to generate the *Tyr:CreER*^{bos} strain, Cre activity should be detectable. If Cre activity was not present this could suggest that co-injection is not a favourable technique for generating transgenic mice. However, lack of expression (in this hypothetical experiment) could also be due to a limited number of founder strains (depending on the number of founders obtained) or it could potentially be due to differences in the method of transgene preparation prior to injection, or due to differences in the injection protocol itself. To test this, we could inject pTCE-B on its own. While these experiments would be informative, the benefit would not necessarily be worth the time and financial investment.

4.2.3 Lack of transgene expression could be due to faults within the pTyr:FlpPR and pTyr:CreER constructs

A third possible explanation is due to faults in the constructs that are not present within pTCE-B. The regulatory regions (enhancer, promoter, IVS, and PolyA) directing pTyr:CreER and pTyr:FlpPR were taken from pTCE-B. pTyr:CreER was sequenced prior to micro-injection, confirming the correct sequences of these elements. Thus, this is unlikely the reason. Similar expression levels of pTCE-B and pTyr:CreER was confirmed *in vitro* using qRT-PCR (Fig. 3-4). However, it is important to note that the RNA detected in this case is total RNA. I was unable to successfully generate highly specific intron-spanning primers that would produce a suitable PCR product for qRT-PCR and therefore I used *Cre*-specific primers. Non-quantitative RT-PCR using intron-spanning primers on the highest concentration of extracted RNA produced PCR products corresponding to spliced mRNA, confirming that the majority of the RNA in the sample was processed RNA (data not shown). Also, I tested cDNA generated from random-primed and polydT-primed RNA, the latter to prime only fully processed mRNA. For both methods of cDNA generation, the level of *Cre* mRNA

detected for each plasmid was the same within 95% confidence intervals (data not shown). The *Cre* mRNA detection level was lower using the polydT primers; however, and thus I decided to carry out the expression comparisons using cDNA generated with random primers. Furthermore, similar function was confirmed when both Cre fusions were specifically activated by 4-HT (and not mifepristone) and demonstrated selectivity for loxP sites (and not Frt sites). Thus, I can conclude that the two constructs function the same *in vitro*.

There are a few subtle differences between the constructs, while producing no adverse effects *in vitro*, could have an unknown role *in vivo*. For one, the cloning regions differ and the insertion of the Gateway cassette into gTyr left behind some residual recombination sequences (each ~25bp long) flanking the cDNAs. Gateway technology is commonly used to build universal vectors in this manner and therefore it is highly unlikely that these remaining sequences have a negative effect on transgene expression. It is conceivable that these sequences could potentially contain microRNA sequences, which are commonly ~21 nucleotides, that could disrupt the protein levels[202]. However, as previously mentioned, the lack of expression is most likely at the transcriptional level and therefore this is unlikely the cause. Another difference between pTyr:CreER and pTyr:FlpPR and the plasmid used to generate the *Tyr:CreER*^{bos} mice, is the presence of 15 nucleotides on the 5' end of the PolyA sequence. When I annotated pTCE-B, I blasted the sequence against the SV40 genome to determine the origin and end sites of the PolyA region. In the construction of gTyr, I used this PolyA sequence. After concluding that the *Tyr:FC* strains were non-functional, I reviewed these annotated sequences. Internet blast searches of pTCE-B identified other expression vectors that contained the same SV40 PolyA region; however, they also contained an identical 15 nucleotides to the 5' end of the sequence. These nucleotides, GATCTTATTAAAGCA, contain sequences characteristic of a PolyA signal. Although the PolyA region of pTyr:CreER and pTyr:FlpPR lack these 15 nucleotides, they do still contain all the essential components of a PolyA sequence, specifically the AATAA sequence and a downstream T-rich region[203,204]. Furthermore, function of the PolyA sequence in both pTCE-B and

pTyr:CreER was tested *in vitro* using qRT-PCR of cDNA generated with PolydT primers (as described above) confirming that the PolyA sequence on pTyr:CreER is sufficient for the proper addition of a polyadenylated 3' tail.

At this point, it is difficult to determine if the lack of functional *Tyr:FC* strain is due to a limited number of founder strains, the co-injection technique, or a flaw in the constructs. Unfortunately there is no robust method to determine which of these possibilities is the actual cause for the lack of expression.

4.3 Possible mechanisms for re-engineering the *Tyr:FC* mice

If one were to attempt to regenerate the *Tyr:FC* mice, or similar mice, in the future there are a few options for improvement to increase the probability that the mice will express the transgenes. One method would be to use a bacterial or yeast artificial chromosome (BAC or YAC respectively) containing larger regions of tyrosinase upstream elements driving expression of both cDNAs. A YAC containing the 80kb tyrosinase locus and 155kb of upstream regulatory elements displayed wild type levels of expression in a position-independent manner[205]. In this case, expression was seen in both neural crest and optic cup-derived cell lineages. Another possibility is to use a bicistronic vector. There are two options for accomplishing this: the use of an internal ribosomal entry site (IRES) of the *Encephalomycarditis virus* (EMCV) or a viral 2a peptide sequence, such as the T2A from the *Thosea asigna virus*. In both cases, the construct could be inserted into gTyr for micro-injection into the genome or could be targeted to a ubiquitously expressed locus.

4.3.1 The *Tyr:FC* mice could be generated using bicistronic vectors

The IRES allows for the inclusion of multiple cDNAs in a single mRNA. The ribosome binds to the IRES in a 5' cap independent manner, thus translating the downstream cDNA independently from the first[206,207]. Vectors containing an IRES have been used for many different applications. The IRES can be used to separate an experimental cDNA of interest from a downstream marker such as GFP[208]. In this case, one could monitor the GFP expression to confirm that the cDNA of interest is being expressed. Similarly, the GFP could be used to FACS

the cells to contain a pure population of vector expressing cells. The IRES can also be used to allow for the expression of two biologically relevant genes. In the past there have been some discrepancies surrounding the expression efficiency of the IRES controlled cDNA[209,210]. In particular, some commercially available vectors contain a modified IRES. In these vectors, the IRES ATG codon has been altered to contain a *HindIII* restriction site to facilitate cloning, while at the same time abolishing the initiation codon. In these vectors, up to a ten-fold decrease in expression levels of the second cDNA have been observed. However, even with the non-modified IRES, expression of the downstream cDNA is commonly observed at a lower level than the first cDNA[209]. This could be problematic considering the expression difficulties we have already encountered. If cDNAs inserted into gTyr are already experiencing weak expression levels *in vivo*, then injecting a bicistronic vector containing an IRES that has weak expression of the downstream cDNA could lead to the generation of a transgenic mouse that would only express the first cistron at a high enough level for functioning recombinase production

Another possible mechanism for producing a bicistronic vector is through the use of a viral 2A peptide. The 2A peptide, consisting of 20 amino acids, has also emerged as a robust technique for expressing two cDNAs under the control of a single promoter[211]. However, unlike the IRES, the 2A peptide functions co-translationally where it prevents the formation of a *Gly-Pro* peptide bond within the 2A peptide sequence due to "ribosomal skipping"[212]. This results in the production of two polypeptides at equimolar ratios from a single mRNA transcript[212]. Functionality of the 2A peptide has been demonstrated *in vivo* through the generation of a transgenic mouse expressing a 2A bicistronic vector in its genome[211]. In this case, the 2A sequence separates the cDNAs of a membrane localized red fluorescent protein and a nuclear localized green fluorescent protein. Correct expression and localization was observed in all tissues at all stages of development and was shown to be passed through the germline[211]. This leaves the 2A peptide as an attractive option for generating the *Tyr:FC* mice. A major problem could arise if the 2A sequence were to not function properly and a single

polypeptide was generated. The concern for the *Tyr:FC* mice if this were to occur would be the production of a single protein containing both CreER and FlpPR, that could potentially lead to co-regulation of the recombinases upon drug administration.

It would be beneficial to build two such constructs and test them *in vitro* to identify which sequence gives the highest level of co-expression and allows for independent regulation of the two recombinase fusions. Furthermore, as suggested above, as an alternative to generating transgenic mice through pro-nuclear microinjection, a single bicistronic transgene could be knocked-into the *Rosa26* locus, eliminating possible position effects.

4.3.2 A *Tyr:FlpPR* strain could be generated to be used in conjunction with *Tyr:CreER^{bos}*

In the event that all methods of co-expressing the two cDNAs were unsuccessful, one could also simply generate a *Tyr:FlpPR* transgenic mouse. The *Tyr:CreER^{bos}* mice could be used in conjunction with the generated *Tyr:FlpPR* mice. This is undesirable because the two transgenes would segregate independently of each other, requiring extra matings to obtain mice with necessary experimental genotypes such as *Tyr:FlpPR Tyr:CreER^{bos} BRAF$^{CA/+}$; PTEN$^{lox/lox}$*. Furthermore, generation of a *Tyr:FlpPR* transgenic strain requires the optimization of protocols for detecting Flp activity *in vitro*. Co-injection or use of a bicistronic vector would also have this requirement; however, strains could be triaged by positive Cre activity. The optimization of a protocol in the absence of a positive control has inherent difficulties.

4.4 A possible mechanism for detecting Flp activity *in vivo*

The ideal method for characterization of Flp activity would be through the use of a *Rosa26* Flp reporter strain, such as *Rosa26$^{Sortm2Dym/J}$*, alkaline phosphatase Flp reporter[190] . At the moment I have still not been able to identify a suitable method for activating the Flp recombinase *in utero*. Unfortunately *in utero* activation of FlpPR (or CrePR) has not been previously published and therefore an established mifepristone dose and timing regime remains unknown. One study

activated CrePR in the brain of adult mice. In this case, Cre activation required administration of 2.5 mg mifepristone intraperitoneally for 8 days consecutively[213]. This level of drug is significantly higher than the amounts I tested. It is difficult to extrapolate information regarding the activation of FlpPR *in utero* from this study due to drastically different experimental features. *In vitro* studies suggest that the modified progesterone and estrogen LBDs are activated by relatively similar levels of their respective drugs[154,183]. In line with this, I hypothesized that similar *in vivo* levels would be required.

Other studies that have assessed lacZ and alkaline phosphatase (AP) activity in embryos, have used similar protocols for the X-gal and AP staining respectively[152]. With this in mind, optimization of an X-gal staining protocol for embryos later in development or on the skin of post-natal mice may be useful in identifying a suitable protocol for AP staining. The X-gal staining of *Tyr:CreER*^{bos} *R26*^{cre} embryos is limited to E13.5 or E14.5 for two reasons: optimal Cre activity can be achieved with a single injection of tamoxifen on E10.5[153] while earlier injection times have not been tested, and the presence of blood vessels later in development makes melanocyte visualization more difficult past E14.5 (my own observations). However, it should be possible to detect β-gal activity (as a result of Cre-mediated recombination of the Cre reporter gene at the *Rosa26* locus) in the skin of post-natal mice. With this in mind, it may be possible to identify a day late in gestation that is suitable for mifepristone injection eliminating abortive effects. At this suitable embryonic day, pregnant females (harbouring *Tyr:CreER*^{bos} *R26*$^{cre/+}$ embryos) can be injected with tamoxifen and the X-gal staining conducted on the skin of new born mice. Optimization of this protocol could then be useful for developing an AP protocol suitable for characterizing Flp activity. The limiting factor for this analysis would then be identifying a date late in gestation that would be conducive to Flp activation by mifepristone injection. Thus far, all injection amounts and dates have been abortive. Mifepristone's abortive effect may be mitigated later in gestation, thus allowing for successful injection of mifepristone and delivery of viable pups. The

skin of these pups could be harvested and subjected to AP staining to detect reporter activity.

4.5 Potential biological uses of the *Tyr:FC* transgenic mouse

The *Tyr:FC* mouse strain was being engineered to build a system where oncogene activation (*BRAF*^{V600E} expression) could be induced independent of TSG (*PTEN)* loss. The use of such a system would allow for the analysis of a variety of biological questions such as the effect of the timing of the two mutations relative to each other, and through the coupled use of ubiquitous TSG loss (e.g. p53), the role of the PI3K pathway in melanoma characteristics such as invasion and metastases.

To determine the effect of *PTEN* loss relative to *BRAF*^{V600E} expression and senescence induction, a thorough understanding of the senescence induction timeline would be required. *BRAF*^{V600E} expression would be induced at some timepoint after birth, and the melanocytic lesions that form assessed for proliferating cells (BrdU or Ki67) and senescence (SA-β-gal). This would allow us to determine when melanocytes exit the cell cycle and become senescent. Once the BRAF^{V600E}-induced senescence timeline has been identified, it would be possible to ask two key biological questions. First, we could determine whether or not it is possible for melanocytes to escape BRAF^{V600E}-induced OIS. Second, we can assess if the timing of *BRAF* and *PTEN* mutations relative to each other have an effect on melanoma development and progression. To do this, *PTEN* would be ablated concomitant with and at various times following the initiation of *BRAF*^{V600E} expression, according to the timeline of senescence induction. The melanocytic lesions would be examined for proliferating and senescent cells before and after *PTEN* is lost. Disease progression would then be assessed based on size and grade of the tumours, as well as extent of invasion and metastases. There are a number of potential outcomes. If nevi rapidly progress to melanoma regardless of when *PTEN* is ablated this would suggest timing of *PTEN* ablation is inconsequential. If however OIS proves to be a barrier to tumour formation,

which has not been proven, then tumor progression would only occur if *PTEN* loss occurs prior to senescence induction.

Using the Tyr:FC mouse system, we could assess in greater detail the exact role *PTEN* loss plays in disease progression. Does *PTEN* loss simply allow for the by-pass of the growth arrest? Is *PTEN* loss involved in the increased metastatic potential of these cells? Such questions could be addressed by combining the conditional *BRAF* and *PTEN* alleles with the silencing of other tumor suppressors capable of by-passing the growth arrest (for example *p53* or *CDKN2A*). Once the growth arrest has been by-passed, the role of *PTEN* loss in invasion and metastases can be assessed. The extent of metastatic spread can be analyzed in tumors with and without intact PTEN. Given that most melanoma patients die due to metastases, information regarding the key players in this process would be instrumental in identifying targets for therapeutic intervention.

The goal of the *Tyr:FC* system is to better understand the physiological interaction of the PI3K and MAPK pathways in melanoma progression. Through the above described experiments, the information to be obtained could highlight different druggable targets as well as key timepoints when therapeutic intervention may have the greatest effect. This information could help lead to the development of drugs that could be used in combination with $BRAF^{V600E}$ inhibitors, such as vemurafenib, which may help by-pass the acquired resistance patients have to these treatments.

5. Final Conclusions and Summary

I attempted to generate a model system that would allow for temporal separation of *BRAF*^{V600E} activation and *PTEN* silencing in melanocytes. To do this, I generated pTyr:CreER and pTyr:FlpPR based on the sequence from pTCE-B, the plasmid used to generate the *Tyr:CreER*^{bos} mice. Although the plasmids I generated functioned in a similar manner as pTCE-B *in vitro*, the generated *Tyr:FC* transgenic strains were non-functional. At the moment, and with the resources on hand, I am unable to conclude definitively the cause behind this lack of expression. As the lab progresses forward, it would be beneficial to alter the mechanism of model generation. This could be done through the use of bicistronic vectors, generating knock-in mice at a ubiquitously expressed locus, through the use of BACs or YACs, or simply through the micro-injection of a single transgene, rather than attempting a co-injection.

FIGURES

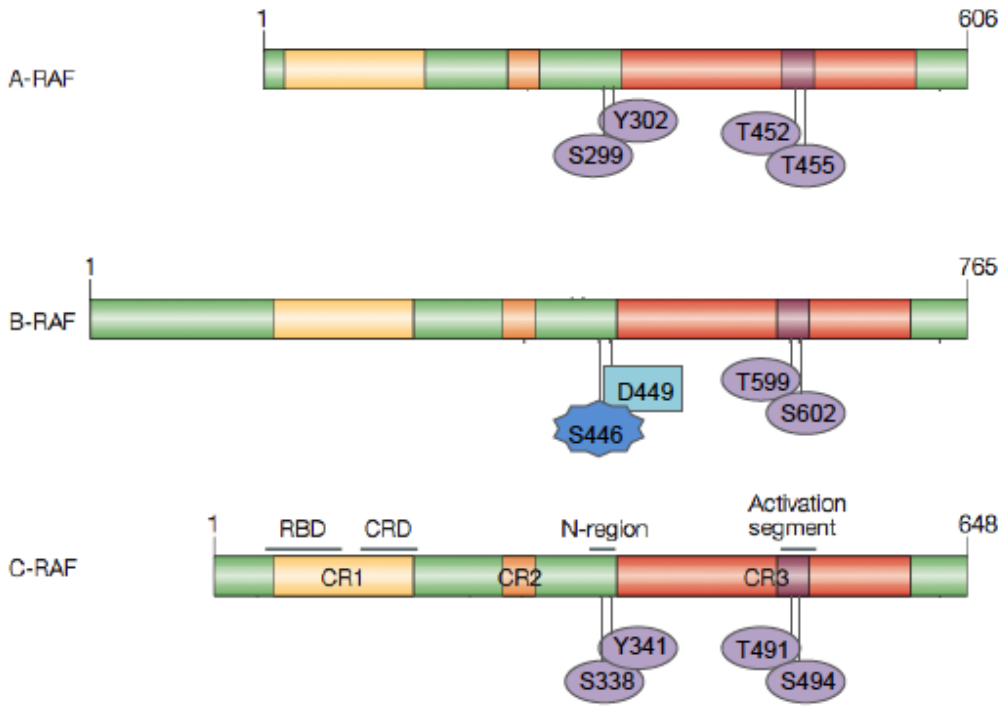

Figure 1-1. Schematic of the RAF proteins – Modified from Wellbrock *et al.*[57] The RAF proteins share three conserved regions: CR1 (yellow), CR2 (orange) and CR3 (red). The amino acids that are highlighted below the individual isoforms refer to known phosphorylation sites. CR1 contains the RAS-binding domain (RBD) and the cysteine-rich domain (CRD), which are both required for membrane recruitment. CR3 contains the catalytic domain (the activation segment is highlighted in pink). The negative-charge regulatory region (N-region) is just upstream of CR3 and contains residue Y341, which is conserved in ARAF (Y302), but is replaced by D449 in BRAF (shown as light blue box). S338 is conserved in all RAF proteins (S299 in ARAF and S446 in BRAF), but is constitutively phosphorylated in BRAF (shown as dark blue star). The catalytic domain contains two activation-segment phosphorylation sites T491 and S494, which are conserved in ARAF (T452 and T455) and BRAF (T599 and S602).

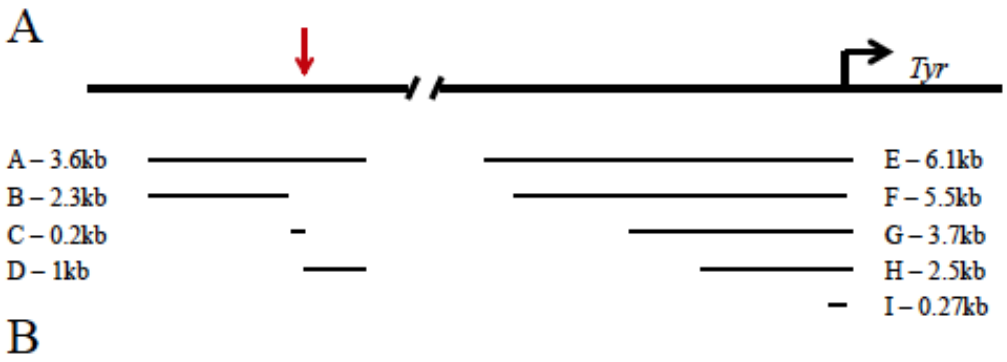

Enhancer	Promoter	cDNA	Mechanism of Detection	Expression	Ref.
--	E, G, I	CAT reporter	*In vitro* activity	Melanocyte-specific expression	130
--	F, I, H	Tyrosinase	Rescue albino phenotype, *in situ* hybridization	Neural crest and optic cup-derived lineages	128,130-133
--	E	LacZ	X-gal activity	Brain	214
A	F	Tyrosinase	Rescue albino phenotype	Neural crest and optic cup-derived lineages	144
A	H	Tyrosinase	Rescue albino phenotype	Increased expression in neural crest-derived cells	141
A A C	E I I	LacZ	X-gal activity	Enhanced expression in neural crest-derived cells and repressed expression in optic cup-derived cells	147
C	I	Luciferase reporter	*In vitro* activity	Melanocyte-specific enhanced activity	146
C	I	CAT reporter	*In vitro* activity	Increased melanocyte-specific expression	144
D	H	Tyrosinase	Rescue albino phenotype	Enhanced expression in neural crest-derived cells	141
B	H	Tyrosinase	Rescue albino phenotype	Enhanced expression in optic cup-derived cells	150
A	I	Cre	Z/AP reporter	Neural crest-derived, optic cup-derived, and neuroepithelial lineages	129
A	H	Cre	*Rosa26* reporter	Neural crest-derived cells, peripheral nerves and brain	153
A	H	$CreER^{T2}$	*Rosa26* reporter	Cutaneous melanocytes	156
A	F	$CreER^{T2}$	*Rosa26* reporter	Cutaneous melanocytes	158

Figure 1-2. Tyrosinase regulatory regions used to generate transgenic mice

(A) Tyrosinase regulatory regions used in transgenic mice. The thick black line represents regulatory sequences upstream of the tyrosinase (*Tyr)* transcription start site (black arrow). The DNAase I hypersensitive site (red arrow) is located at -15kb.

(B) Summary of transgenic mice and plasmids generated using different tyrosinase regulatory regions

A

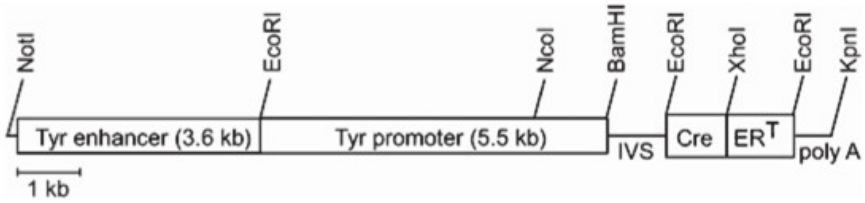
NotI
EcoRI
NcoI
BamHI
EcoRI
XhoI
EcoRI
KpnI
Tyr enhancer (3.6 kb)
Tyr promoter (5.5 kb)
IVS
Cre
ER^T
poly A
1 kb

B

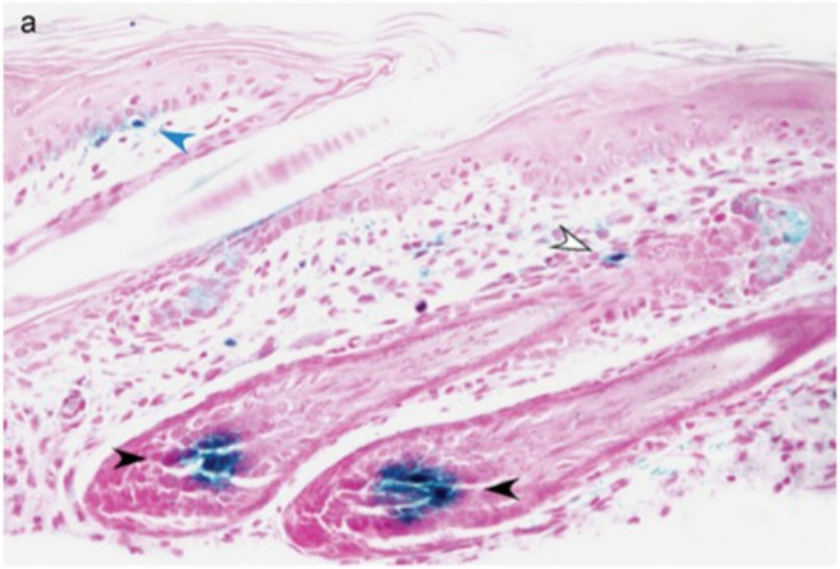
a

Figure 1-3. Melanocyte-specific expression of inducible Cre under the control of tyrosinase regulatory regions – Figure modified from Bosenberg *et al.*[158]

(A) Schematic of the Tyr:CreER^{T2} transgene construct. The 3.6kb tyrosinase enhancer sequence and the 5.5kb tyrosinase promoter sequence are derived from phsTyr4[144]. Cre and ER^{T} represent the sequences encoding the CreER^{T2} fusion protein, beta-globin intervening sequence (intron) are denoted by IVS, and SV40-derived polyadenylation sequences are labelled poly A. Restriction sites used to make the construct are listed.

(B) X-gal staining of mouse tissue following Cre induction. X-gal staining of tail skin following perinatal topical 4-HT treatment of *Tyr:CreER^{bos} R26$^{cre/+}$* mice showing staining of follicular bulb melanocytes (black arrowheads), a putative follicular bulge melanocytic stem cell (open arrowhead), and an epidermal/junctional melanocyte (blue arrowhead). Mild staining due to endogenous β-gal activity was observed in the sebaceous gland (right of open arrowhead) of both treated *Tyr:CreER^{bos} R26$^{cre/+}$* and control *R26$^{cre/+}$* mice.

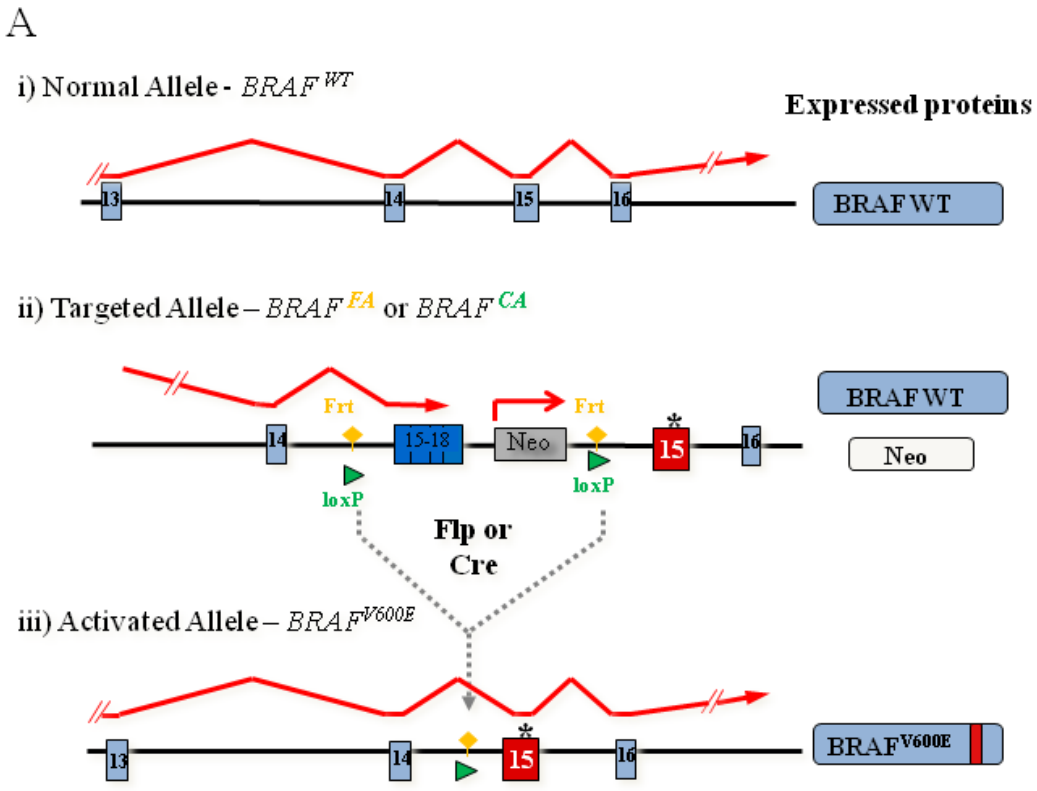
A
i) Normal Allele - BRAF WT
Expressed proteins
13
14
15
16
BRAF WT
ii) Targeted Allele – BRAF FA or BRAF CA
Frt
Frt
14
15-18
Neo
15
16
BRAF WT
Neo
loxP
loxP
Flp or
Cre
iii) Activated Allele – BRAF V600E
13
14
15
16
BRAF V600E
B
1
2
3
loxP
4
5
loxP
6
Cre
1
2
3
loxP
6

Figure 1-4. Genetic alterations of the *BRAF* and *PTEN* loci

(A) Cre and Flp Activated *BRAF^{V600E}* alleles i. Wild type *BRAF*. Exons 13 through 16 of wild type *BRAF* are depicted. *BRAF* has 18 exons. **ii.** *BRAF^{FA}* and *BRAF^{CA}* constructs. *BRAF* exons 15-18 are fused together and found upstream of a neomycin resistance gene. These two components are flanked by loxP sites and this whole cassette is found upstream of a *BRAF* exon 15 encoding the *T1799A* point mutation. Downstream of the mutant exon 15 are wild type exons 16-18. This construct directs the expression of wild type *BRAF* and the neomycin resistance gene. **iii.** Activated *BRAF^{V600E}*. In the presence of Flp or Cre, the two Frt or loxP sites will undergo recombination removing the Frt/loxP flanked cassette, allowing for the expression of *BRAF^{V600E}*.

(B) Conditional *PTEN* construct. Wild-type *PTEN* containing loxP sites flanking exons 4 and 5. Upon Cre-mediated recombination exons 4 and 5 will be lost resulting in *PTEN* silencing.

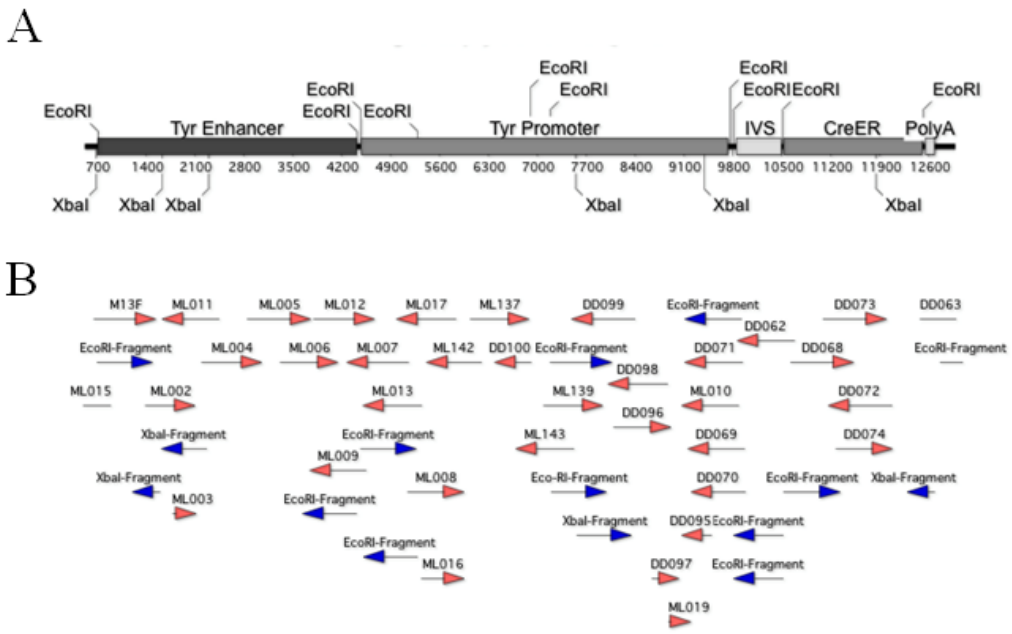

Figure 3-1. Sequencing pTCE-B

(A) Schematic of pTCE-B . Schematic includes annotated regions and the restriction cut sites used for shotgun cloning. The tyrosinase enhancer contains the 3.6kb enhancer region located 15kb upstream of the transcription site and the tyrosinase promoter consists of a 5.5kb promoter region located directly upstream of the transcription start site. The intervening sequence (IVS), consisting of an intron, is from rabbit β-globin, and the PolyA from the SV40 polyadenylation sequence. The *EcoRI* and *XbaI* restriction sites were initially identified through the generation of a detailed restriction map. *EcoRI* and *XbaI* fragments were shotgun cloned into pCR2.1 and sequenced to begin the sequencing process.

(B) Sequencing runs used to sequence pTCE-B. Sequencing runs for the shotgun cloned fragments (blue) and generated sequencing primers (red).

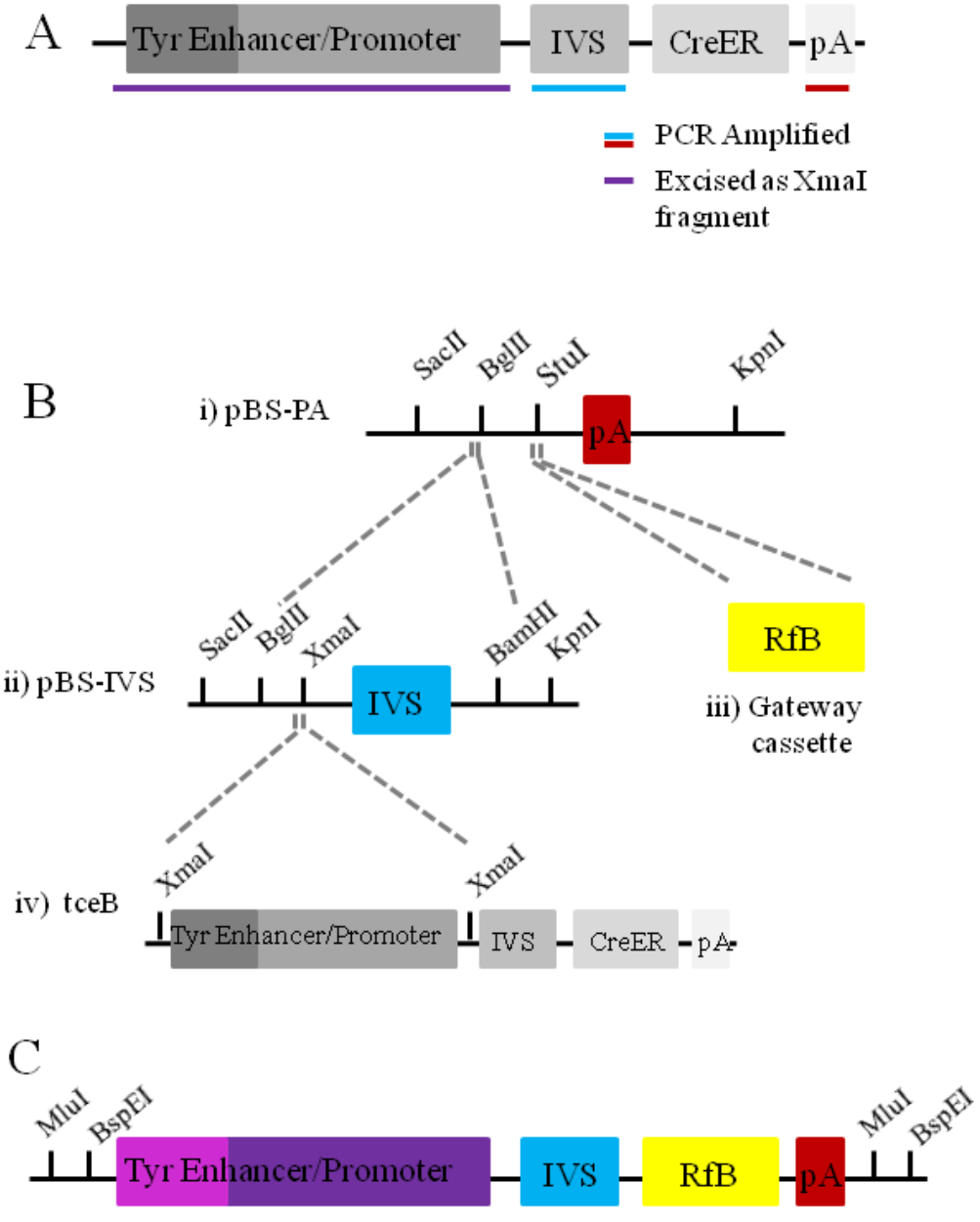
A
Tyr Enhancer/Promoter
IVS
CreER
pA
PCR Amplified
Excised as XmaI fragment
B
i) pBS-PA
SacII
BglII
StuI
KpnI
pA
ii) pBS-IVS
SacII
BglII
XmaI
BamHI
KpnI
IVS
RfB
iii) Gateway cassette
iv) tceB
XmaI
XmaI
Tyr Enhancer/Promoter
IVS
CreER
pA
C
MluI
BspEI
Tyr Enhancer/Promoter
IVS
RfB
pA
MluI
BspEI

Figure 3-2. Generation of gTyr gateway destination vector

(A) pTCE-B regions used in the generation of gTyr. The 3.6kb tyrosinase enhancer and 5.5kb promoter regions were excised as an *XmaI* fragment. The intervening sequence (IVS) and polyadenylation sequence (pA) were PCR-amplified off pTCE-B and sequence confirmed prior to use in gTyr.

(B) The stepwise construction of gTyr. PCR-amplified pA and IVS were initially inserted into pBluescript as *SacII-KpnI* fragments to generate **i**. pBS-PA and **ii.** pBS-IVS. The IVS was inserted into the *BglII* site of pBS-PA as a *BglII-BamHI* fragment. **iii.** The reading frame B (RfB) gateway cassette containing a ccdB gene, chloramphenicol resistance gene, and recombination sites for the entry of cDNAs from an entry vector, was inserted into the *StuI* site. **iv.** The tyrosinase enhancer and promoter were excised from pTCE-B and inserted into the *XmaI* site, all leading to the generation of gTyr.

(C) Schematic of gTyr. The light purple represents the 3.6kb tyrosinase enhancer region and the dark purple represents the 5.5kb tyrosinase promoter. The rabbit β-globin IVS will help to increase expression levels of the construct. The RfB gateway cassette will allow for entry of any cDNA of interest contained within a pENTR/D vector. The SV40 minimal polyadenylation sequence will signal the addition of a polyA tail to the transcribed mRNAs.

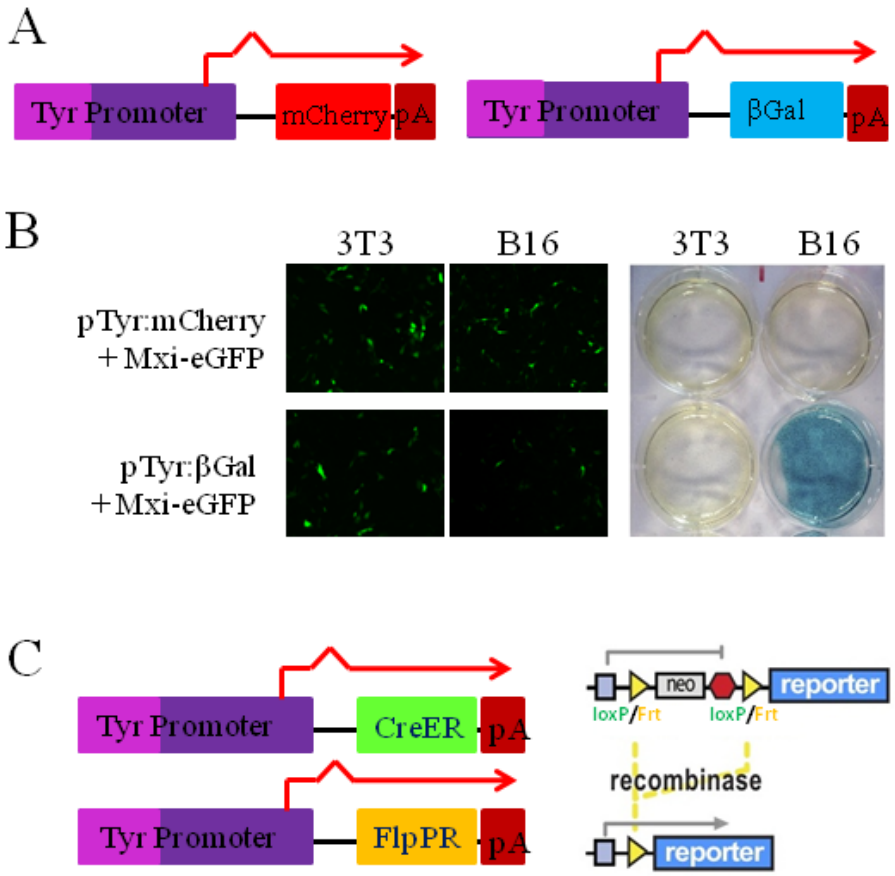
A
Tyr Promoter
mCherry
pA
Tyr Promoter
βGal
pA
B
3T3
B16
3T3
B16
pTyr:mCherry
+Mxi-eGFP
pTyr:βGal
+Mxi-eGFP
C
Tyr Promoter
CreER
pA
Tyr Promoter
FlpPR
pA
neo
reporter
loxP/Frt
loxP/Frt
recombinase
reporter
D
EtOH
4-HT
Mif
pTyr:CreER
pTyr:FlpPR

Figure 3-3. pTyr:CreER and pTyr:FlpPR are functional *in vitro*

(A) The pTyr:mCherry and pTyr:βGal constructs. mCherry encodes a red fluorescent protein and β-gal encodes the β-galactasidase gene. **(A, C)** The light and dark purple regions represent the 3.6kb tyrosinase enhancer and 5.5kb promoter respectively.

(B) gTyr directs melanocyte-specific expression. Mouse NIH 3T3 fibroblast and B16 melanoma-derived cells were co-transfected with a ubiquitously expressed GFP (Mxi-eGFP) and either pTyr:mCherry or pTyr:βGal. Twenty four hours post-transfection, the cells were observed under fluorescence and active GFP was seen in all 4 wells. X-gal staining was carried out on the cells and within 3 hours positive β-gal activity was detected only in the B16 cells. Image is after 72 hours of staining.

(C) pTyr:FlpPR, pTyr:CreER, and Flp and Cre reporter plasmids. FlpPR refers to the codon optimized and 37°C stable Flp recombinase fused to a modified LBD of the progesterone receptor[181-183] and CreER refers to the Cre recombinase fused to a modified LBD of the estrogen receptor[154]. The reporter plasmids contain a neomycin resistance gene followed by a stop codon flanked by either Frt or loxP sites for the Flp and Cre reporters respectively. Post recombinase-mediate recombination, the Cre reporter expressed a red fluorescent protein (DSRed) and the Flp reporter expresses a green fluorescent protein (eGFP).

(D) pTyr:FlpPR and pTyr:CreER are functional. B16 cells were co-transfected with either pTyr:CreER or pTyr:FlpPR with both Cre and Flp reporter plasmids. Twenty-four hours post-transfection the cells were treated with 1nM 4-HT, mifepristone (Mif), or ethanol (EtOH) solvent control. Twenty-four hours later the cells were observed under fluorescence. Both Flp and Cre demonstrate inducibility for their respective drugs and specificity for their respective recombination sequences. Insets correspond to bright-field view of cells at time of fluorescence.

A

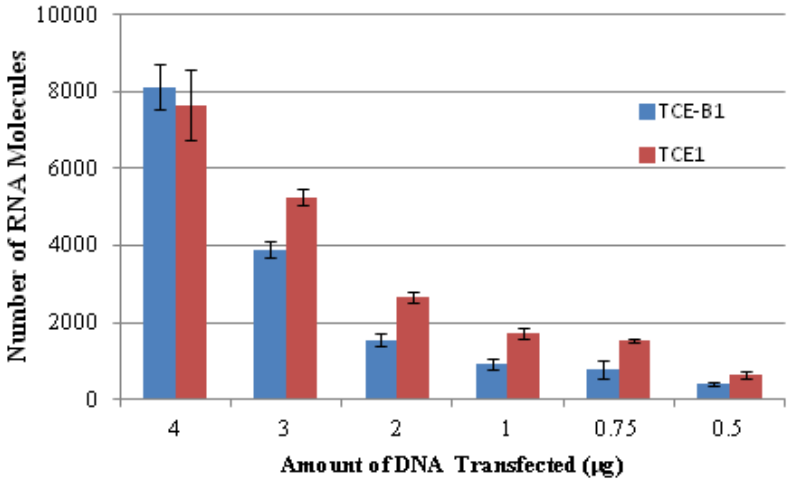
10000
8000
6000
4000
2000
0
Number of RNA Molecules
TCE-B1
TCE1
4
3
2
1
0.75
0.5
Amount of DNA Transfected (µg)

B

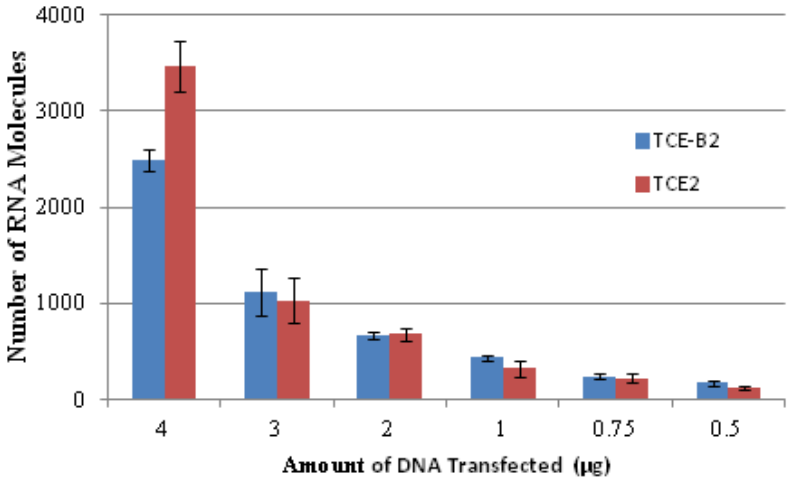
4000
3000
2000
1000
0
Number of RNA Molecules
TCE-B2
TCE2
4
3
2
1
0.75
0.5
Amount of DNA Transfected (µg)

Figure 3-4. pTCE-B and pTyr:CreER are expressed at comparable levels *in vitro*

B16 F10 cells were transfected in duplicate with different amounts of pTCE-B and pTyr:CreER. Forty-eight hours post transfection, the cells were harvested and the RNA extracted. cDNA was generated from random primed RNA, and subjected to qRT-PCR where each sample was measured in triplicate. Primers amplifying a 150bp product in *Cre* were used (Table 2-1). Salmon sperm was included as a negative control and the number of RNA molecules for the samples were corrected for the value of salmon sperm molecules. Error bars represent 95% confidence intervals. **(A)** and **(B)** represent independent experiments using independent plasmid preparations.

A

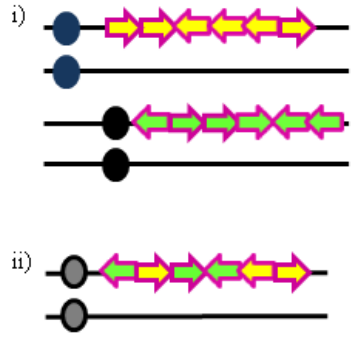

B

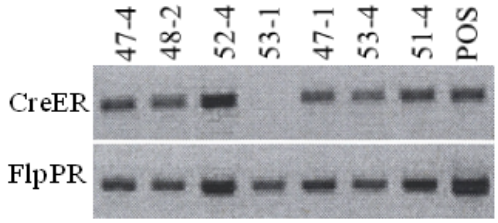

C

Founder Strain	Strain	Genotype	F1 Progeny	Co-Integrated
47-4	1	*Tyr:FC*	-	-
48-2	2	*Tyr:FC*	*Tyr:FC*	Yes
52-4	3	*Tyr:FC*	*Tyr:FC*	Yes
53-1	4	*Tyr:FlpPR*	-	-
47-1	5	*Tyr:FC*	*Tyr:FC*	Yes
53-4	6	*Tyr:FC*	*Tyr:FC*	Yes
51-4	7	*Tyr:FC*	*Tyr:FC*	Yes

Figure 3-5. Pro-nuclear microinjection of *Tyr:FlpPR* and *Tyr:CreER*

(A) The hypothetical genetic structure of transgenic lines for *Tyr:FlpPR* and *Tyr:CreER*. The yellow and green arrows represent *Tyr:FlpPR* and *Tyr:CreER* respectively. **i.** Individual transgenic lines generated for each transgene. For both *Tyr:FlpPR* and *Tyr:CreER*, the transgenes are integrated in one location on any given chromosome. The transgenes are depicted on separate chromosomes showing that they will segregate independently of each other. The transgenes are inserted in tandem repeats in both orientations. **ii.** Co-injection of *Tyr:CreER* and *Tyr:FlpPR*. When the transgenes are co-injected, they will integrate in the same location of the genome, there will be approximately equal copy numbers of each transgene, and the transgenes will integrate as tandem repeats in both orientations **(B) Genotyping the seven founder strains**. *Tyr:FC* strains were genotyped for *CreER* and *FlpPR* using polymerase chain reaction. Strains 1, 2, 3, 5, 6, and 7 are positive for both *Tyr:CreER* and *Tyr:FlpPR,* whereas strain 4 is only positive for *Tyr:FlpPR*.

(C) Summary table of micro-injection results. Seven strains contained at least one of the transgenes, and only five of these strains passed the transgenes to their F1 progeny. Progeny of the five strains are genotyped for both *FlpPR* and *CreER* and the two transgenes have not yet been observed to segregate independent of each other, thus concluding that the transgenes are co-integrated for all five strains.

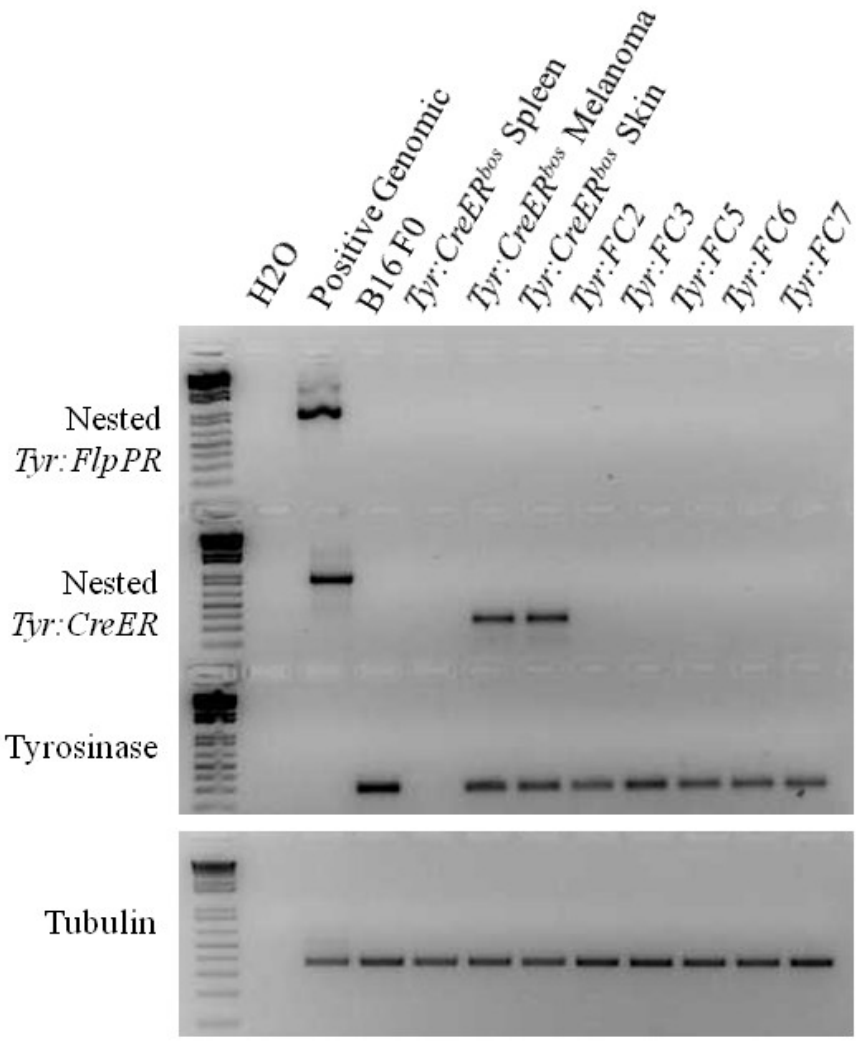
H2O
Positive Genomic
B16 F0
Tyr:CreER^bos Spleen
Tyr:CreER^bos Melanoma
Tyr:CreER^bos Skin
Tyr:FC2
Tyr:FC3
Tyr:FC5
Tyr:FC6
Tyr:FC7
Nested Tyr:FlpPR
Nested Tyr:CreER
Tyrosinase
Tubulin

Figure 3-6. *FlpPR* and *CreER* mRNA are not expressed in skin tissue of *Tyr:FC* mice

Expression of *FlpPR* and *CreER* mRNA was analyzed in the skin tissue of adult *Tyr:FC* mice by RT-PCR using primers outlined in Table 2-2. Amplified products of 428bp and 100bp correspond to spliced and unspliced *Tyr:FlpPR*, and products of 354bp and 926bp, and 316bp and 888bp correspond to spliced and unspliced *Tyr:CreER*^{bos} and *Tyr:CreER* respectively. To increase detection levels, a nested PCR system was employed for both genes. RNA was extracted from the flank of *Tyr:CreER*^{bos} or *Tyr:FC* mice with TRIzol. All RNA was treated with DNaseI prior to analysis to remove any DNA present in the samples. Tubulin was tested as an internal control for RNA extraction, and tyrosinase was tested as a control for melanocytic RNA contribution to the skin sample. RNA samples from a *Tyr:CreER*^{bos} *BRAF*$^{CA/+}$*; PTEN*$^{lox/lox}$ tumor and from a *Tyr:CreER*^{bos} skin sample were tested as positive controls for spliced *Tyr:CreER*^{bos}, B16 F10 as a positive control for tyrosinase, and *Tyr:CreER*^{bos} spleen sample as a negative control.

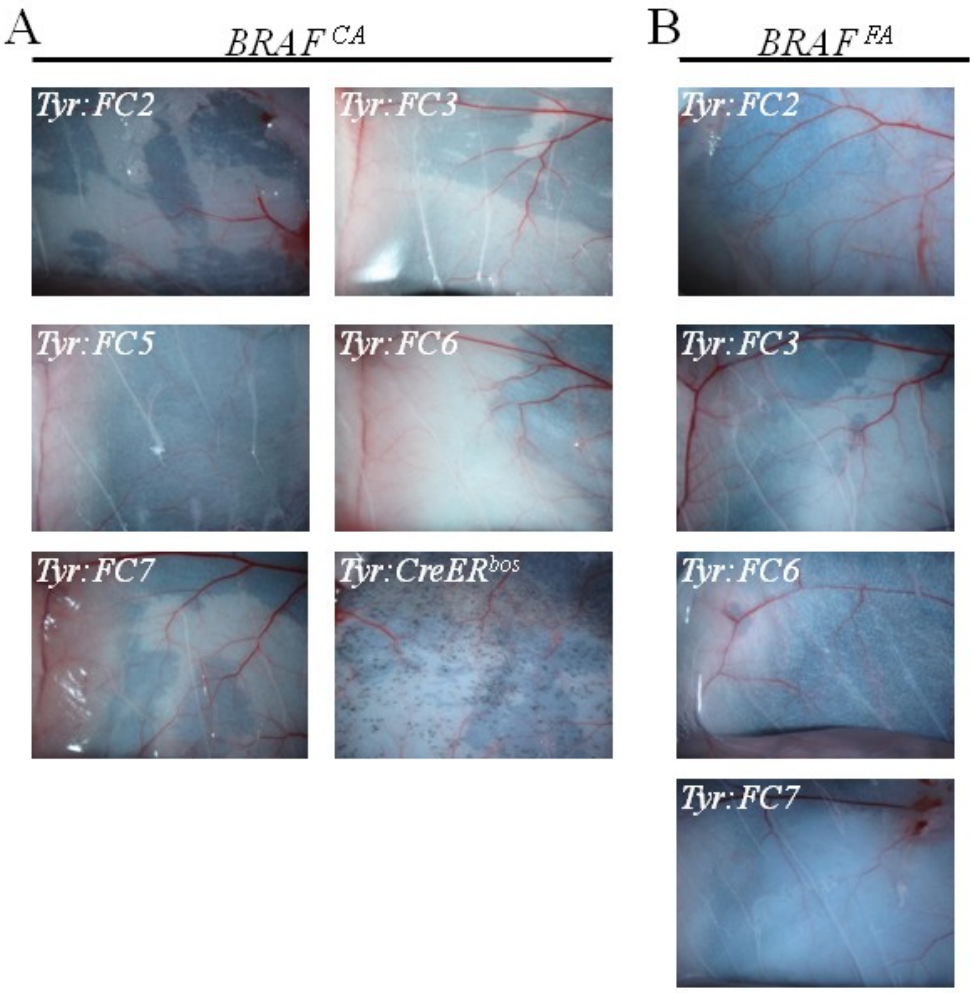

Figure 3-7. *Tyr:FC* strains do not mediate nevi formation

Inside flanks of treated *Tyr:FC* experimental or *Tyr:CreER*^{bos} control strains harbouring the **(A)** *BRAF*^{CA} or **(B)** *BRAF*^{FA} alleles. Mice were treated topically on their right ear, flank and tail on three separate days within the first week of birth. Four to 11 weeks post-treatment, the mice were sacrificed and analyzed.

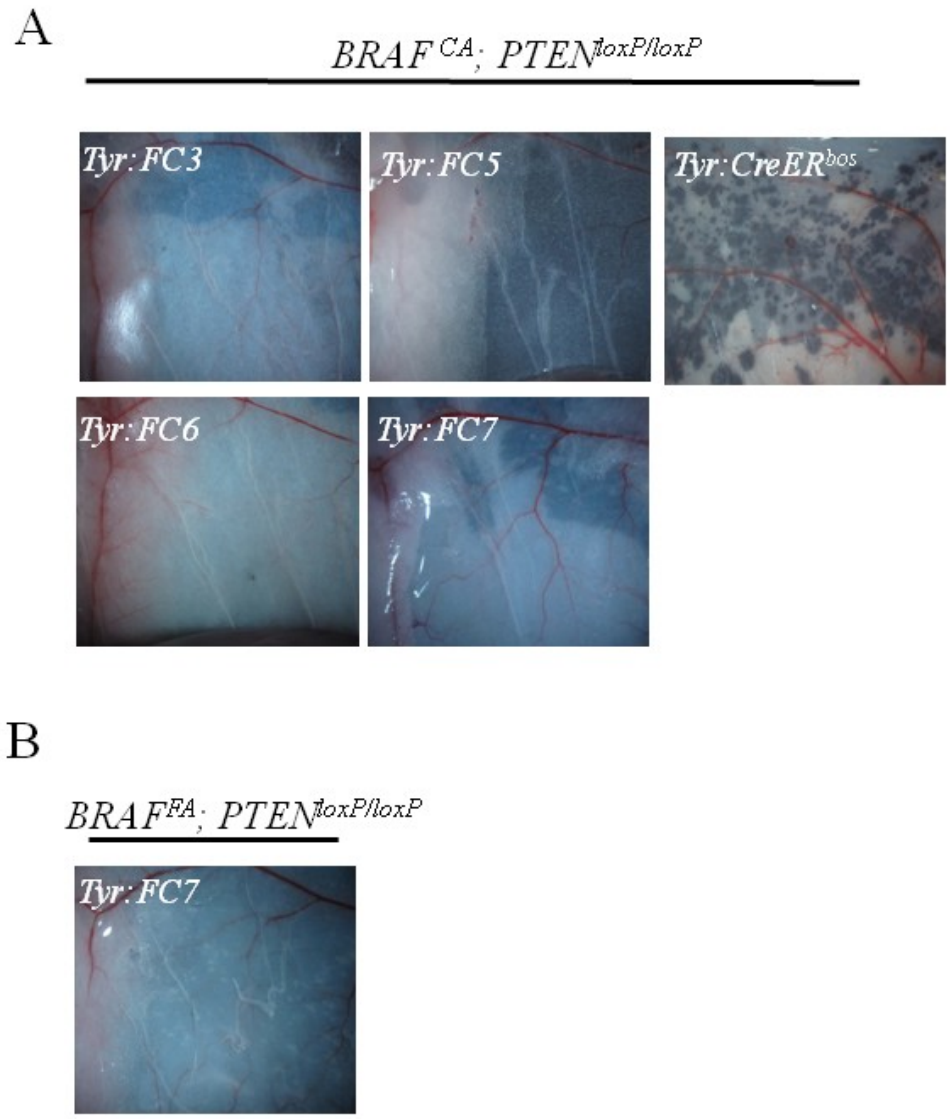

Figure 3-8. *Tyr:FC* strains do not mediate melanoma formation

(A) Cre-mediated melanoma formation. *Tyr:FC* strains or *Tyr:CreER*^{bos} control strains harbouring the *BRAF*$^{CA/+}$*; PTEN*$^{lox/lox}$ genotype were treated topically on their right ear, flank and tail on three separate days within the first week of birth. Four to six weeks post-treatment, the mice were sacrificed and the inside of their treated flank was analyzed.

(B) Cre- and Flp-mediated melanoma formation. *Tyr:FC BRAF*$^{FA/+}$*; PTEN*$^{lox/lox}$ mice were treated as in A and analyzed 6 weeks post-treatment.

A

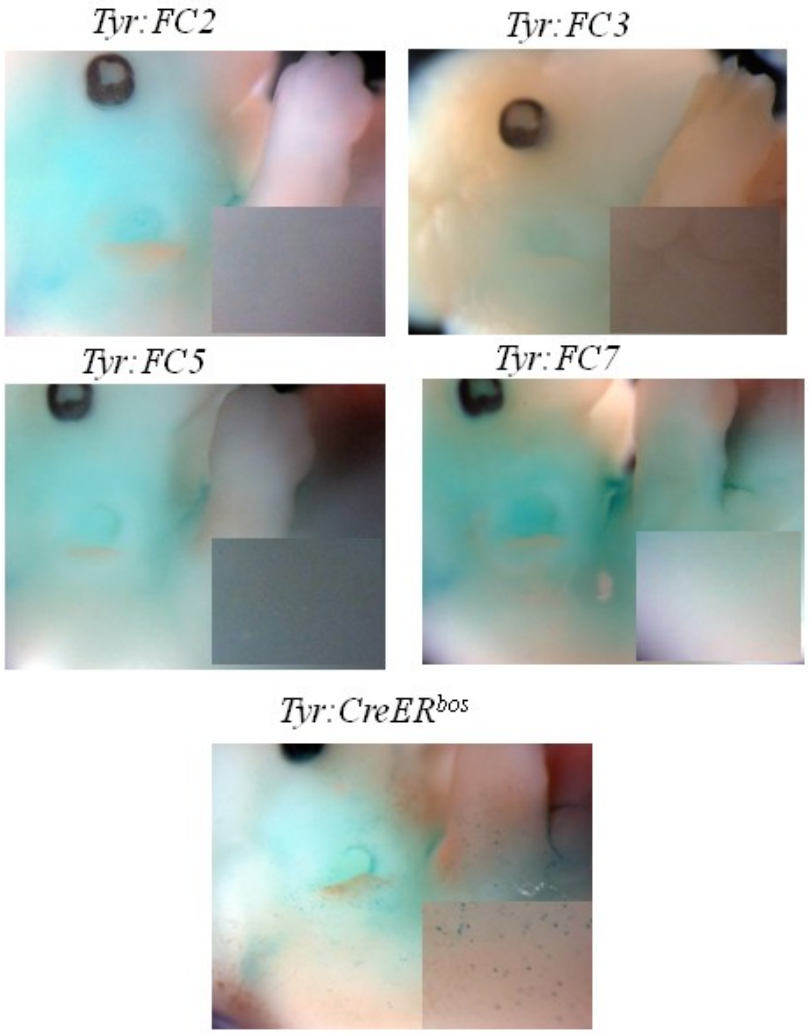
Tyr:FC2
Tyr:FC3
Tyr:FC5
Tyr:FC7
Tyr:CreER^bos

B

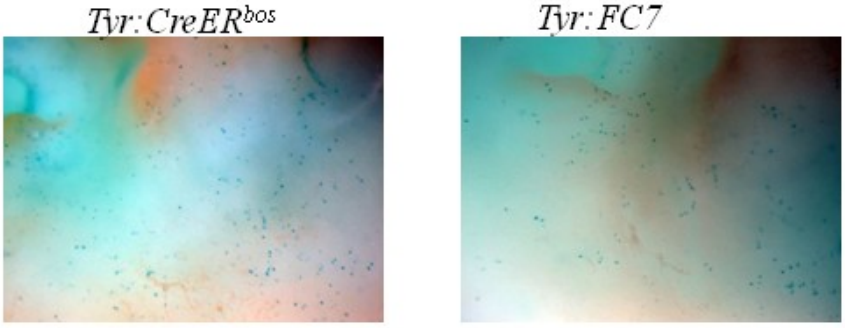
Tyr:CreER^bos
Tyr:FC7

Figure 3-9. *Tyr:FC* strains do not mediate β-galactasidase expression in melanocytes

Tyr:FC R26$^{Cre/+}$ and *Tyr:CreER*^{bos} *R26*$^{Cre/+}$ embryos were treated with tamoxifen on days E10.5, E11.5, E12.5 and analyzed on E13.5 by whole embryo X-gal staining. For all embryos tested, DNA was extracted from portions of the embryo body by proteinase K digestion and genotyped for *FlpPR, CreER* and *R26*^{Cre}. **(A)** Representative images of each strain tested. Insets correspond to magnified view of the right bottom corner of the image. **(B)** *Tyr:CreER*^{bos} and *Tyr:FC7* embryos at higher magnification. This strain 7 embryo was the only *Tyr:FC* embryo to test positive in this assay. The result was not reproducible.

TABLES

Table 2-1 Primers used for genotyping, cloning, and qRT-PCR analysis

Allele	Primers			Tm (°C)	Product Size (bp)
	Fwd or Rev	Primer	Sequence (5'--3')		
Genotyping					
BRAF^{CA} or BRAF^{FA}	Fwd	DD106	GGAAAGCCTGTCACGGGTC	59	Mut: 413, WT: 357
	Rev	DD105	AGATTCGTATGTCCTCTGAAAGTC		
PTEN^{lox}	Fwd	DD032	AAAAGTTCCCCTGCTGATGATTTGT	59	Mut: ~ 400, WT: 342
	Rev	DD033	TGTTTTTGACCAATTAAAGTAGGCTGTG		
	Fwd	DD034	CCCCCAAGTCAATTGTTAGGTCTGT		
Rosa26^{tm1Sor} (R26^{cre})	Fwd1	DD054	GCGAAGAGTTTGTCCTCAACC	59	Mut: 340, WT: 650
	Fwd2	DD055	GGAGCGGGAGAAATGGATATG		
	Rev	DD056	AAAGTCGCTCTGAGTTGTTAT		
FlpPR	Fwd	ML085	CGTGCTGGTTATTGTGCTGTCTC	66	Mut: 327, WT: no band
	Rev	ML086	TGTTGCTGATGATGGTGTTGTAGC		
CreER	Fwd	ML115	CCTGGAAGGGATTTTTGAAGCAAC	66	Mut: 396, WT: no band
	Rev	ML116	ATAGAGTATGGGGGGCTCAGCATC		
Cloning					
IVS	Fwd	ML021	CACCCCGCGGACGCGTCCGGACTCGAG AGATCTCCCGGGATCGATCCTGAGAAC TTCAGGGTGA	55	745
	Rev	ML022	GTAGGTACCTCCGGACGCGTCTCGAGCA TGCGGCCGAGGCCTGGATCCTGCGGCCG CACAATTCTTTGCCAAAATGATGAG		
PolyA	Fwd	ML024	CTCATCATTTTGGCAAAGAATTGTGCG GCCGCAGGATCCAGGCCTCGGCCGCATG CTCGAGACGCGTCCGGAGGTACCTAC	55	215
	Rev	ML025	GTAGGTACCTCCGGACGCGTCTCGAGCA TGCGGCCGACCAGACATGATAAGATAC ATTGAT		
qRT-PCR					
Cre	Fwd	ML132	TTCCCGCAGAACCTGAAGATG	62	150
	Rev	ML134	GCATAACCAGTGAAACAGCATTGC		

Table 2-2 Sequencing primers

Primers		Plasmids		
Name	**Sequence (5' → 3')**	**pTCE-B**	**pTCE[1]**	**pTFP[1]**
M13R	GGAAACAGCTATGACCATG		x	x
M13F	GTAAAACGACGGCCAGT	x	x	x
ML001	AAAAGACTCCAAATCCCCCCCG	x	x	x
ML002	CCTCAAAGTCATCCAGTAGGG	x	x	
ML003	CCTTGCTTTGGGGACATAG	x		
ML004	TGTGTATGTGGGTGTGTTTG	x	x	
ML005	CAGTATGACCCTTCAAGCAG	x	x	
ML006	AGAGTGAAGTCAAAGGTCTGC	x	x	
ML007	TCCAAGGGTCAGGAAGCAAC	x	x	x
ML008	CTGTAAGGCAAAAGACACCATC	x	x	
ML009	AGGTTTTTTGTTATTCCAGATG	x	x	
ML010	TGAAAACTTTGCCCCCTCC	x	x	x
ML011	CTCTTGCTACTAATCATCACTGC	x	x	
ML012	CATTGGTCTACTTGTCTGTTGC	x		
ML013	CTGACTGATGTGAGATGGAAT	x		
ML015	CCAAAAGGGAACATAACAGC	x		
ML016	GGAATACCAAATGGCTGAGAA	x		
ML017	GCAAGACCAAGAAACCTCTC	x	x	
ML019	AAGCAGCATAGAGAAGGGAG	x	x	
ML095	GTTACCTCACTATGGGCTATG			x
ML096	AATATTTCCACGCCAGCCAG		x	x
ML137	GTGGGTATAGGGAACTTTCAG	x	x	
ML138	CTAATTTCCACTGAGGTATC		x	
ML139	ATGCCCAGAAGACCATCTC	x	x	
ML140	TCTAGATTCTGAATACAAGCC		x	
ML141	GAAACTTTATGCATTGAAGCAG		x	
ML142	TTAAACTCCTGTCTTCAGGC	x	x	
ML143	GAGTCATAGAAGAGCAGAATAGC	x	x	
DD009	CAAACGCTCTAAGAAGAACAGC		x	
DD010	TGCTGGCTACATCATCTCGG		x	
DD011	TCACTGAAGGGTCTGGTAGG		x	
DD012	AGGGTGCTGGACAGAAATG		x	
DD013	GCCAGAGATTCACTTTTTCACC			x
DD014	GAACAGCGGATGAAAGAATC			x
DD015	TCACATCTGGTTCAATGCTC			x

[1] pTCE and pTFP refer to pTyr:CreER and pTyr:FlpPR

Table 2-2 continued.

Primers		Plasmids		
Name	**Sequence (5' → 3')**	**pTCE-B**	**pTCE[1]**	**pTFP[1]**
DD016	CTGGGTTTGACTTCGTAGC			x
DD018	TGGCAGAACGAAAACGCTG		x	
DD020	ATTGCTGTCACTTGGTCGTGGC		x	
DD021	GGCAAAACAGGTAGTTATTCGG		x	
DD022	GAGTTCACCATCATCCCTTAC			x
DD023	AAGAGAGTGAACAGGACCG			x
DD024	ATGTCGGTGATGTCGCTCTG			x
DD025	TGATAGCGAAGATGGGGTAG			x
DD062	ATCTTCAGGTTCTGCGG	x		
DD063	CGGGCTCTACTTCATCGC	x		
DD068	GAGTGATGAGGTTCGCAAG	x		
DD069	GTGAAAGAAACAAAATTATCATGA	x		
DD070	GGAGACAATGGTTGTCAACAGAG	x		
DD071	CATGAGGGTCCATGGTGATAC	x		
DD072	TCTTCCAGAGACTTCAGGG	x		
DD073	AGGCACACAAACTCCTCTCC	x		
DD074	ATGTGCCTGATGTGGGAGAGGATG	x		
DD095	ATGACTAACTTTTTCTTGGAG	x		
DD096	AGAAAGAGCAGGACTGGTG	x	x	x
DD097	CACTGTTCTTTCTACCTGCC	x	x	
DD098	GGATGGTTTGAATAGCACTG	x		
DD099	TAACACAGGACCTCGTTCC	x	x	

[1] pTCE and pTFP refer to pTyr:CreER and pTyr:FlpPR

Table 2-3 Non-quantitative RT-PCR primers

Gene	Primers		Spanning Intron or Within Exon	Outer vs inner primers[1]	Product size (bp)
	Position & Number	Sequence			
Tubulin	Fwd ML52	AAGACCATTGGGGGAGGAGATG	Within Exon	N/A	370
	Rev ML53	TTCCGTAATCCACAGAGAGCCG			
Tyrosinase	Fwd ML81	GGTCGTCACCCTGAAAATCCTAAC	Spanning Intron	N/A	Unspl: -/-, Spl: 293
	Rev ML82	GAGTGGACTGGCAAATCCTTCC			
Tyr:CreER	Fwd ML111	CACTCATTAACCTATTGGTGCAG	Spanning Intron	Outer	Unspl: 1009 Spl: 437
	Rev ML113	GAACATCTTCAGGTTCTGCG			
Tyr:CreER	Fwd ML110	AGGCACTAGTTCTAGGGGGATC	Spanning Intron	Inner	Unspl: 888 Spl: 316
	Rev ML112	GCATTTTCCAGGTATGCTCAG			
Tyr:CreER^{bos}	Fwd ML111	CACTCATTAACCTATTGGTGCAG	Spanning Intron	Outer	Unspl: 1047 Spl: 475
	Rev ML113	GAACATCTTCAGGTTCTGCG			
Tyr:CreER^{bos}	Fwd ML110	AGGCACTAGTTCTAGGGGGATC	Spanning Intron	Inner	Unspl: 926 Spl: 354
	Rev ML112	GCATTTTCCAGGTATGCTCAG			
Tyr:FlpPR	Fwd ML111	CACTCATTAACCTATTGGTGCAG	Spanning Intron	Outer	Unspl: 1126 Spli: 554
	Rev ML106	CGTTGTAAGGGATGATGGTGAACTC			
Tyr:FlpPR[2]	Fwd ML110	AGGCACTAGTTCTAGGGGGATC	Spanning Intron	Inner	Unspl: 1000 Spl: 428
	Rev ML108	TGTTGCTGATGATGGTGTTGTAGC			

[1] Primers for nested PCRs. Outer refers to primers for the first PCR and inner refers to primers for the second PCR.

[2] The second nested PCR for Tyr:FlpPR was the only reaction with an annealing temperature of 65°C. All other PCRs were completed using an annealing temperature of 62°C

Table 2-4 Allelic nomenclature

Allele	Nomenclature
Cre-Activated *BRAF*^{V600E}	*BRAF*^{CA}
Flp-Activated *BRAF*^{V600E}	*BRAF*^{FA}
Pten^{lox4-5}	*PTEN*^{lox}
Rosa26^{tm1Sor}	*R26*^{cre}
Tg(Tyr-cre/ERT2)13Bos/J	*Tyr:CreER*^{bos}
Tyr:FlpPR/Tyr:CreER	*Tyr:FC*

Table 3-1. Overview of functional analyses completed on *Tyr:CreER*^{bos} control strain and *Tyr:FC* experimental strains

Strain	Nevi		Melanoma		Whole Embryo X-Gal Staining
	BRAF$^{CA/+}$	***BRAF***$^{FA/+}$	***BRAF***$^{CA/+}$***; PTEN***$^{lox/lox}$	***BRAF***$^{FA/+}$***; PTEN***$^{lox/lox}$	
Tyr:FC2	0/10	0/11	--	--	0/6
Tyr:FC3	0/11	0/5	0/4	--	0/8
Tyr:FC5	0/13	--	0/1	--	0/12
Tyr:FC6	0/11	0/2	0/4	--	--
Tyr:FC7	0/5	0/4	0/4	0/5	1/10
Tyr:CreER^{bos}	14/14	--	8/8	--	38/38

Table 3-2. Testing conditions for activating FlpPR *in utero*

Mifepristone Amount (relative molar percentage of tamoxifen)[1]	Progesterone or DMSO	Embryonic Days of Treatment	Embryonic Day of Analysis	Result
--	DMSO[2]	10.5, 11.5, 12.5	13.5	Non-abortive
--	DMSO[3]	10.5, 11.5, 12.5	13.5	Non-abortive
--	Progesterone	10.5, 11.5, 12.5	13.5	Non-abortive
100%	--	10.5, 11.5, 12.5	13.5	Abortive
15%	--	10.5, 11.5, 12.5	13.5	Abortive
100%	Progesterone	10.5, 11.5, 12.5	13.5	Abortive
50%	Progesterone	10.5, 11.5, 12.5	13.5	Abortive
25%	Progesterone	10.5, 11.5, 12.5	13.5	Abortive
15%	Progesterone	10.5, 11.5, 12.5	13.5	Abortive
15%	Progesterone	11.5, 12.5	13.5	Abortive
15%	Progesterone	10.5	13.5	Abortive
15%	Progesterone[4]	12.5	13.5	Abortive
15%	Progesterone	13.5	14.5	Abortive

[1] Mifepristone was administered to the same molar concentration as standard tamoxifen (5.4μmoles per 40g mouse weight)

[2] Inject 16.5μL per 40g mouse weight

[3] Inject 2.5μL DMSO per 40g mouse weight

[4] Progesterone was administered 5 hours prior to mifepristone injection

REFERENCES

1 Kuphal, S. & Bosserhoff, A. Recent progress in understanding the pathology of malignant melanoma. *J Pathol* **219**, 400-409 (2009).

2 Jemal, A., Siegel, R., Xu, J. & Ward, E. Cancer statistics, 2010. *CA Cancer J Clin* **60**, 277-300 (2010).

3 Ibrahim, N. & Haluska, F. G. Molecular pathogenesis of cutaneous melanocytic neoplasms. *Annu Rev Pathol* **4**, 551-579 (2009).

4 Bauer, J. & Garbe, C. Acquired melanocytic nevi as risk factor for melanoma development. A comprehensive review of epidemiological data. *Pigment Cell Res* **16**, 297-306 (2003).

5 de Snoo, F. A., Bergman, W. & Gruis, N. A. Familial melanoma: a complex disorder leading to controversy on DNA testing. *Fam Cancer* **2**, 109-116 (2003).

6 Gray-Schopfer, V., Wellbrock, C. & Marais, R. Melanoma biology and new targeted therapy. *Nature* **445**, 851-857 (2007).

7 Chin, L. The genetics of malignant melanoma: lessons from mouse and man. *Nat Rev Cancer* **3**, 559-570 (2003).

8 Michaloglou, C. *et al.* BRAFE600-associated senescence-like cell cycle arrest of human naevi. *Nature* **436**, 720-724 (2005).

9 Nguyen, D. X., Bos, P. D. & Massague, J. Metastasis: from dissemination to organ-specific colonization. *Nat Rev Cancer* **9**, 274-284 (2009).

10 Avril, M. F. *et al.* Fotemustine compared with dacarbazine in patients with disseminated malignant melanoma: a phase III study. *J Clin Oncol* **22**, 1118-1125 (2004).

11 Bedikian, A. Y. *et al.* Bcl-2 antisense (oblimersen sodium) plus dacarbazine in patients with advanced melanoma: the Oblimersen Melanoma Study Group. *J Clin Oncol* **24**, 4738-4745 (2006).

12 Chapman, P. B. *et al.* Phase III multicenter randomized trial of the Dartmouth regimen versus dacarbazine in patients with metastatic melanoma. *J Clin Oncol* **17**, 2745-2751 (1999).

13 Middleton, M. R. *et al.* Randomized phase III study of temozolomide versus dacarbazine in the treatment of patients with advanced metastatic malignant melanoma. *J Clin Oncol* **18**, 158-166 (2000).

14 Bollag, G. *et al.* Clinical efficacy of a RAF inhibitor needs broad target blockade in BRAF-mutant melanoma. *Nature* **467**, 596-599 (2010).

15 Chapman, P. B. *et al.* Improved survival with vemurafenib in melanoma with BRAF V600E mutation. *N Engl J Med* **364**, 2507-2516 (2011).

16 Johannessen, C. M. *et al.* COT drives resistance to RAF inhibition through MAP kinase pathway reactivation. *Nature* **468**, 968-972 (2010).

17 Montagut, C. *et al.* Elevated CRAF as a potential mechanism of acquired resistance to BRAF inhibition in melanoma. *Cancer Res* **68**, 4853-4861 (2008).

18 Nazarian, R. *et al.* Melanomas acquire resistance to B-RAF(V600E) inhibition by RTK or N-RAS upregulation. *Nature* **468**, 973-977 (2010).

19 Villanueva, J. *et al.* Acquired resistance to BRAF inhibitors mediated by a RAF kinase switch in melanoma can be overcome by cotargeting MEK and IGF-1R/PI3K. *Cancer Cell* **18**, 683-695 (2010).

20 Wagle, N. *et al.* Dissecting therapeutic resistance to RAF inhibition in melanoma by tumor genomic profiling. *J Clin Oncol* **29**, 3085-3096 (2011).
21 Dankort, D. *et al.* BrafV600E cooperates with Pten loss to induce metastatic melanoma. *Nature Genetics* **41**, 544-552 (2009).
22 Soufir, N. *et al.* Prevalence of p16 and CDK4 germline mutations in 48 melanoma-prone families in France. The French Familial Melanoma Study Group. *Hum Mol Genet* **7**, 209-216 (1998).
23 Chao, E., Gabree, M. & Tsao, H. in *Principles of Clinical Cancer Genetics: A Handbook from the Massachusetts General Hospital* (eds Daniel Chung & Daniel Haber) 129-144 (Springer; 1st Edition, Boston, MA, 2010).
24 Sharpless, E. & Chin, L. The INK4a/ARF locus and melanoma. *Oncogene* **22**, 3092-3098 (2003).
25 Quelle, D. E., Zindy, F., Ashmun, R. A. & Sherr, C. J. Alternative reading frames of the INK4a tumor suppressor gene encode two unrelated proteins capable of inducing cell cycle arrest. *Cell* **83**, 993-1000 (1995).
26 Pomerantz, J. *et al.* The Ink4a tumor suppressor gene product, p19Arf, interacts with MDM2 and neutralizes MDM2's inhibition of p53. *Cell* **92**, 713-723 (1998).
27 Haupt, Y., Maya, R., Kazaz, A. & Oren, M. Mdm2 promotes the rapid degradation of p53. *Nature* **387**, 296-299 (1997).
28 Offer, H. *et al.* The onset of p53-dependent DNA repair or apoptosis is determined by the level of accumulated damaged DNA. *Carcinogenesis* **23**, 1025-1032 (2002).
29 Efeyan, A. & Serrano, M. p53: guardian of the genome and policeman of the oncogenes. *Cell Cycle* **6**, 1006-1010 (2007).
30 Zhang, Y., Xiong, Y. & Yarbrough, W. G. ARF promotes MDM2 degradation and stabilizes p53: ARF-INK4a locus deletion impairs both the Rb and p53 tumor suppression pathways. *Cell* **92**, 725-734 (1998).
31 Stott, F. J. *et al.* The alternative product from the human CDKN2A locus, p14(ARF), participates in a regulatory feedback loop with p53 and MDM2. *Embo J* **17**, (1998).
32 Serrano, M., Hannon, G. J. & Beach, D. A new regulatory motif in cell-cycle control causing specific inhibition of cyclin D/CDK4. *Nature* **366**, 704-707 (1993).
33 Chellappan, S. P., Hiebert, S., Mudryj, M., Horowitz, J. M. & Nevins, J. R. The E2F transcription factor is a cellular target for the RB protein. *Cell* **65**, 1053-1061 (1991).
34 Zuo, L. *et al.* Germline mutations in the p16INK4a binding domain of CDK4 in familial melanoma. *Nature genetics* **12**, 97-99 (1996).
35 Castellano, M. *et al.* CDKN2A/p16 is inactivated in most melanoma cell lines. *Cancer Res* **57**, 4868-4875 (1997).
36 Orlow, I. *et al.* CDKN2A germline mutations in individuals with cutaneous malignant melanoma. *The Journal of investigative dermatology* **127**, 1234-1243 (2007).
37 Randerson-Moor, J. A. *et al.* A germline deletion of p14(ARF) but not CDKN2A in a melanoma-neural system tumour syndrome family. *Hum Mol Genet* **10**, 55-62 (2001).
38 Rizos, H. *et al.* A melanoma-associated germline mutation in exon 1beta inactivates p14ARF. *Oncogene* **20**, 5543-5547 (2001).
39 Castresana, J. S. *et al.* Lack of allelic deletion and point mutation as mechanisms of p53 activation in human malignant melanoma. *Int J Cancer* **55**, 562-565 (1993).

40 Lin, J. Y. & Fisher, D. E. Melanocyte biology and skin pigmentation. *Nature* **445**, 843-850 (2007).
41 Chakraborty, A. K. *et al.* UV light and MSH receptors. *Ann N Y Acad Sci* **885**, 100-116 (1999).
42 Busca, R. *et al.* Ras mediates the cAMP-dependent activation of extracellular signal-regulated kinases (ERKs) in melanocytes. *Embo J* **19**, 2900-2910 (2000).
43 Bertolotto, C. *et al.* Microphthalmia gene product as a signal transducer in cAMP-induced differentiation of melanocytes. *J Cell Biol* **142**, 827-835 (1998).
44 Loercher, A. E., Tank, E. M., Delston, R. B. & Harbour, J. W. MITF links differentiation with cell cycle arrest in melanocytes by transcriptional activation of INK4A. *J Cell Biol* **168**, 35-40 (2005).
45 Rana, B. K. *et al.* High polymorphism at the human melanocortin 1 receptor locus. *Genetics* **151**, 1547-1557 (1999).
46 Ringholm, A. *et al.* Pharmacological characterization of loss of function mutations of the human melanocortin 1 receptor that are associated with red hair. *The Journal of investigative dermatology* **123**, 917-923 (2004).
47 Goldstein, A. M. *et al.* Linkage of cutaneous malignant melanoma/dysplastic nevi to chromosome 9p, and evidence for genetic heterogeneity. *Am J Hum Genet* **54**, 489-496 (1994).
48 Cachia, A. R., Indsto, J. O., McLaren, K. M., Mann, G. J. & Arends, M. J. CDKN2A mutation and deletion status in thin and thick primary melanoma. *Clin Cancer Res* **6**, 3511-3515 (2000).
49 Curtin, J. A., Busam, K., Pinkel, D. & Bastian, B. C. Somatic activation of KIT in distinct subtypes of melanoma. *J Clin Oncol* **24**, 4340-4346 (2006).
50 Chabot, B., Stephenson, D. A., Chapman, V. M., Besmer, P. & Bernstein, A. The proto-oncogene c-kit encoding a transmembrane tyrosine kinase receptor maps to the mouse W locus. *Nature* **335**, 88-89 (1988).
51 Hemesath, T. J., Price, E. R., Takemoto, C., Badalian, T. & Fisher, D. E. MAP kinase links the transcription factor Microphthalmia to c-Kit signalling in melanocytes. *Nature* **391**, 298-301 (1998).
52 Graziani, A., Gramaglia, D., dalla Zonca, P. & Comoglio, P. M. Hepatocyte growth factor/scatter factor stimulates the Ras-guanine nucleotide exchanger. *J Biol Chem* **268**, 9165-9168 (1993).
53 Tsang, M. & Dawid, I. B. Promotion and attenuation of FGF signaling through the Ras-MAPK pathway. *Sci STKE* **2004**, pe17 (2004).
54 McKay, M. M. & Morrison, D. K. Integrating signals from RTKs to ERK/MAPK. *Oncogene* **26**, 3113-3121 (2007).
55 Marshall, C. J. Ras effectors. *Curr Opin Cell Biol* **8**, 197-204 (1996).
56 Gray-Schopfer, V. C., da Rocha Dias, S. & Marais, R. The role of B-RAF in melanoma. *Cancer Metastasis Rev* **24**, 165-183 (2005).
57 Wellbrock, C., Karasarides, M. & Marais, R. The RAF proteins take centre stage. *Nat Rev Mol Cell Biol* **5**, 875-885 (2004).
58 Bonner, T. I. *et al.* Structure and biological activity of human homologs of the raf/mil oncogene. *Mol Cell Biol* **5**, 1400-1407 (1985).
59 Michaloglou, C., Vredeveld, L. C., Mooi, W. J. & Peeper, D. S. BRAF(E600) in benign and malignant human tumours. *Oncogene* **27**, 877-895 (2008).

60 Marais, R., Light, Y., Paterson, H. F., Mason, C. S. & Marshall, C. J. Differential regulation of Raf-1, A-Raf, and B-Raf by oncogenic ras and tyrosine kinases. *J Biol Chem* **272**, 4378-4383 (1997).
61 Lin, S. L., Le, T. X. & Cowen, D. S. SptP, a Salmonella typhimurium type III-secreted protein, inhibits the mitogen-activated protein kinase pathway by inhibiting Raf activation. *Cell Microbiol* **5**, 267-275 (2003).
62 Demunter, A., Stas, M., Degreef, H., De Wolf-Peeters, C. & van den Oord, J. J. Analysis of N- and K-ras mutations in the distinctive tumor progression phases of melanoma. *The Journal of investigative dermatology* **117**, 1483-1489 (2001).
63 Davies, H. *et al.* Mutations of the BRAF gene in human cancer. *Nature* **417**, 949-954 (2002).
64 Wan, P. T. *et al.* Mechanism of activation of the RAF-ERK signaling pathway by oncogenic mutations of B-RAF. *Cell* **116**, 855-867 (2004).
65 Marais, R. *et al.* Inducible expression of (V600E)Braf using tyrosinase-driven Cre recombinase results in embryonic lethality. *Pigm Cell Melanoma R* **23**, 112-120 (2010).
66 Ichii-Nakato, N. *et al.* High frequency of BRAFV600E mutation in acquired nevi and small congenital nevi, but low frequency of mutation in medium-sized congenital nevi. *The Journal of investigative dermatology* **126**, 2111-2118 (2006).
67 Brash, D. E. *et al.* A role for sunlight in skin cancer: UV-induced p53 mutations in squamous cell carcinoma. *Proc Natl Acad Sci U S A* **88**, 10124-10128 (1991).
68 Kimura, E. T. *et al.* High prevalence of BRAF mutations in thyroid cancer: genetic evidence for constitutive activation of the RET/PTC-RAS-BRAF signaling pathway in papillary thyroid carcinoma. *Cancer Res* **63**, 1454-1457 (2003).
69 Rajagopalan, H. *et al.* Tumorigenesis: RAF/RAS oncogenes and mismatch-repair status. *Nature* **418**, 934 (2002).
70 Singer, G. *et al.* Mutations in BRAF and KRAS characterize the development of low-grade ovarian serous carcinoma. *J Natl Cancer Inst* **95**, 484-486 (2003).
71 Pollock, P. M. *et al.* High frequency of BRAF mutations in nevi. *Nature Genetics* **33**, 19-20 (2003).
72 Tsao, H., Goel, V., Wu, H., Yang, G. & Haluska, F. G. Genetic interaction between NRAS and BRAF mutations and PTEN/MMAC1 inactivation in melanoma. *The Journal of investigative dermatology* **122**, 337-341 (2004).
73 Hayflick, L. & Moorhead, P. S. The serial cultivation of human diploid cell strains. *Exp Cell Res* **25**, 585-621 (1961).
74 Hayflick, L. The Limited in Vitro Lifetime of Human Diploid Cell Strains. *Exp Cell Res* **37**, 614-636 (1965).
75 Bodnar, A. G. *et al.* Extension of life-span by introduction of telomerase into normal human cells. *Science* **279**, 349-352 (1998).
76 d'Adda di Fagagna, F. *et al.* A DNA damage checkpoint response in telomere-initiated senescence. *Nature* **426**, 194-198 (2003).
77 Campisi, J. & d'Adda di Fagagna, F. Cellular senescence: when bad things happen to good cells. *Nat Rev Mol Cell Biol* **8**, 729-740 (2007).
78 Serrano, M., Lin, A. W., McCurrach, M. E., Beach, D. & Lowe, S. W. Oncogenic ras provokes premature cell senescence associated with accumulation of p53 and p16INK4a. *Cell* **88**, 593-602 (1997).

79 Newbold, R. F. & Overell, R. W. Fibroblast immortality is a prerequisite for transformation by EJ c-Ha-ras oncogene. *Nature* **304**, 648-651 (1983).
80 Land, H., Parada, L. F. & Weinberg, R. A. Tumorigenic conversion of primary embryo fibroblasts requires at least two cooperating oncogenes. *Nature* **304**, 596-602 (1983).
81 Ruley, H. E. Adenovirus early region 1A enables viral and cellular transforming genes to transform primary cells in culture. *Nature* **304**, 602-606 (1983).
82 Lin, A. W. *et al.* Premature senescence involving p53 and p16 is activated in response to constitutive MEK/MAPK mitogenic signaling. *Gene Dev* **12**, 3008-3019 (1998).
83 Zhu, J., Woods, D., McMahon, M. & Bishop, J. M. Senescence of human fibroblasts induced by oncogenic Raf. *Gene Dev* **12**, 2997-3007 (1998).
84 Rizos, H. & Scurr, L. L. in *Melanoma Development: Molecular Biology, Genetics and Clinical Application* (ed A. Bosserhoff) (Springer, 2011).
85 Irani, K. *et al.* Mitogenic signaling mediated by oxidants in Ras-transformed fibroblasts. *Science* **275**, 1649-1652 (1997).
86 Lee, A. C. *et al.* Ras proteins induce senescence by altering the intracellular levels of reactive oxygen species. *J Biol Chem* **274**, 7936-7940 (1999).
87 Dimri, G. P. *et al.* A biomarker that identifies senescent human cells in culture and in aging skin in vivo. *Proc Natl Acad Sci U S A* **92**, 9363-9367 (1995).
88 Kurz, D. J., Decary, S., Hong, Y. & Erusalimsky, J. D. Senescence-associated (beta)-galactosidase reflects an increase in lysosomal mass during replicative ageing of human endothelial cells. *J Cell Sci* **113 (Pt 20)**, 3613-3622 (2000).
89 Campisi, J. Senescent cells, tumor suppression, and organismal aging: good citizens, bad neighbors. *Cell* **120**, 513-522 (2005).
90 Collado, M. & Serrano, M. The power and the promise of oncogene-induced senescence markers. *Nat Rev Cancer* **6**, 472-476 (2006).
91 Narita, M. *et al.* Rb-mediated heterochromatin formation and silencing of E2F target genes during cellular senescence. *Cell* **113**, 703-716 (2003).
92 Jackson, J. G. & Pereira-Smith, O. M. p53 is preferentially recruited to the promoters of growth arrest genes p21 and GADD45 during replicative senescence of normal human fibroblasts. *Cancer Res* **66**, 8356-8360 (2006).
93 Kuilman, T. & Peeper, D. S. Senescence-messaging secretome: SMS-ing cellular stress. *Nat Rev Cancer* **9**, 81-94 (2009).
94 Kuilman, T. *et al.* Oncogene-induced senescence relayed by an interleukin-dependent inflammatory network. *Cell* **133**, 1019-1031 (2008).
95 Kodaki, T. *et al.* The activation of phosphatidylinositol 3-kinase by Ras. *Curr Biol* **4**, 798-806 (1994).
96 Vivanco, I. & Sawyers, C. L. The phosphatidylinositol 3-Kinase AKT pathway in human cancer. *Nat Rev Cancer* **2**, 489-501 (2002).
97 Stokoe, D. *et al.* Dual role of phosphatidylinositol-3,4,5-trisphosphate in the activation of protein kinase B. *Science* **277**, 567-570 (1997).
98 Alessi, D. R. *et al.* Characterization of a 3-phosphoinositide-dependent protein kinase which phosphorylates and activates protein kinase Balpha. *Curr Biol* **7**, 261-269 (1997).
99 Chan, T. O. & Tsichlis, P. N. PDK2: a complex tail in one Akt. *Sci STKE* **2001**, pe1 (2001).
100 Datta, S. R. *et al.* Akt phosphorylation of BAD couples survival signals to the cell-intrinsic death machinery. *Cell* **91**, 231-241 (1997).

101 Dhawan, P., Singh, A. B., Ellis, D. L. & Richmond, A. Constitutive activation of Akt/protein kinase B in melanoma leads to up-regulation of nuclear factor-kappaB and tumor progression. *Cancer Res* **62**, 7335-7342 (2002).
102 Diehl, J. A., Cheng, M., Roussel, M. F. & Sherr, C. J. Glycogen synthase kinase-3beta regulates cyclin D1 proteolysis and subcellular localization. *Gene Dev* **12**, 3499-3511 (1998).
103 Madhunapantula, S. V. & Robertson, G. P. The PTEN-AKT3 signaling cascade as a therapeutic target in melanoma. *Pigm Cell Melanoma R* **22**, 400-419 (2009).
104 Stahl, J. M. *et al.* Deregulated Akt3 activity promotes development of malignant melanoma. *Cancer Res* **64**, 7002-7010 (2004).
105 Engelman, J. A. Targeting PI3K signalling in cancer: opportunities, challenges and limitations. *Nat Rev Cancer* **9**, 550-562 (2009).
106 Omholt, K., Krockel, D., Ringborg, U. & Hansson, J. Mutations of PIK3CA are rare in cutaneous melanoma. *Melanoma Res* **16**, 197-200 (2006).
107 Li, D. M. & Sun, H. TEP1, encoded by a candidate tumor suppressor locus, is a novel protein tyrosine phosphatase regulated by transforming growth factor beta. *Cancer Res* **57**, 2124-2129 (1997).
108 Li, J. *et al.* PTEN, a putative protein tyrosine phosphatase gene mutated in human brain, breast, and prostate cancer. *Science* **275**, 1943-1947 (1997).
109 Steck, P. A. *et al.* Identification of a candidate tumour suppressor gene, MMAC1, at chromosome 10q23.3 that is mutated in multiple advanced cancers. *Nature Genetics* **15**, 356-362 (1997).
110 Tsao, H., Mihm, M. C., Jr. & Sheehan, C. PTEN expression in normal skin, acquired melanocytic nevi, and cutaneous melanoma. *J Am Acad Dermatol* **49**, 865-872 (2003).
111 Tamguney, T. & Stokoe, D. New insights into PTEN. *J Cell Sci* **120**, 4071-4079 (2007).
112 Maehama, T. & Dixon, J. E. The tumor suppressor, PTEN/MMAC1, dephosphorylates the lipid second messenger, phosphatidylinositol 3,4,5-trisphosphate. *J Biol Chem* **273**, 13375-13378 (1998).
113 Ramaswamy, S. *et al.* Regulation of G1 progression by the PTEN tumor suppressor protein is linked to inhibition of the phosphatidylinositol 3-kinase/Akt pathway. *Proc Natl Acad Sci U S A* **96**, 2110-2115 (1999).
114 Marsh, D. J. *et al.* Germline mutations in PTEN are present in Bannayan-Zonana syndrome. *Nature genetics* **16**, 333-334 (1997).
115 Nelen, M. R. *et al.* Germline mutations in the PTEN/MMAC1 gene in patients with Cowden disease. *Hum Mol Genet* **6**, 1383-1387 (1997).
116 Liaw, D. *et al.* Germline mutations of the PTEN gene in Cowden disease, an inherited breast and thyroid cancer syndrome. *Nature genetics* **16**, 64-67 (1997).
117 Bonneau, D. & Longy, M. Mutations of the human PTEN gene. *Hum Mutat* **16**, 109-122 (2000).
118 Carnero, A., Blanco-Aparicio, C., Renner, O., Link, W. & Leal, J. F. The PTEN/PI3K/AKT signalling pathway in cancer, therapeutic implications. *Curr Cancer Drug Targets* **8**, 187-198 (2008).
119 Zhou, X. P. *et al.* Epigenetic PTEN silencing in malignant melanomas without PTEN mutation. *Am J Pathol* **157**, 1123-1128 (2000).
120 Di Cristofano, A., Pesce, B., Cordon-Cardo, C. & Pandolfi, P. P. Pten is essential for embryonic development and tumour suppression. *Nature Genetics* **19**, 348-355 (1998).

121 Tamura, M. *et al.* Inhibition of cell migration, spreading, and focal adhesions by tumor suppressor PTEN. *Science* **280**, 1614-1617 (1998).
122 Freeman, D. J. *et al.* PTEN tumor suppressor regulates p53 protein levels and activity through phosphatase-dependent and -independent mechanisms. *Cancer Cell* **3**, 117-130 (2003).
123 Dai, D. L., Martinka, M. & Li, G. Prognostic significance of activated Akt expression in melanoma: a clinicopathologic study of 292 cases. *J Clin Oncol* **23**, 1473-1482 (2005).
124 Tsao, H., Zhang, X., Fowlkes, K. & Haluska, F. G. Relative reciprocity of NRAS and PTEN/MMAC1 alterations in cutaneous melanoma cell lines. *Cancer Res* **60**, 1800-1804 (2000).
125 Murisier, F., Guichard, S. & Beermann, F. Distinct distal regulatory elements control tyrosinase expression in melanocytes and the retinal pigment epithelium. *Dev Biol* **303**, 838-847 (2007).
126 Ruppert, S., Muller, G., Kwon, B. & Schutz, G. Multiple transcripts of the mouse tyrosinase gene are generated by alternative splicing. *Embo J* **7**, 2715-2722 (1988).
127 Hearing, V. J., Jr. Mammalian monophenol monooxygenase (tyrosinase): purification, properties, and reactions catalyzed. *Methods Enzymol* **142**, 154-165 (1987).
128 Beermann, F., Schmid, E., Ganss, R., Schutz, G. & Ruppert, S. Molecular characterization of the mouse tyrosinase gene: pigment cell-specific expression in transgenic mice. *Pigment Cell Res* **5**, 295-299 (1992).
129 Tonks, I. D. *et al.* Tyrosinase-Cre mice for tissue-specific gene ablation in neural crest and neuroepithelial-derived tissues. *Genesis* **37**, 131-138 (2003).
130 Kluppel, M. *et al.* The mouse tyrosinase promoter is sufficient for expression in melanocytes and in the pigmented epithelium of the retina. *Proc Natl Acad Sci U S A* **88**, 3777-3781 (1991).
131 Beermann, F. *et al.* Rescue of the albino phenotype by introduction of a functional tyrosinase gene into mice. *Embo J* **9**, 2819-2826 (1990).
132 Tanaka, S., Yamamoto, H., Takeuchi, S. & Takeuchi, T. Melanization in albino mice transformed by introducing cloned mouse tyrosinase gene. *Development* **108**, 223-227 (1990).
133 Beermann, F., Schmid, E. & Schutz, G. Expression of the mouse tyrosinase gene during embryonic development: recapitulation of the temporal regulation in transgenic mice. *Proc Natl Acad Sci U S A* **89**, 2809-2813 (1992).
134 Jackson, I. J. & Bennett, D. C. Identification of the albino mutation of mouse tyrosinase by analysis of an in vitro revertant. *Proc Natl Acad Sci U S A* **87**, 7010-7014 (1990).
135 Yokoyama, T. *et al.* Conserved cysteine to serine mutation in tyrosinase is responsible for the classical albino mutation in laboratory mice. *Nucleic Acids Res* **18**, 7293-7298 (1990).
136 Ganss, R., Schutz, G. & Beermann, F. The mouse tyrosinase gene. Promoter modulation by positive and negative regulatory elements. *J Biol Chem* **269**, 29808-29816 (1994).
137 Lowings, P., Yavuzer, U. & Goding, C. R. Positive and negative elements regulate a melanocyte-specific promoter. *Mol Cell Biol* **12**, 3653-3662 (1992).

138 Hodgkinson, C. A. *et al.* Mutations at the mouse microphthalmia locus are associated with defects in a gene encoding a novel basic-helix-loop-helix-zipper protein. *Cell* **74**, 395-404 (1993).
139 Jackson, I. J. *et al.* Genetics and molecular biology of mouse pigmentation. *Pigment Cell Res* **7**, 73-80 (1994).
140 Porter, S., Larue, L. & Mintz, B. Mosaicism of tyrosinase-locus transcription and chromatin structure in dark vs. light melanocyte clones of homozygous chinchilla-mottled mice. *Dev Genet* **12**, 393-402 (1991).
141 Porter, S. D. & Meyer, C. J. A distal tyrosinase upstream element stimulates gene expression in neural-crest-derived melanocytes of transgenic mice: position-independent and mosaic expression. *Development* **120**, 2103-2111 (1994).
142 Forrester, W. C. *et al.* A deletion of the human beta-globin locus activation region causes a major alteration in chromatin structure and replication across the entire beta-globin locus. *Gene Dev* **4**, 1637-1649 (1990).
143 Vyas, P. *et al.* Cis-acting sequences regulating expression of the human alpha-globin cluster lie within constitutively open chromatin. *Cell* **69**, 781-793 (1992).
144 Ganss, R., Montoliu, L., Monaghan, A. P. & Schutz, G. A cell-specific enhancer far upstream of the mouse tyrosinase gene confers high level and copy number-related expression in transgenic mice. *Embo J* **13**, 3083-3093 (1994).
145 Montoliu, L., Umland, T. & Schutz, G. A locus control region at -12 kb of the tyrosinase gene. *Embo J* **15**, 6026-6034 (1996).
146 Murisier, F., Guichard, S. & Beermann, F. The tyrosinase enhancer is activated by Sox10 and Mitf in mouse melanocytes. *Pigment Cell Res* **20**, 173-184 (2007).
147 Camacho-Hubner, A. & Beermann, F. Increased transgene expression by the mouse tyrosinase enhancer is restricted to neural crest-derived pigment cells. *Genesis* **29**, 180-187 (2001).
148 Gasser, S. M. & Laemmli, U. K. A glimpse at chromosomal order. *Trends in Genetics* **3**, 16-22 (1987).
149 Wilson, C., Bellen, H. J. & Gehring, W. J. Position effects on eukaryotic gene expression. *Annu Rev Cell Biol* **6**, 679-714 (1990).
150 Porter, S. D., Hu, J. & Gilks, C. B. Distal upstream tyrosinase S/MAR-containing sequence has regulatory properties specific to subsets of melanocytes. *Dev Genet* **25**, 40-48 (1999).
151 Nagy, A. Cre recombinase: the universal reagent for genome tailoring. *Genesis* **26**, 99-109 (2000).
152 Lobe, C. G. *et al.* Z/AP, a double reporter for cre-mediated recombination. *Dev Biol* **208**, 281-292 (1999).
153 Delmas, V., Martinozzi, S., Bourgeois, Y., Holzenberger, M. & Larue, L. Cre-mediated recombination in the skin melanocyte lineage. *Genesis* **36**, 73-80 (2003).
154 Feil, R., Wagner, J., Metzger, D. & Chambon, P. Regulation of Cre recombinase activity by mutated estrogen receptor ligand-binding domains. *Biochem Biophys Res Commun* **237**, 752-757 (1997).
155 Picard, D. Regulation of protein function through expression of chimaeric proteins. *Curr Opin Biotechnol* **5**, 511-515 (1994).
156 Yajima, I. *et al.* Spatiotemporal gene control by the Cre-ERT2 system in melanocytes. *Genesis* **44**, 34-43 (2006).
157 Soriano, P. Generalized lacZ expression with the ROSA26 Cre reporter strain. *Nature Genetics* **21**, 70-71 (1999).

158 Bosenberg, M. *et al.* Characterization of melanocyte-specific inducible Cre recombinase transgenic mice. *Genesis* **44**, 262-267 (2006).
159 Ahuja, D., Saenz-Robles, M. T. & Pipas, J. M. SV40 large T antigen targets multiple cellular pathways to elicit cellular transformation. *Oncogene* **24**, 7729-7745 (2005).
160 Sablina, A. A. & Hahn, W. C. SV40 small T antigen and PP2A phosphatase in cell transformation. *Cancer Metastasis Rev* **27**, 137-146 (2008).
161 Bradl, M., Klein-Szanto, A., Porter, S. & Mintz, B. Malignant melanoma in transgenic mice. *Proc Natl Acad Sci U S A* **88**, 164-168 (1991).
162 Mintz, B. & Silvers, W. K. Transgenic mouse model of malignant skin melanoma. *Proc Natl Acad Sci U S A* **90**, 8817-8821 (1993).
163 Kelsall, S. R. & Mintz, B. Metastatic cutaneous melanoma promoted by ultraviolet radiation in mice with transgene-initiated low melanoma susceptibility. *Cancer Res* **58**, 4061-4065 (1998).
164 Serrano, M. *et al.* Role of the INK4a locus in tumor suppression and cell mortality. *Cell* **85**, 27-37 (1996).
165 You, M. J. *et al.* Genetic analysis of Pten and Ink4a/Arf interactions in the suppression of tumorigenesis in mice. *Proc Natl Acad Sci U S A* **99**, 1455-1460 (2002).
166 Chin, L. *et al.* Cooperative effects of INK4a and ras in melanoma susceptibility in vivo. *Gene Dev* **11**, 2822-2834 (1997).
167 Jafari, M. *et al.* Analysis of ras mutations in human melanocytic lesions: activation of the ras gene seems to be associated with the nodular type of human malignant melanoma. *J Cancer Res Clin Oncol* **121**, 23-30 (1995).
168 Chin, L. *et al.* Essential role for oncogenic Ras in tumour maintenance. *Nature* **400**, 468-472 (1999).
169 Eskandarpour, M. *et al.* Frequency of UV-inducible NRAS mutations in melanomas of patients with germline CDKN2A mutations. *J Natl Cancer Inst* **95**, 790-798 (2003).
170 Ackermann, J. *et al.* Metastasizing melanoma formation caused by expression of activated N-RasQ61K on an INK4a-deficient background. *Cancer Res* **65**, 4005-4011 (2005).
171 Dhomen, N. *et al.* Oncogenic Braf induces melanocyte senescence and melanoma in mice. *Cancer Cell* **15**, 294-303 (2009).
172 Goel, V. K. *et al.* Melanocytic nevus-like hyperplasia and melanoma in transgenic BRAFV600E mice. *Oncogene* **28**, 2289-2298 (2009).
173 Woods, D. *et al.* Raf-induced proliferation or cell cycle arrest is determined by the level of Raf activity with arrest mediated by p21Cip1. *Mol Cell Biol* **17**, 5598-5611 (1997).
174 Dankort, D. *et al.* A new mouse model to explore the initiation, progression, and therapy of BRAFV600E-induced lung tumors. *Gene Dev* **21**, 379-384 (2007).
175 Mercer, K. *et al.* Expression of endogenous oncogenic V600EB-raf induces proliferation and developmental defects in mice and transformation of primary fibroblasts. *Cancer Res* **65**, 11493-11500 (2005).
176 Chen, Z. *et al.* Crucial role of p53-dependent cellular senescence in suppression of Pten-deficient tumorigenesis. *Nature* **436**, 725-730 (2005).
177 Sambrook, J. & Russell, D. W. *The Condensed Protocols From Molecular Cloning: A Laboratory Manual*. 1st edn, (Cold Spring Harbor Lab Press, 2006).

178 Kinniburgh, A. J., Mertz, J. E. & Ross, J. The precursor of mouse beta-globin messenger RNA contains two intervening RNA sequences. *Cell* **14**, 681-693 (1978).
179 Palmiter, R. D., Sandgren, E. P., Avarbock, M. R., Allen, D. D. & Brinster, R. L. Heterologous introns can enhance expression of transgenes in mice. *Proc Natl Acad Sci U S A* **88**, 478-482 (1991).
180 Choi, T., Huang, M., Gorman, C. & Jaenisch, R. A generic intron increases gene expression in transgenic mice. *Mol Cell Biol* **11**, 3070-3074 (1991).
181 Buchholz, F., Angrand, P. O. & Stewart, A. F. Improved properties of FLP recombinase evolved by cycling mutagenesis. *Nat Biotechnol* **16**, 657-662 (1998).
182 Raymond, C. S. & Soriano, P. High-efficiency FLP and PhiC31 site-specific recombination in mammalian cells. *PLoS One* **2**, e162 (2007).
183 Wunderlich, F. T., Wildner, H., Rajewsky, K. & Edenhofer, F. New variants of inducible Cre recombinase: a novel mutant of Cre-PR fusion protein exhibits enhanced sensitivity and an expanded range of inducibility. *Nucleic Acids Res* **29**, E47 (2001).
184 Brinster, R. L. *et al.* Somatic expression of herpes thymidine kinase in mice following injection of a fusion gene into eggs. *Cell* **27**, 223-231 (1981).
185 Burdon, T., Sankaran, L., Wall, R. J., Spencer, M. & Hennighausen, L. Expression of a whey acidic protein transgene during mammary development. Evidence for different mechanisms of regulation during pregnancy and lactation. *J Biol Chem* **266**, 6909-6914 (1991).
186 Clark, A. J., Cowper, A., Wallace, R., Wright, G. & Simons, J. P. Rescuing transgene expression by co-integration. *Biotechnology (N Y)* **10**, 1450-1454 (1992).
187 Lacy, E., Roberts, S., Evans, E. P., Burtenshaw, M. D. & Costantini, F. D. A foreign beta-globin gene in transgenic mice: integration at abnormal chromosomal positions and expression in inappropriate tissues. *Cell* **34**, 343-358 (1983).
188 McKnight, R. A., Wall, R. J. & Hennighausen, L. Expression of genomic and cDNA transgenes after co-integration in transgenic mice. *Transgenic Res* **4**, 39-43 (1995).
189 Lim, C. K. *et al.* A comparative study of tamoxifen metabolism in female rat, mouse and human liver microsomes. *Carcinogenesis* **15**, 589-593 (1994).
190 Awatramani, R., Soriano, P., Mai, J. J. & Dymecki, S. An Flp indicator mouse expressing alkaline phosphatase from the ROSA26 locus. *Nature genetics* **29**, 257-259 (2001).
191 el-Refaey, H., Rajasekar, D., Abdalla, M., Calder, L. & Templeton, A. Induction of abortion with mifepristone (RU 486) and oral or vaginal misoprostol. *N Engl J Med* **332**, 983-987 (1995).
192 Cao, T., He, W., Roop, D. R. & Wang, X. J. K14-GLp65 transactivator induces transgene expression in embryonic epidermis. *Genesis* **32**, 189-190 (2002).
193 Murisier, F., Guichard, S. & Beermann, F. A conserved transcriptional enhancer that specifies Tyrp1 expression to melanocytes. *Dev Biol* **298**, 644-655 (2006).
194 Sutton, R., Gordon-Thomson, C., Cree, I. A., Mason, R. S. & Moore, G. P. Tyr-TGFalpha transgenic mice develop ocular melanocytic lesions. *Melanoma Res* **12**, 435-439 (2002).
195 Moltó, E., Vicente-Garcia, C., Fernández, A. & Montoliu, L. in *MOUSE AS A MODEL ORGANISM* (eds Cord Brakebusch & Taina Pihlajaniemi) (Springer, 2011).

196 Gasser, S. M. & Laemmli, U. K. Improved methods for the isolation of individual and clustered mitotic chromosomes. *Exp Cell Res* **173**, 85-98 (1987).
197 Hsiao, E. C. *et al.* Constitutive Gs activation using a single-construct tetracycline-inducible expression system in embryonic stem cells and mice. *Stem Cell Res Ther* **2**, 11 (2011).
198 Strathdee, D., Ibbotson, H. & Grant, S. G. Expression of transgenes targeted to the Gt(ROSA)26Sor locus is orientation dependent. *PLoS One* **1**, e4 (2006).
199 Behringer, R. R. *et al.* Synthesis of functional human hemoglobin in transgenic mice. *Science* **245**, 971-973 (1989).
200 Beermann, F., Ruppert, S., Hummler, E. & Schutz, G. Tyrosinase as a marker for transgenic mice. *Nucleic Acids Res* **19**, 958 (1991).
201 Overbeek, P. A. *et al.* Coinjection strategy for visual identification of transgenic mice. *Transgenic Res* **1**, 31-37 (1991).
202 Lu, J. *et al.* MicroRNA expression profiles classify human cancers. *Nature* **435**, 834-838 (2005).
203 Hart, R. P., McDevitt, M. A., Ali, H. & Nevins, J. R. Definition of essential sequences and functional equivalence of elements downstream of the adenovirus E2A and the early simian virus 40 polyadenylation sites. *Mol Cell Biol* **5**, 2975-2983 (1985).
204 Levitt, N., Briggs, D., Gil, A. & Proudfoot, N. J. Definition of an efficient synthetic poly(A) site. *Gene Dev* **3**, 1019-1025 (1989).
205 Schedl, A. *et al.* A method for the generation of YAC transgenic mice by pronuclear microinjection. *Nucleic Acids Res* **21**, 4783-4787 (1993).
206 Jang, S. K. *et al.* A segment of the 5' nontranslated region of encephalomyocarditis virus RNA directs internal entry of ribosomes during in vitro translation. *J Virol* **62**, 2636-2643 (1988).
207 Jang, S. K. & Wimmer, E. Cap-independent translation of encephalomyocarditis virus RNA: structural elements of the internal ribosomal entry site and involvement of a cellular 57-kD RNA-binding protein. *Gene Dev* **4**, 1560-1572 (1990).
208 Reya, T. *et al.* A role for Wnt signalling in self-renewal of haematopoietic stem cells. *Nature* **423**, 409-414 (2003).
209 Martin, P., Albagli, O., Poggi, M. C., Boulukos, K. E. & Pognonec, P. Development of a new bicistronic retroviral vector with strong IRES activity. *BMC Biotechnol* **6**, 4 (2006).
210 Mizuguchi, H., Xu, Z., Ishii-Watabe, A., Uchida, E. & Hayakawa, T. IRES-dependent second gene expression is significantly lower than cap-dependent first gene expression in a bicistronic vector. *Mol Ther* **1**, 376-382 (2000).
211 Trichas, G., Begbie, J. & Srinivas, S. Use of the viral 2A peptide for bicistronic expression in transgenic mice. *BMC Biol* **6**, 40 (2008).
212 Donnelly, M. L. *et al.* Analysis of the aphthovirus 2A/2B polyprotein 'cleavage' mechanism indicates not a proteolytic reaction, but a novel translational effect: a putative ribosomal 'skip'. *J Gen Virol* **82**, 1013-1025 (2001).
213 Kellendonk, C. *et al.* Inducible site-specific recombination in the brain. *J Mol Biol* **285**, 175-182 (1999).
214 Tief, K., Schmidt, A. & Beermann, F. New evidence for presence of tyrosinase in substantia nigra, forebrain and midbrain. *Brain Res Mol Brain Res* **53**, 307-310 (1998).